



Dynamic reference points for improved vertical accuracy of GNSS

MASTER'S THESIS AT AALBORG UNIVERSITY

SURVEYING, PLANNING AND LAND MANAGEMENT

- SPECIALISATION IN SURVEYING AND MAPPING -

Authors:

Filip NØRHOLM

Jens Henrik Friis OVERGAARD

The 4th of June, 2021



**AALBORG
UNIVERSITY**



Department of Planning
Technical Faculty of IT and Design
Rendsburggade 14
9000 Aalborg
plan.aau.dk

AALBORG UNIVERSITY

STUDENT REPORT

Education and semester:

Master's programme in Surveying,
Planning and Land Management
with specialisation in
Surveying and Mapping.
4th semester.

Title:

Dynamic reference points for
improved vertical accuracy of GNSS

Semester Theme:

Master's Thesis

Project Period:

February 2021 - June 2021

Participants:

Filip Nørholm
Jens Henrik Friis Overgaard

Supervisor:

Jens Peter Cederholm

Number of pages and words:

61 normal pages, 21934 words and 158
printed pages including appendices.

Date of Completion:

The 4th of June, 2021

Synopsis:

Orthometric height determination with GNSS suffers from poor precision and accuracy, compared to the determination of planar coordinates. This project examines the capabilities of single-baseline RTK (SRTK) in interaction with the "dynamic reference point (DRP)". The examinations are done by collecting observations at different baseline lengths, along with levelling and examinations of geoid models. A GNSS observation with corrections from an SRTK setup is examined to have a precision of $2.4 \text{ mm} + 1.3 \text{ mm/km}$ baseline length. Different geoid models are examined to have systematic biases, but within a limited area, the bias is constant. The orthometric height in the DRP solves the bias problem, by correcting the base height. Because of the corrected bias, an SRTK+DRP orthometric height observation can be accurate within $2.4 \text{ mm} + 1.3 \text{ mm/km}$ baseline length. The applicability and potential of the method are present. Resource demands of the method are significantly lower than competing and conventional methods, though the accuracy can not compete with geometric levelling.

Resumé

Kotebestemmelse er normalt dyrt og besværligt, da det er nødvendigt at udføre nivellerment. GNSS er meget hurtigere og billigere, men giver typisk en markant dårligere præcision. Derudover bidrager geoidmodellen typisk med absolutte fejl i størrelsesordenen 0-2 cm. Den initierende hypotese er at en nøjagtig kote i GNSS basestationen, kan korrigere for fejlen i geoidmodellen. Det dynamiske fikspunkt, udviklet af Geopartner A/S, kan sikre at basestationen kan tilknyttes en kote med høj absolut nøjagtighed. Derudover er fikspunktet baseret på radar teknologi, som giver mulighed for efterfølgende monitorering og opdatering af koten, hvorved fikspunktet betegnes som dynamisk.

Problemstillingen formuleres som; *Hvad er mulighederne ved enkeltstations RTK i relation til et "dynamisk fikspunkt"?*. Geopartner A/S har initieret projektidéen, og har bidraget med problemstillinger og faglig indsigt i teknologien bag det dynamiske fikspunkt. De problemstillinger, som der har manglet empiri om er; *præcisionen af enkeltstations RTK samt nøjagtigheden af SRTK* begge parametre med afsæt i også at indrage nyligt tilkomne satellitprogrammer (Galileo og BeiDou). Ift. nøjagtigheden har det været essentielt at undersøge præcisionen af geoidmodeller, samt nøjagtigheden af målte ellipsoidehøjder og geoidmodeller. Udover de kvantitative problemstillinger er brugbarheden og potentialet af teknologien også vurderet.

Præcision og nøjagtighed undersøges empirisk vha. egen dataindsamling. Afledt af en hypotese om at større dataindsamling bør øge præcisionen testes forskellige opmålingstider eller intervaller (time averaging window). Der opmåles i intervallerne 5, 15, 30, 60, 120, 240 og 600 sekunder. Resultatet viser ingen signifikant forskel på præcisionen, hvorfor det ikke umiddelbart kan anbefales at bruge lange tidsintervaller for at øge præcisionen. Efterfølgende dataindsamlingerne er foretaget med 60 sekunders opmåling.

Grundet tekniske problemer har det ikke været muligt at udføre enkeltstations RTK med egen basestation, hvorfor er der brugt basestationer ved TAPAS, som er et regionalt netværk af basestationer i Aarhus. Over 5 dage i løbet af en måned, er der indsamlet ca. 40 observationer med følgende baseline længder [m]; 22, 286, 686, 1409, 2944, 4469, 7401, 12401, 21991, 32561. Som målestok indsamles der i ét punkt med korrektioner fra Leica Smartnet IMAX netværkstjeneste.

Undersøgelsen af præcisionen af kort baseline enkeltstations RTK viser at grundfejlen er 2,4 mm og den afstandafhængige fejl $1,3 \text{ mm/km}$. For længere baselines, over 5 km, er præcisionen $5,3 \text{ mm} + 0,3 \text{ mm/km}$.

Undersøgelsen af præcision og nøjagtighed af geoidmodeller er lavet på et lokalt niveau. Der udført geometrisk nivellerment mellem respekterede højdefikspunkter og 4 af de punkter, som er placeret indenfor en afstand på ca. 1450 m, som er målt i test af præcision af enkeltstations RTK. De nivellerede koter og de målte ellipsoidehøjder sammenlignes med geoidhøjder i to forskellige geoidmodeller. Det viser sig at begge geoidmodeller har en vis unøjagtighed, men til gengæld har høj præcision. Det vil sige, at der i alle 4 punkter er en systematisk forskydning i geoidhøjden, men det er den samme forskydning i alle punkter.

GNSS-observationerne er i sin rå form ellipsoidehøjder. De målte ellipsoidehøjder sammenlignes i 5 baseline afstande med den opgivne ellipsoidehøjde i et såkaldt 10 km fikspunkt. Der viser sig en systematisk fejl, som er korreleret med forskellen mellem koten ved basestationen og koten ved roveren. Hypotesen er at fejlen skyldes en fejl i modelleringen af troposfære forsinkelse. Fejlen er i størrelsesordenen 0,2 mm pr. m forskel.

Rapporten beviser empirisk hvordan der i basestationen kan korrigeres for lokale systematiske fejl (geoidmodellens forskydning), og hvordan det overfører korrektionen til roverens observationer.

Grundet geoidmodellernes høje præcision kan en måling med enkeltstations RTK i relation til et dynamisk fikspunkt konkluderes at have en nøjagtighed på $2,4 \text{ mm} + 1,3 \text{ mm/km}$. Det forudsættes at der ikke er signifikant forskel mellem koten i base og rover, medmindre at der opnås en bedre modellering af troposfæreforsinkelsen. Det forudsættes også at geoidmodellen har en høj præcision.

Brugbarheden af enkeltstations RTK i relation til et dynamisk fikspunkt er vurderet vha. egne erfaringer med anvendelse, vurdering af implementering af teknologien, samt de opnåelige nøjagtighedsniveauer sammenlignet med alternative metoder. Det vurderes at teknologien har fordele og ulemper. Det er muligt at spare betydelige ressourcer, men nøjagtigheden kan ikke konkurrere med præcisionsniveauet.

Potentialet for teknologien vurderes ift. specifikke opgavetyper og samfundsmæssige problemstillinger vha. bl.a. ekspertudtalelser. Der konkluderes at ved ledningsregistrering af forsyningsledninger, hvor nøjagtighedskravet typisk er 1 cm (95%), vil enkeltstations RTK have et relevant potentiale. Teknologien vil potentielt kunne opfylde kravet inden for en radius af 2 km fra basestationen ved bare en måling.

Preface

Geopartner A/S and especially Karsten Vognsen, Chief Advisor, have been the initiating force, that presented the basic problems of the examined technologies. The company have fortunately been helpful with delivering research areas, survey equipment and presenting practical experiences.

SDFE and especially Kristian Keller, Geodesist, have in several circumstances helped with knowledge about geoid models, and with delivering the present geoid model and a draft of the newest version among other things.

A huge gratitude is also expressed to Jens Peter Cederholm, who have been supervising, encouraging and guiding the project group during this final semester, as well as several previous semesters.

Instructions for reading

Current thesis is written in a scientific language. Knowledge about surveying, mapping, positioning and basic statistics is a prerequisite of reading.

The examinations in the thesis are based on several GNSS observations performed by the project group. The observations are delivered along with the report as a separate zip compressed folder.

The folder contains:

- Text files with raw and grouped GNSS observations (before detection of outliers)
- Excel sheet of grouped observations from time averaging window test (after detection and removing of outliers)
- Excel sheet of grouped observations from baseline distance test (after detection and removing of outliers)

The thesis is separated in 4 parts. The first three parts examines the 3 research questions were the last part contains the main conclusion, discussion and perspectives.

The citation form used is the *Harvard Method*, which is expressed by [author, year].

A list of the used scientific abbreviations is seen in table 1

Table of used abbreviations	
Abbreviation	Description
RTK	Real Time Kinematics
DVR90	Dansk Vertikal Reference 1990, <i>Vertical reference system</i>
STD	STandard Deviation
GNSS	Global Navigation Satellite System
RTCM	Radio Technical Commission for Maritime Services
NTRIP	Networked Transport of RTCM via Internet Protocol
TAPAS	Testbed for Precise positioning and Autonomic Systems
GNSS	Global Navigation Satellite System
GPS	Global Positioning System
GLONASS	GLObalnaya NAVigatsionnaya Sputnikovaya Sistema
SDFE	Agency for Data Supply and Efficiency
ECEF	Earth Centered Earth Fixed
NRTK	Network RTK
SRTK	Single baseline RTK
DRP	Dynamic Reference Point
iMAX	Idividualized Master AuXiliary concept
ETRS89	European Terrestrial Reference System 1989
WGS84	World Geodetic System of 1984
GSM	Global System for Mobile communications
VHF	Very High Frequency
UHF	Ultra High Frequency
SIM	Subscriber Identification Module
IP	Internet Protocol
DNS	Domain Name System

Table 1: Table of abbreviations

Contents

Resumé	v
Preface	vii
1 Introduction	1
1.1 Idea	3
2 Problem statement	7
3 Method	9
3.1 Part I	10
3.2 Part II	12
3.3 Part III	14
3.4 Part IV	15
Part I Precision of SRTK	17
4 Relative GNSS positioning	19
4.1 Relative positioning	19
4.2 Error sources	20
4.3 Available GNSS programmes	21
5 Test design	23
5.1 Possible unintentional error sources of testing	23
5.2 Averaging time window test	24
5.3 Baseline distance test	25
5.4 Disclaimer for not performing SRTK with own base station	26
5.5 Approach for data examination	27
6 Test of averaging time window	31
6.1 Data collection	31
6.2 Data examination	34
6.3 Conclusion	37
7 Baseline distance test	39
7.1 Data collection	39
7.2 Data examination	41
8 Conclusion - Part I - Precision of SRTK	51
Part II Accuracy of SRTK in interaction with the DRP	53
9 Introduction to examination of accuracy of SRTK in interaction with the DRP	55
9.1 Orthometric heights	55

9.2	Ellipsoidal heights	55
9.3	Geoid heights	56
10	Assessment of accuracy and precision of geoid models	57
10.1	Regional examination	57
10.2	Local examination	59
10.3	Height differences	60
11	Accuracy (Trueness) of SRTK	65
11.1	Ellipsoidal heights	65
11.2	Orthometric heights	69
12	Conclusion - Part II - Accuracy of SRTK	73
 Part III Applicability and potential		75
13	Applicability of using SRTK with DRPs	77
13.1	Procedure for setting up base station at the DRP	77
13.2	RTK correction transmitting method	77
13.3	Procedures for RTK corrections from DRP base station	78
13.4	Performance of SRTK in relation to DRP's	79
14	Potential for SRTK in interaction with the DRP	81
14.1	Satellite data and radar reflectors	81
14.2	The dynamic reference point	82
14.3	Potential of SRTK in interaction with the DRP	83
15	Conclusion - Part III - Applicability and potential	85
 Part IV Main conclusion, discussion and perspectives		87
16	Main conclusion	89
17	Discussion	91
18	Perspectives	93
Bibliography		95
Appendix A Understanding the dynamic reference point		99
A.1	Sentinel 1	99
A.2	Dynamic reference point - concept	99
Appendix B Accuracy of RTK GNSS		107
Appendix C Absolute positioning		111
C.1	Error sources	111

Appendix D	Number of satellites, DOP-values and elevation of satellites	114
Appendix E	Individual data examination of test of averaging time window	117
E.1	Data collected in Aalestrup	118
E.2	Data collected in Sabro	125
Appendix F	Individual data examination of baseline distance test	133
Appendix G	Precision of a height difference	145

Introduction

1

Determination of orthometric heights or stake out of heights in an absolute coordinate system is a classic survey discipline, but not necessarily easy or straightforward. Orthometric heights are only absolute when in a relation to the chosen geoid model, which describes the ocean surface affected by the gravity field throughout the extent of the model. Figure 1.1 visualizes the principle of height determination by GNSS, where the geoid model is illustrated by the red dashed line. The geoid is often defined as the mean sea level and the zero point, which heights are to be related to.

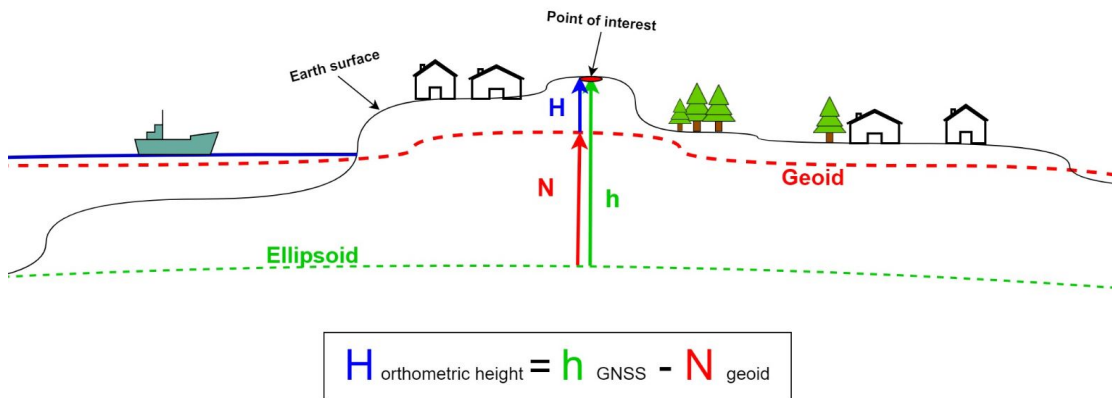


Figure 1.1: Principle for orthometric height determination

In Denmark, the national geoid (DVR90) is related to the European reference frame ETRS89 by 13 permanent GNSS stations [SDFE, 2021a]. ETRS89 is based on the GRS80 ellipsoid, which at figure 1.1 is illustrated by the green dashed line. An ellipsoid is earth-centred and a regular geometric shape, which approximates the shape of the earth. However, this is a rough assumption as the earth's shape is not regular, and the geoid model is required. When using GNSS, positions are based on the global WGS84 reference frame. WGS84 is a **E**arth **C**entered **E**art **F**ixed (**ECEF**) global reference defined by a ellipsoid with origin in the mass centre of the earth [Hofmann-Wellenhof et al., 2008]. Positions are converted into the European ETRS89 reference frame, and the height subsequently transformed into orthometric heights by the formula shown at figure 1.1, ($H = h - N$) [Hofmann-Wellenhof et al., 2008].

For the physical realization of the DVR90, and to offer available height references a large network of reference points are established throughout the country. Establishing new points or maintenance of already existing points relies on labour-consuming levelling surveys from one point to another or repeating intervals of static GNSS. This is a costly process, which leads to many of the 67.000 height reference points in Denmark not being maintained or updated periodically, and in some regions not at all maintained [SDFE, 2021a]. This approach does not entirely result in reliable or accurate height references.

Land subsidence, elevation, or physical damage of the reference points are obvious reasons why maintenance is a returning demand, but the cost is often too high. In general, surveyors in Denmark only rarely need height reference points because most work can be done by using GNSS - also height determination. GNSS and associated network RTK providers are approved for cadastral work in Denmark why this is the convenient solution in most cases. But GNSS and RTK have their limit, especially when determining heights, where Leica claims to have a height accuracy typically better than 4 cm using their network service Smartnet [Leica Geosystems, 2021b]. Practical experience show RTK GNSS accuracy in a certain case only to be in the range of 7 cm (95%) as appendix B on page 107 shows [Vognsen, 2021].

The accuracy of GNSS or RTK measured heights is affected by two factors (h and N), which are visualized in figure 1.2. In other words, the determining factors are the accuracy of the reference (N) and the precision of GNSS (h). To describe the issues the figure also visualizes theoretical true values illustrated by black.

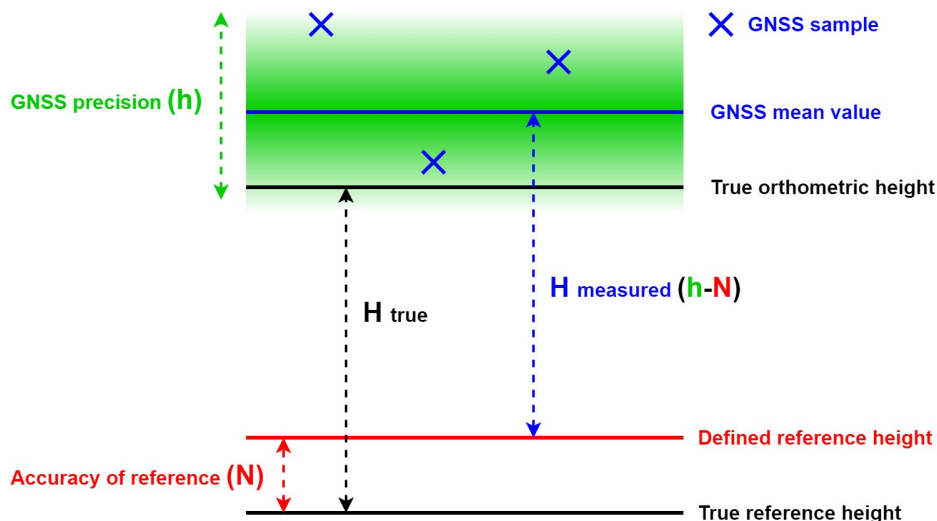


Figure 1.2: Determining factors N and h - Accuracy of N and precision of h

The accuracy of the reference (N) consists of how accurate the geoid model is related to the ellipsoid, but also how the geoid model represents the earth's gravity field. A geoid model is realized by a matrix, i.e. a regular grid, of geoid heights at certain planar positions. When desiring a geoid height within the grid, interpolating is done. The accuracy of the model will vary throughout the extent of the model. Therefore, the accuracy might vary from one point to another, but for a specific point of interest be constant. The inaccuracy of the geoid model will propagate directly to every height determination in relation to the geoid, which at the figure is illustrated by the "defined reference height" being placed a bit higher than the "true reference height". The measured H has the same length as the true H , but because the "defined reference height" is placed too high so will the determined orthometric height.

The GNSS precision is not constant and will vary from time to time when measuring the same point. GNSS is characterized by relatively low precision compared to other survey

methods and in practice, it can be difficult to predict the level of precision due to varying satellite constellation and atmospheric conditions. High precision GNSS positions are obtainable by static GNSS or larger series of data, which at the figure is illustrated by the "GNSS mean value". This can be considered as the best obtainable GNSS value, which in this case lies higher than the true orthometric height due to the inaccuracy of the reference. If only measuring once or for a short time this GNSS sample is not necessarily close to the mean value. As illustrated, it is possible to get a sample closer to the true value, but more likely to add an error and thereby magnify the inaccuracy of the measured H .

Eventually, this leads to a situation where the majority of orthometric heights are determined by GNSS with only limited certainty and consistency of the accuracy. The demand for accurate heights however seems to be more crucial than ever. Preparation and protection against climate changes is a topic of immediate interest in a flat and porous country like Denmark, why accurate heights are an important factor. Intensive urban development and large infrastructure are also relying on the ability to determine accurate heights. When accurate heights are needed GNSS is not suitable, but what is the alternative option if only a few reliable reference points are available several kilometres away?

1.1 Idea

The danish company Geopartner A/S has developed a "Dynamic Reference Point" (DRP) based on satellite radar technology, which is an alternative approach of delivering a reliable and accurate height reference point. The DRP is not just a point, but a radar reflector, which is a cube-formed iron screen designed to reflect satellite radar signals. An example of a DRP is seen in figure 1.3. This iron screen returns a strong signal, which is clear and more precise in the radar images. The reflectors can be used to calibrate or fix radar images for higher precision of the surrounding natural objects. As a DRP the important factor is the continuous relative radar data provided every time the satellite passes by is used to detect the vertical movement of the reflector. A Sentinel satellite passes by every six days and when a data series of about a year is generated, vertical movement in a magnitude of just a millimetre can be registered.



Figure 1.3: Dynamic Reference Point



Figure 1.4: Height reference point of DRP

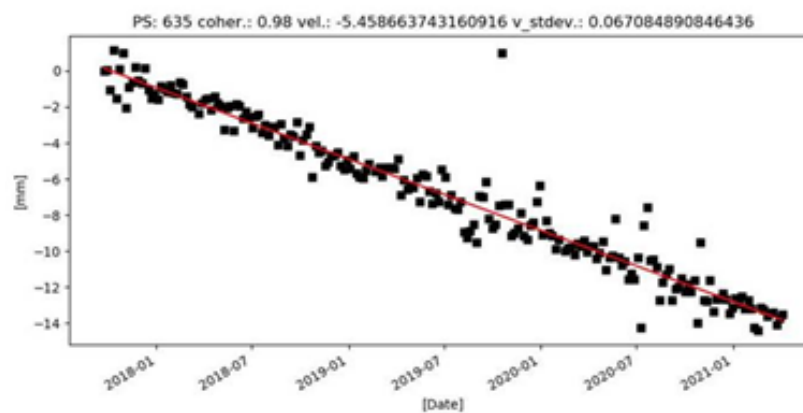


Figure 1.5: Time series of data from radar reflector located in Thyborøn, Denmark. Movement / subsidence of 5.5 mm/year [Vognsen, 2021]

The physical height reference point is placed at the bottom of the radar reflector, as seen in figure 1.4. When establishing the DRP levelling is needed to provide it with an absolute orthometric height, but afterwards, the benefits are remarkable. The continuous radar data offer the opportunity of easy maintenance and updating of the reference height in case of land subsidence, why the DRP is considered dynamic. An example of a time series, showing the dynamic change of the orthometric height is seen in figure 1.5. Over time most reference points need maintenance, but in exposed areas such as coastal regions or areas with intensive urban development, land subsidence can be several millimetres per year. This control or update could be done for example once a year, and

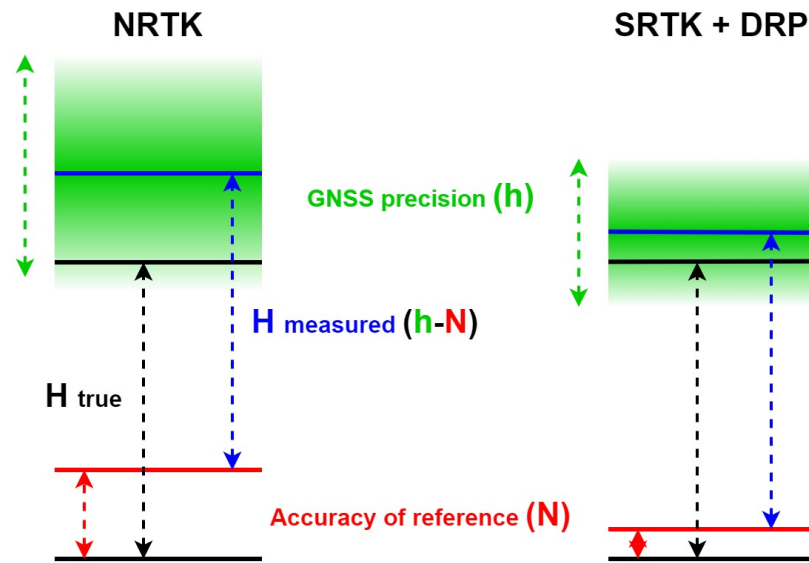
for at a larger number of reference points, the cost for this process would be a fraction compared to traditional maintenance by levelling. This cost-beneficial process should be a basis for updated and more reliable reference points, or just more accurate reference points. A more adequate description of the DRP is seen in appendix A on page 99, including more photos as well.

Despite the accuracy, the DRP is not a convenient solution if the presumption is levelling to a DRP whenever a reference height is needed. However, by combining the DRP with GNSS positioning it might be possible to create a method for height measurement, which is both accurate and convenient.

GNSS for survey purposes relies on the technology of RTK, where the precision is improved by measuring relatively to a known reference point. A GNSS receiver, called the base station, is placed in the known point, which allows sending corrections to another receiver, called the rover, used to measure new points. Naturally, the accuracy of the RTK rover is affected by the accuracy of the reference point, but also by random uncertainty of GNSS, which in figure 1.2 was illustrated as "GNSS precision". An important and known parameter to affect the random errors or the precision is the distance between base and rover. As corrections are made relative to the base, these are only usable for the rover if the two receivers are exposed to approximately the same atmospheric conditions. In theory, the shortest distance between base and rover should result in the highest GNSS precision. Today RTK positioning is almost entirely based on network services where the distance to a reference station can be about 20 or 40 kilometres.

Single-baseline RTK (SRTK) where the surveyor establishes the base station himself can be considered as the traditional method as this was the only opportunity before the network services. Establishing the base station by yourself is not at all convenient compared to the network services, but it allows the opportunity to locate the base station very close to the rover, and thereby have what is called a short baseline. The short baseline should in theory result in high GNSS precision, so all you need for high accuracy positioning with SRTK is an accurate reference point nearby. Geopartner considers a DRP network with a density of about 5 km a realistic scenario in areas of interest, for example, larger urban areas or coastal areas. The DRP's are prepared to be used as an SRTK base station by having mounts for a GNSS antenna with a registered reference height.

The overall aim of this thesis is to investigate if SRTK and the DRP is an applicable method for determining orthometric heights. The hypothesis of how SRTK in interaction with the DRP is anticipated to improve height determination is visualized in figure 1.6. In the figure, the SRTK + DRP scenario is compared to network RTK (NRTK), where the NRTK part is a replica of the earlier explained scenario from figure 1.2. The DRP is supposed to improve the accuracy of the reference (N) and therefore the red line is placed closer to the true reference height at figure 1.6. SRTK is supposed to improve the GNSS precision (h) and therefore the green area at figure 1.6 is narrower. A single GNSS sample will be placed somewhere in the green area, and consequently, the SRTK + DRP scenario offers a higher probability of this sample being close to the true orthometric height.

Figure 1.6: Determining factors N and h - NRTK vs SRTK + DRP

The DRP is a completed and proven set-up to provide high accuracy, and the relatively low-cost establishment and maintenance give the DRP a potential for expansion to a larger network of DRPs in Denmark or other countries. GNSS positioning is continuously improved by newly available satellites and more advanced multi-frequency signals, which should make GNSS positioning more precise than ever. SRTK is however not a method commonly used, which constitutes some uncertainty about what SRTK is capable of when using modern equipment and the current number of available satellites. This project will investigate the performance of SRTK and combine it with the potential of the DRP.

Problem statement 2

As described in the introduction the idea is to use the DRP as a basis for accurate height determination by SRTK. The DRP concept will offer a high accuracy reference point based on satellite radar technology, which is prepared to work as a base station for SRTK. The DRP should be an accurate reference for the base station, as the short baseline should potentially offer high precision for SRTK. To investigate this method for height determination the following problem statement has been formed:

What are the capabilities of single-baseline RTK in interaction with the “dynamic reference point”?

By capabilities are meant **precision** and **accuracy** of the orthometric height, as well as the **applicability** and **potential** for this approach of height determination. The relationship between precision and accuracy is described in the research method in section 3.1.1, but generally, the precision is a topic focused at SRTK, when the accuracy will involve the SRTK in interaction with the DRP, and how it cooperates towards accurate orthometric heights.

By interaction is meant the cooperation and synergy advantages the SRTK technology earns from having the base station placed in a DRP, with an accurate orthometric height.

To do a thorough examination of the problem statement, the following three research questions have been formed:

1. *What is the vertical precision of SRTK?*
2. *What is the vertical accuracy of SRTK in interaction with the DRP?*
3. *How is SRTK in interaction with the DRP applicable, and what is the potential?*

The research questions will be the basis for corresponding examinations, which combined are designed to answer the problem statement.

Research question 1

In this project, the capability of the DRP for GNSS survey relies on the technique of SRTK, where the initial idea is that short distances between base and rover should be the groundwork for high precision surveying. Research question 1 is the basis of examining the precision of SRTK unbiased. The analysis will relate distances and practical conditions to usage with the DRP, but the aim is to examine SRTK independently. The analysis will determine the obtainable precision under certain conditions. The analysis will determine how the distance between base and rover affects the precision and clarify other decisive parameters.

Research question 2

In the context of GNSS positioning accuracy describes the ability to determine a position in a certain reference system. This project aims to determine orthometric heights in the

danish vertical reference system DVR90. The DRP and the geoid model can be considered as the link between the SRTK survey and the reference system. Research question 2 will be the basis of examining the accuracy in DVR90 for heights determined by DRP and SRTK.

Research question 3

Research question 3 is the basis of examining the applicability and potential of height determination by DRP and SRTK. To consider the technique as a practical solution for height determination, high accuracy should not only be obtainable but also be a usable and applicable solution. In the case of potential, the DRP and SRTK concept is put into perspective with specific tasks, where potential advantages can be obtained. The expansion potential of the DRP concept is also assessed.

Main thesis structure

In the following chapter 3 on the next page the method for answering the three research question, and thereby the problem statement, is presented. Subsequently, the thesis is divided into parts where the examinations for research question 1, 2 and 3 is described in thesis part I, II and III.

Method 3

This chapter presents the method for answering the problem statement; *What are the capabilities of single-baseline RTK in interaction with the “dynamic reference point”?*

To answer the problem statement three research questions have been formed as presented in chapter 2.

1. *What is the vertical precision of SRTK?*
2. *What is the vertical accuracy of SRTK in interaction with the DRP?*
3. *How is SRTK in interaction with the DRP applicable, and what is the potential?*

The three research questions are the basis for each part of the thesis as visualized in figure 3.1.

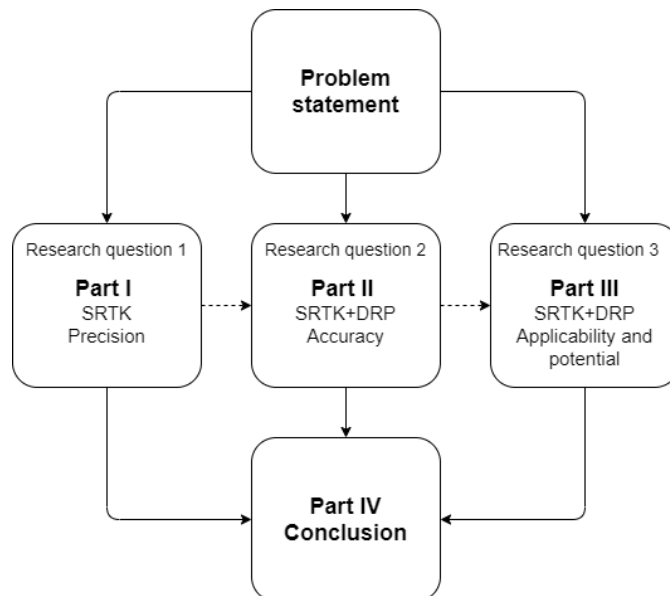


Figure 3.1: Main flowchart for the project thesis

Examining the precision of SRTK is considered an independent process, which is described in part I of this project thesis.

Part II will analyze the accuracy of SRTK, by examining the danish height reference system and put these into perspective with results of SRTK precision from part I, to assess the obtainable accuracy of SRTK. The geoid model is an important factor of this part because it is essential when deriving orthometric heights from GNSS. The realization of the SRTK technology, when combined with a DRP, will also be examined.

Part III of the thesis will examine the applicability and potential for SRTK in interaction with the “dynamic reference point”. Will the accuracy and applicability of the method meet the current and potential needs for determining orthometric heights? This part will

be based on the results of part I and II, and the practical experiences of working with SRTK.

The conclusion of the problem statement will be derived from the examinations in part I, II, and III.

The following sections will describe the method of how part I, part II and part III are answering their respective research question.

3.1 Part I

This part of the thesis is set up to answer the research question; *What is the vertical precision of SRTK?*

The only parameter of analysis in this part is precision, and therefore the subject and measuring method need to be defined. The definition of precision and accuracy is seen in section 3.1.1 on the facing page.

To examine the precision of SRTK, part I will have a deductive approach where variables to affect the precision initially are identified and later tested. This course of action for part I is visualized in figure 3.2.

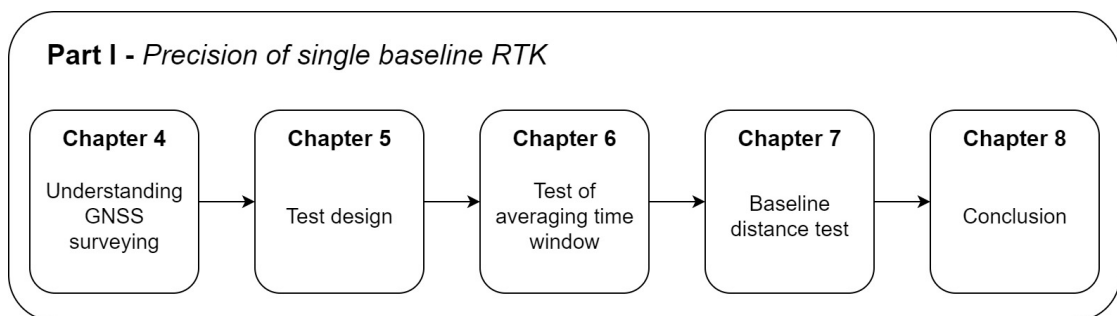


Figure 3.2: Flowchart of part I

Chapter 4 on page 19 provides the primary knowledge of GNSS surveying through an empirical analysis, which is the basis of identifying test variables and error sources for SRTK. Chapter 5 on page 23 describes how relevant variables and error sources are tested in practice.

Through chapter 4 and 5 two variables for SRTK precision, *time* and *distance*, are identified and setup for testing.

Chapter 6 on page 31 examines the effect of "the averaging time window", or the time used to measure the height of a certain point. This test will also be the basis for choosing a suitable time window for the following test.

Chapter 7 on page 39 is the main analysis of this part, where the effect of the distance between the RTK base and rover is examined. The analysis consists of a larger number of observations to investigate this well-known error source for RTK surveying.

Chapter 8 on page 51 will answer research question 1 based on the testings in chapter 6 and 7.

3.1.1 Precision and accuracy

The current section defines and describes the term "precision", which is used as a key term in research question 1; *What is the vertical precision of SRTK?*. The section will also describe how the precision is being quantified and measured, to test the obtainable precision.

Figure 3.3 describes how systematic errors (trueness) and random errors (precision) affects the total error (accuracy).

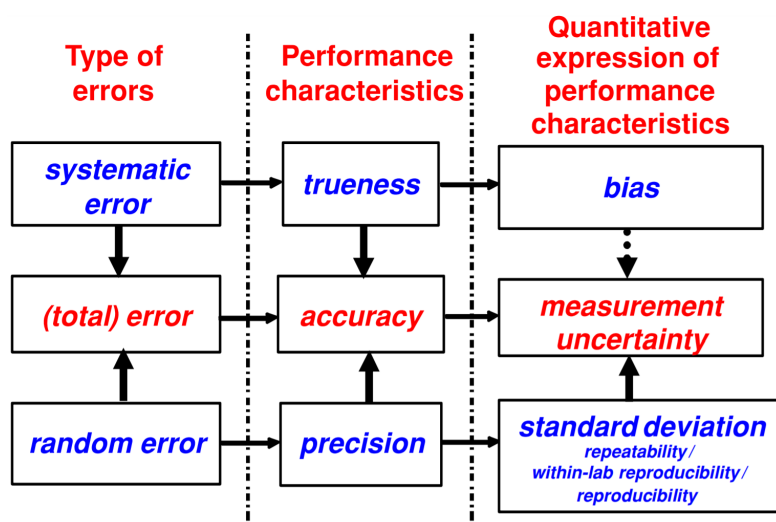


Figure 3.3: Relationships between type of error, qualitative performance characteristics and their quantitative expression. [Menditto et al., 2007]

It is seen that the error contribution in the third row, which describes the qualitative performance characteristic "precision", is only derived from "random errors". It is necessary to identify the random errors and systematic errors, as to isolate the random errors when maintaining the same level of systematic error in every observation. According to the figure, precision is quantitatively expressed by the standard deviation to describe repeatability. The way of quantifying precision, by standard deviations, will be done by examining the collected data sets. The data sets will be examined with equation 3.1:

$$\sigma = \sqrt{\frac{\sum |x - \bar{x}|^2}{n - 1}} \quad (3.1)$$

Where:

σ = the standard deviation of the sample

x = the unique observation in the sample

\bar{x} = the mean of all of the unique observations in the sample

n = the number of unique observations in the sample

Equation 3.1 presumes that the sample is without outliers. When examining standard distributed data sets, the empirical rule ($1\sigma = 68\%$, $2\sigma = 95\%$ and $3\sigma = 99,7\%$) can be used. The level of standard distribution in the data sets will be examined.

The equation computes a quantitative measure for the closeness of the sample.

The method for examining precision is applied in a practical test design, which is described in chapter 5 on page 23.

3.1.2 Equipment

The initial idea of using SRTK in interaction with the DRP will be based on equipment, which usually would be available to surveyors. To examine SRTK as a potential method of determining orthometric height, it is considered essential to use ordinary GNSS survey equipment.

Requirements and the specific choice of equipment will be described in chapter 5 about the test design.

3.2 Part II

This part of the thesis is aiming to answer the research question; *What is the vertical accuracy of SRTK in interaction with the DRP?*. The current section is describing the used method for answering the research question.

According to figure 3.3 on the previous page the accuracy is the product of the precision of the observations, and their trueness. Quantitatively the precision is examined by computing standard deviations in relation to the repeatability. The quantitative expression of the trueness is expressed as a bias. As to determine the bias between the observations and the "true" orthometric height, the mean value of the observations needs to be calculated. The bias will be the difference between the mean observation and the true orthometric height. Equation 3.2 describes the bias quantification.

$$\varepsilon = \bar{x} - x_{true} \tag{3.2}$$

Where:

ε = the bias

\bar{x} = the mean of all of the unique observations in the sample

x_{true} = the true value

To visualize the bias of orthometric heights figure 3.4 can be used.

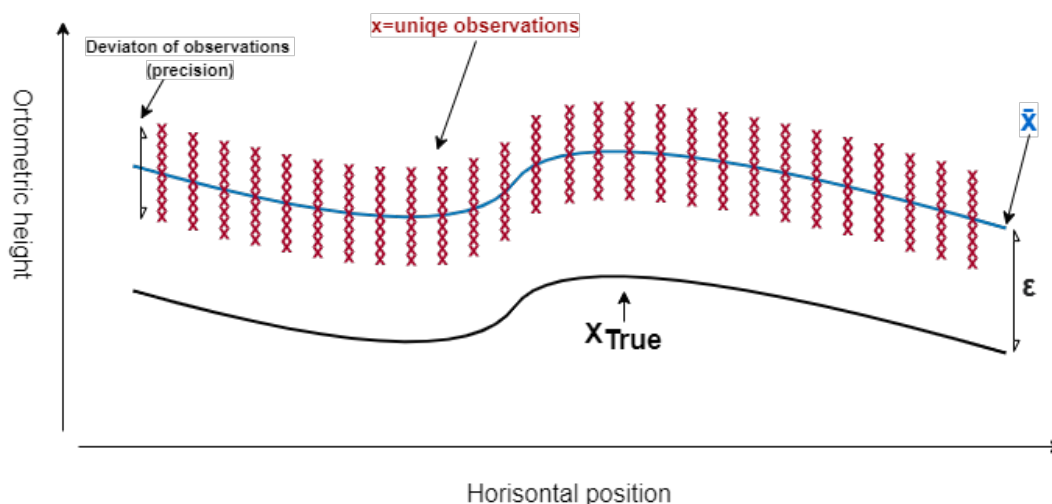


Figure 3.4: Trueness and bias of observations, in relation to the true value, in a context of orthometric heights

The figure shows that the mean observation can be offset by a constant value, ε , which systematically translates every observation away from the true value. The uncertainty of the \bar{x} and the x_{true} is affecting the precision of the quantified bias, ε , why it is necessary to obtain a decent degree of certainty of the two elements.

Flowchart for Part II

Figure 3.5 visualizes the flowchart for part II.

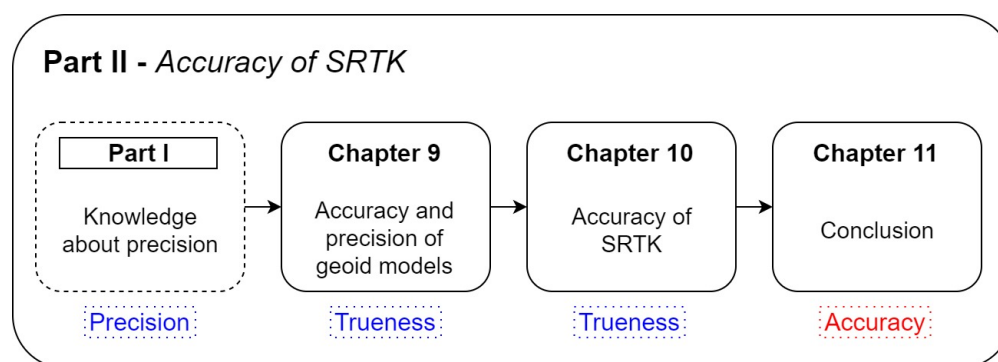


Figure 3.5: Flowchart of part II

It is necessary to identify the factors affecting the accuracy and assess the magnitude of the error. According to figure 3.3 on page 11 and section 3.2 on the preceding page the accuracy is affected by both the precision and the trueness. The flowchart expresses how the conclusions from part I, will function as the knowledge about SRTK's precision, while chapter 10 and 11 will assess the trueness. The geoid model is an essential factor when deriving orthometric heights from GNSS, and the accuracy or trueness of this model is assessed in chapter 10. For this analysis, two versions of the DVR90 geoid model are compared to both ellipsoidal heights and levelled orthometric heights. In chapter 11

the accuracy is calculated empirical, with observations collected in part I, examined in relation to "true values" derived from levelling surveys.

3.3 Part III

This part of the thesis is aiming to answer the research question; *How is SRTK in interaction with the DRP applicable, and what is the potential?*. The current section is describing the used method for answering the research question.

The keywords of the research question is *applicability* and *potential*. These words are interpreted as follows:

Synonyms of *applicability* can be *relevant*, *suitable*, *appropriate* etc.. The applicability of SRTK and DRP's will be assessed by the performance of the technology, in comparison to other comparable technologies, without a particular survey task in mind. The key parameters of the performance comparison are time/cost usage in relation to obtainable precision/accuracy.

The flowchart of part III is seen in figure 3.6.

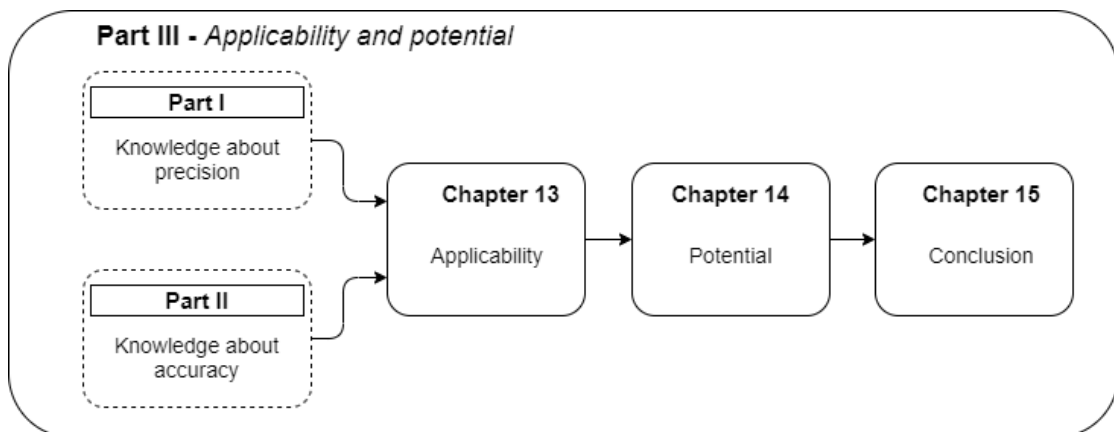


Figure 3.6: Flowchart for part III

It is seen that the assessed applicability is highly dependent on the conclusions and knowledge derived from part I (precision) and part II (accuracy). The time/cost usage has not been examined earlier. Own experiences of working with SRTK are the basis of comparison on this parameter.

The other keyword, *potential*, is interpreted as a more broad and futuristic word than applicability. The potential of SRTK and DRP's will be discussed with specific survey tasks in mind, where the technology seems to have a force. Own experiences and statements from acknowledged specialists will be used, to arrive at a conclusion on the future potentials of the technology.

3.4 Part IV

The objective of part IV is to present the conclusion, discussion, and perspectives of the entire thesis and the problem statement; *What are the capabilities of single-baseline RTK in interaction with the “dynamic reference point”?*. All three previous parts serve as inputs for the three chapters in part IV.

The flowchart of part IV is seen in figure 3.7

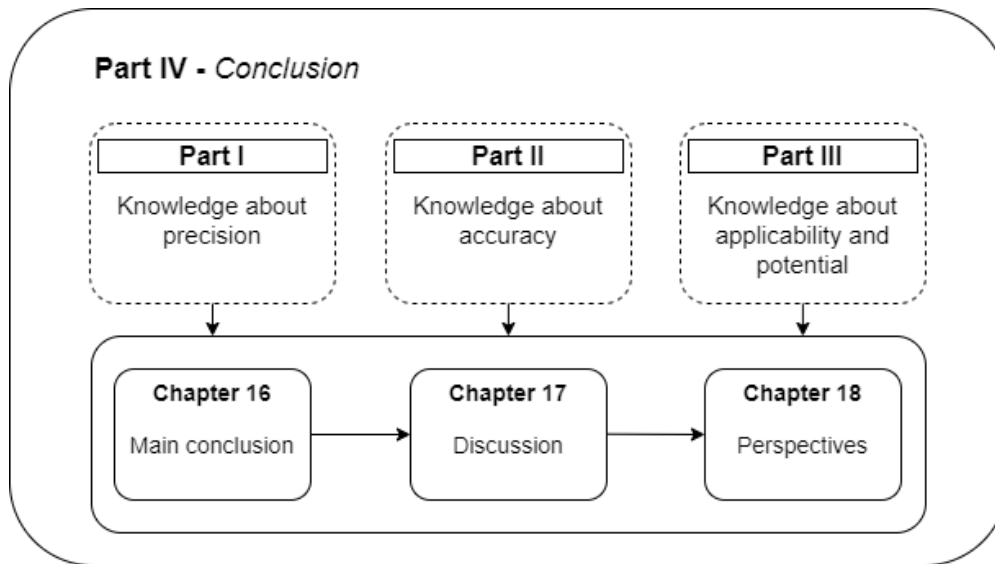


Figure 3.7: Flowchart for part IV.

The *Discussion* serves as relevant arguments and doubts about the used method and approach for answering the problem statement. The objective of the chapter, *Perspectives*, is to put the thesis conclusion into a broader perspective and suggest relevant further studies which could further validate the conclusions.

Part I

Precision of SRTK

Relative GNSS positioning 4

The current part is answering research question 1; "*What is the vertical precision of SRTK?*".

To examine the precision of SRTK it is essential to know which variables are affecting the precision and to identify possible error sources. This chapter will present primary knowledge about RTK surveying, and be the basis of determining test variables. General understanding of how relative GNSS positioning works and error sources are considered essential to set up a suitable test design in chapter 5 on page 23.

4.1 Relative positioning

The fundamental way of positioning by GNSS is with absolute positions, where only one receiver computes an absolute position. The position is calculated by observing distances to several satellites with known positions. The current section is to some extent based on the foundation of absolute positioning, described in appendix C on page 111

For improved accuracy, carrier phase measurement is used, and modern surveying receivers also multi-frequent signal, but the fundamental difference of survey equipment compared to standalone GNSS receivers is relative positioning.

Relative positioning involves two GNSS receivers, where one of them, referred to as the base, is placed in a known position. The method aims to determine the unknown position of the other receiver called the rover. The position of the rover is determined relative to the base receiver, which allows high accuracy positioning at a level of a few centimetres. The basic concept of relative positioning is that the two receivers at the same time are observing the same constellation of satellites, which means the receivers also are affected by similar errors. Having the base receiver placed in a known position allows the opportunity to calculate the error and generate a correction that can be transmitted to the rover. As shown in figure 4.1 the vector between the base and the rover is called the baseline. Calculating corrections at the base station and using them at the rover is possible because the baseline is short compared to the distances to the satellites at about 20,000 km altitudes. [PennState, 2021a]

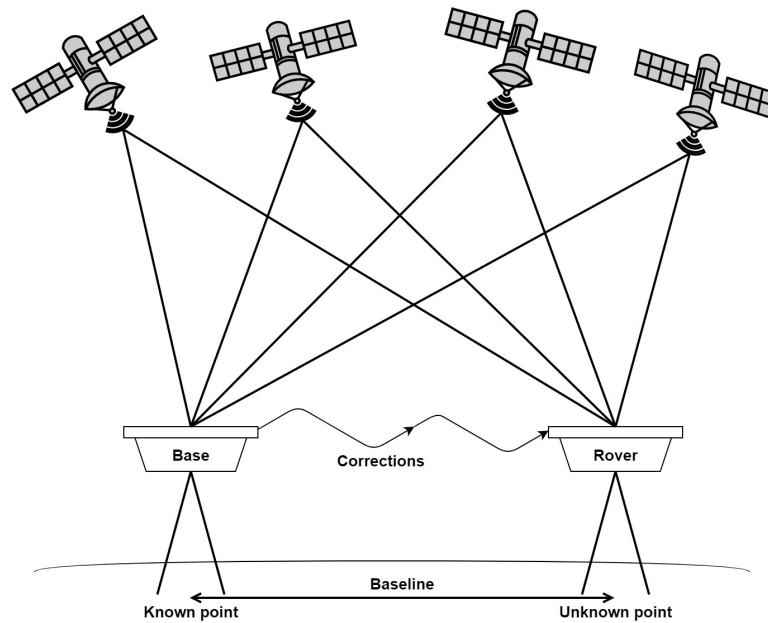


Figure 4.1: Principle for relative GNSS positioning

Different implementations of relative GNSS positioning can be used, where SRTK and NRTK is the main type of methods.

4.2 Error sources

The error sources of GNSS positioning in general can be listed as following:

- Orbital error
- Satellite Clock Error
- Ionospheric Error
- Tropospheric Error
- Multipath
- Receiver Noise
- *Impact of Geometry*

[Olynik et al., 2002] [Trimble Inc., 2021]

When performing relative positioning the errors does decrease significantly. In the following the error characteristics are listed, when measuring relatively from a known point (base station).

Orbital error and Satellite Clock Error

Errors will be eliminated when performing relative positioning

Ionospheric Error, Tropospheric Error

Errors will be reduced when using relative positioning. As baseline grows, the error grows, due to different atmospheric paths of satellite signals. Multifrequency receivers reduce atmospheric errors. Errors are also being modelled, to some extent.

Multipath

Errors can not be reduced by using relative positioning. Some receivers can be more multipath resistant than others. Increasing cut off angle reduces multipath error. Multifrequency receivers reduce multipath error.

Receiver noise

The error can not be reduced by using relative positioning. Receiver noise is correlated with receiver quality and price.

Impact of geometry

Geometry does not behave like the other error sources. The geometry of satellites in a specific point of interest is always an issue. The geometry can be improved by using more satellites, ie. more satellite programmes and reducing cut off-angle.

[Olynik et al., 2002] [Trimble Inc., 2021]

All of the above errors is in theory normally distributed, and should therefore be reduceable, by making several observations. A position can be calculated in a fraction of a second, with modern hardware and software. Though several positions are often collected, to calculate a more precise mean value.

4.3 Available GNSS programmes

As discussed in the above a minimum of 4 satellites is required to compute a position. Expanding the number of observations makes an overdetermined system. As another benefit, the geometry of the satellites is more likely to be beneficial, when using more satellites.

The number of GNSS satellite programmes available has been increasing in recent years, so has the number of healthy satellites within each programme. Galileo and BeiDou have particularly increased the number of satellites. In the following list the available programmes are stated (regional programmes are not stated).

- GPS (32)
- GLONASS (22)
- Galileo (20)
- BeiDou (49 (not all in a global orbit))

List of available GNSS satellite programmes. Number of healthy satellites (by the 09-02-2021) in parentheses. [Trimble, 2021]

It should be noted that the different satellites emit different positioning signals, and uses different clocks.

Modern GNSS-receivers can receive signals from all 4 programmes [Leica Geosystems, 2021a]. In Denmark the two most used RTK-services are also able to deliver corrections relating to all 4 systems [Leica Geosystems, 2021b] [GeoTeam A/S, 2021].

The 3 figures shown in appendix D on page 114 shows the number of available satellites, elevations and DOP-values during a random day in Central Jutland. The figures visualize the view of satellites in perfect conditions, trees, buildings etc. can block the sky.

In figure D.1 it is seen that the number of available satellites varies between approximately 30 and 40 when using a cut off angle of 10 °.

4.3.1 Potential benefit from new satellite programmes

In Denmark, GLONASS is commonly used and compliments GPS for RTK surveying. Through the work on this project, for example, communication with Leica Denmark, it is the impression that the newer programmes are used to a limited extend. Galileo is generally included in newer equipment, while it is not common for 3-4-year-old equipment. The usage of Beidou is far more exceptionally, and not a significant part of RTK surveys in Denmark. It is assumed that the usage of Galileo will continue to increase, as well as Beidou will be implemented in years to come.

Swedish research from 2009 concludes through simulation of network RTK, that the future satellite systems Galileo and Beidou has the potential of reducing the vertical error from 27 mm to 20 mm [Emardson et al., 2010]. This would be a potential error reduction of about 25 %. In the Danish master thesis from 2019 the effect of Galileo is tested and found to be insignificant in an open rural environment, but with a noticeable effect in an open urban environment [Skoffer and Larsen, 2019]. The magnitude of the effect on the vertical component is about 10 %, but compared to the Swedish research it is noticeable that Galileo was not fully operational in 2019 and the testing did not include Beidou. In Swiss testing from 2017 the Galileo programme is found to have a significant positive effect regarding multipath and reliability [Luo et al., 2017].

Overall, it is assessed that including Galileo and Beidou should offer a more robust GNSS positioning, and have an effect on the precision in a difficult environment. The exact effect on GNSS positioning in suitable conditions is more questionable. Since both Galileo and Beidou only recently became fully operational the amount of research is also limited. The effect will also differ by the location of the testing, which combined with not fully operational programmes can reduce the reliability of both foreign and earlier research.

Test design 5

Chapter 4 on page 19 presents the error sources affecting the precision of relative RTK positioning. This chapter describes which sources is picked for further testing.

According to the idea of DRP's and using them for reference points for SRTK, it is perceived as important to test different baseline lengths effect on the precision. To be able to vary the baseline length, and isolate only this parameter, it is necessary to maintain all other parameters. The parameters are listed in the following:

- Satellite constellation and frequencies used
- Hardware, ie. receivers
- Cut off angle
- Time averaging window

To exploit the potential of the available satellite constellations and frequencies, it is decided to use the latest generation of survey equipment. Using Leica GS16 and Leica GS18 multi-frequency receivers with all global satellite programmes available should in theory result in better precision than lower-end hardware with fewer satellites.

The cut off angle is to some extent a trade-off between multipath resistance and additional satellites which increases precision [Maciuk, 2018]. A cut off angle of 10 degrees is chosen to be suitable, with the test environment in mind, which do not include major building or dense urban areas.

A suitable time-averaging window can be difficult to determine. Higher time averaging windows requires more labour, but will in theory increase precision. As to have an empirical basis for deciding an appropriate time-averaging window, it is decided to test different time averaging windows. After the test the quantified precision derived empirically, will become the basis of determining a proper time-averaging window to use, when testing different baseline lengths.

5.1 Possible unintentional error sources of testing

For the project it is decided to perform two separate tests; a test of how the averaging time window affects precision, and a test of how different baseline distances affects precision. The tests aim to isolate the two factors, why other error sources need to be taken into consideration. According to the theoretic background discussed and presented in section 4.2 on page 20, the error sources which needs to be considered when testing averaging time window and baseline distances are listed in table 5.1.

Sources of Gaussian errors in SRTK GNSS	Can be reduced by
Satellite constellation (excl. cut off angle)	Using all available satellite programs, at multiple frequencies
Cut off angle decreases number of observable satellites	Choosing an appropriate cut off angle, as to avoid multipath
Hardware and software capabilities of GNSS receivers	Choosing modern and high end geodesian receivers
Centering of antenna at survey point	Using tripod or threaded reference point
Wrong offset of antenna relatively to survey point	Using tripod or threaded reference point
Outliers affecting computed position	Increasing averaging time window <i>Errors examined in tests</i>
Difference in ionospheric and tropospheric conditions due to different location of base station and rover	Shortening baseline distance <i>Errors examined in tests</i>

Table 5.1: Selected Gaussian error sources in relation to SRTK GNSS, and how they are reduced when testing

The errors according to satellite constellation (geometry) and atmospheric distortions are varying due to different activity of the sun and to the unevenness of the satellites orbits. The errors can be presumed as Gaussian errors when observations are collected at different cycle stages of the sidereal time and with days and weeks in between, as to change the conditions of the atmosphere and geometry of satellites. This will be done, to reflect realistic and average conditions.

The Gaussian errors are reduced by using threaded reference points when possible and using all available satellite programs with a high-end multi-frequency receiver. The error sources which the project aims to investigate ie. *Averaging time window* and *baseline distance* are varied throughout the two tests. Though they are only varied one by one, as to isolate the effect to a large extent. In the following, the aims and designs of the two tests are described and discussed.

5.2 Averaging time window test

The test is set to determine the influence of the averaging time window of SRTK measuring, to establish a basis of determining an appropriate time-averaging window for testing different baseline lengths and provide knowledge about how this parameter affects the precision. It is decided to focus the test on seven different averaging time settings, which are:

- 5 seconds
- 15 seconds
- 30 seconds
- 1 minute (60 seconds)
- 2 minutes (120 seconds)
- 4 minutes (240 seconds)
- 10 minutes (600 seconds)

The averaging time window can be changed in the settings on the controller of the receiver.

The general assumption is that longer averaging time windows will result in higher precision, but also increase the workload and be disadvantageous for the method. This test

aims to decide an appropriate compromise between precision and the practical performance of the method. The decided compromise will be used in the baseline distance test.

The different averaging time window intervals are chosen to enable the possibility to describe the dependencies between averaging time window and precision, by a curve. Studies of SRTK with baseline distances of 15 km show that the maximum outlier, and presumably the standard deviation, decreases drastically (up to 400%) when going from 0 to 60 seconds of the time-averaging window. The effect of increasing the averaging time window flattens between 1 minute and 10 minutes. [Janssen et al., 2012]. Presumably, the precision should increase close to infinite, if an infinite averaging time window is used. Though averaging time windows longer than 10 minutes are assumed to benefit more from different satellite constellations, than from the averaging time window itself. No studies describe benefits from increased averaging time windows with short baseline distances (0-2.5 km.). To isolate the influence of the averaging time window the same baseline distance will be used in this test. It is decided the baseline distance should be about 1 kilometre, which will be a representative distance for the following baseline distance test.

The momentary satellite constellation will have an important effect on the achievable precision, wherefore it is decided to build up a test data set where every sample of the same averaging time window has a different satellite constellation. The satellite constellation can be considered as different after 10-30 minutes [Janssen et al., 2012].

The atmospheric conditions of the current day or longer period can also be influential on the achieved precision. The optimal option would be data collected at several days over a period of months. For this project, it is decided to have at least five different days of data collection throughout a minimum of one month.

5.3 Baseline distance test

As mentioned earlier, increasing the distance between base and rover when using SRTK, will theoretically lower the precision. This test is set up to determine the influence of the error depending on the baseline length or distance between base and rover, and the precision to be expected from various baseline lengths.

As mentioned in chapter 1.1 on page 3, Geopartner considers a 5 km network of DRPs to be a realistic possibility in Denmark, which will result in a maximum baseline length of about 2.5 km. To have a thorough investigation of the distance-dependent error and consider the opportunity of a lower density DRP network it is decided to focus on baseline lengths up to about 5 km. Even longer baseline length can be tested to investigate the propagation of the error.

It is decided that the testing should include 5-7 different baseline distances between 0 and 5 km. The chosen baselines should be representative for the interval of 0-5 km, but the exact distances will be decided with consideration of the physical conditions of the test area. This includes considerations of establishing stable test points and avoiding the

surrounding environment to affect the GNSS survey.

The averaging time window of this test will be based on and decided by the averaging time window test.

Quality control of the survey pole for correct offset is considered an important factor for this test.

5.4 Disclaimer for not performing SRTK with own base station

This project aims to test SRTK for height determination in interaction with the DRP. To use this method in practice a base and rover setup of two geodetic GNSS receivers are required. The aim for the testing was to use high end, but also regular GNSS receivers available to surveyors, to set up a realistic scenario. This assessment has proven more difficult than anticipated, as there have been significant problems related to base and rover communication.

During test preparations and the initial tests, the attempts of sending and receiving RTK correction has been unsuccessful when using Leica GS16 or GS18 with the software Capivate. These two models were chosen because they are multi frequent, and the specific hardware available to the project group also compatible with Galileo and Beidou. The attempts to set up this solution have involved several days of trial, information retrieval and repeated contact with Leica Support, but in the end not successful in time for the data collection of the project.

The project group has to some extent been successful in setting up base and rover communication using Leicas older model GS14 with the software Viva. This model is only dual frequent and the available hardware only compatible with GPS and GLONASS, which therefore is not the preferred test setup. Furthermore, the communication of these receivers has for reasons unknown proved to be unreliable throughout the initial tests. This has led to several hours of fieldwork affected by communication breakdown with no possibility of collecting data.

These technical issues have forced the project group to search for an alternative solution to test the precision of SRTK. Therefore, it has been chosen to carry out the testing at TAPAS (Testbed in Aarhus for Precision positioning and Autonomous Systems). This test facility offers a high-density network of GNSS reference stations with the opportunity of receiving corrections from one chosen station. Using TAPAS with Leica GS16 and GS18 makes the initial idea of multi frequent receivers using all global satellite systems possible. It is assumed that TAPAS will offer an ideal condition to set up tests of how the baseline length and the averaging time windows affect the precision. Despite the possibility of receiving corrections from a single reference station, this test setup will not offer the same realistic conditions as using your own GNSS receiver as a base station.

5.5 Approach for data examination

The test design is tightly connected to the approach for data examination. The approach for data examination is separated into two steps. The initial data examination and the combined data examination. The initial data examination secures that the grouped observations do not contain outliers and that the sample is normally distributed. The combined data examination combines the different grouped samples to be able to examine the tendencies.

5.5.1 Initial data examination (grouped observations)

The output of the test design and the data collection are several observations. The test design strives for producing normally distributed data sets without outliers. To be able to verify the test design and prepare the data for further examinations, the collected data sets need to be tested. Figure 5.1 visualizes the approach for the initial data examination.

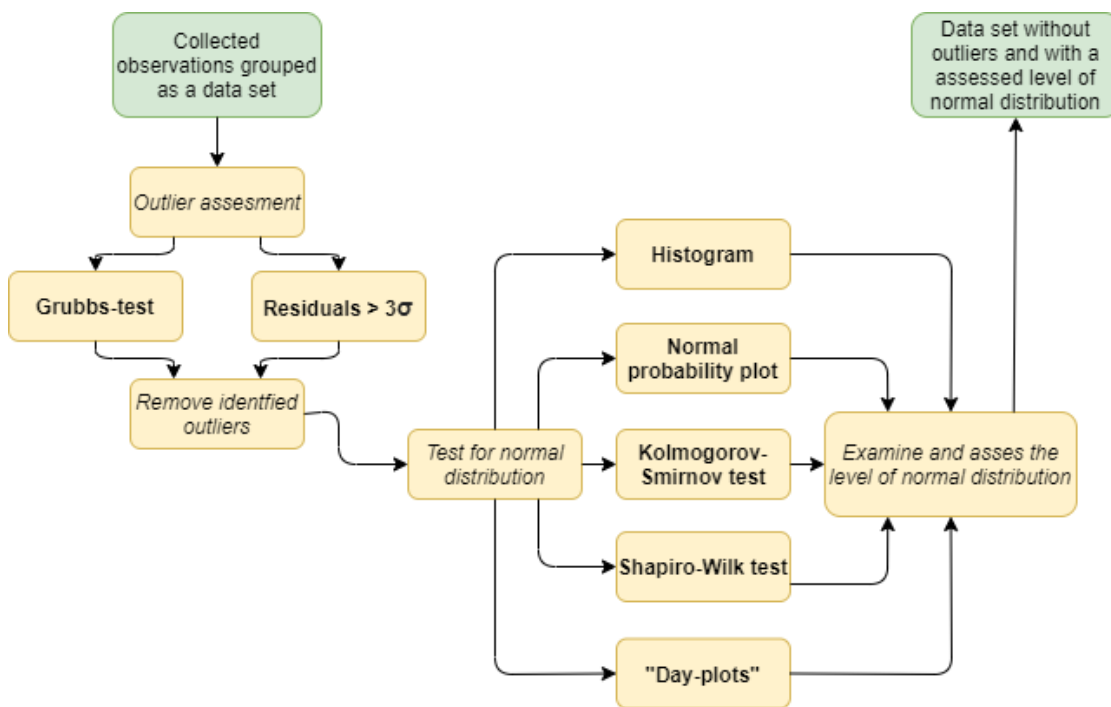


Figure 5.1: Approach for initial data examination. Green boxes symbolizes input and output. Yellow boxes symbolizes tasks and ways to achieve the output. Bold font symbolizes statistical analytical tools.

The approach is used on grouped data sets collected at the same point, with the same hardware and with the same averaging time window. The approach strives to examine both potential outliers and the level of standard distribution in the data set. Both parameters are dependent on each other. It is therefore assumed that the data set is normally distributed, to be able to remove outliers not fitting in the normal distribution. After the outliers are removed, the level of normal distribution is assessed.

According to section 3.1.1 on page 11 the examination of the term precision is quantified

by computing standard deviations, by using deviations from the mean value. However, the mean-value can be sensitive to outliers, especially when using few observations. It is necessary to detect outliers and remove them from the dataset before examining the deviations from the mean value.

Different approaches can be used for detecting outliers. In this examination, the way of detecting outliers is done partly by the "3 sigma rule", where normalized residuals exceeding 3σ are considered as outliers and removed. Pros and cons can be considered when using this method, and it should be mentioned that the outlier(s) itself affects the mean-value, and therefore also the computed residuals. As the collected data are not expected to be affected by a large number of outliers, hence the threaded mount of the rover and the non-multipathing environment, the "3 sigma rule" is perceived as a suitable method for detecting outliers. The second method is a Grubbs-test, which can be used to find one single outlier in a sample [Grubbs, 1969]. Both methods assume normally distributed data sets, which the test design should ensure.

After removing potential outliers, the data set will be tested and examined for the level of normal distribution. The five test methods assume no outliers, to perform well. If the data set is not examined as normally distributed, the test design could be rethought and more data collection done. The five methods of evaluating normal distribution are used as following; Not all five methods need to be agreeing, it is accepted that some of the five methods suggest a not normally distributed data set if the other suggests the opposite. The tests for normal distribution is broadly a subjective overall assessment.

In the following the two hypothesis testing methods, and the three visual methods are described.

The two hypothesis testing methods; *Kolmogorov-Smirnov test* and *Shapiro-Wilk test* both have the same H_0 , that the data set is normally distributed at a confidence interval of 95%. The two tests supplements each other as the Kolmogorov-Smirnov test is supposed to find and quantify the largest vertical difference between the hypothesized and empirical distribution of samples. The Shapiro-Wilk test is also testing the skewness and kurtosis of the data set.[Mohd Razali and Yap, 2011] The statistical visual methods; *Histogram* and *Normal Propability Plot* are more simple to use, but still acknowledged, though they are more exposed to subjective prerequisites and biases of the analyzer. At last, a "Day-plot" is used. The day-plot is separating the data set into different days of collection. The plot will visualize if there are significant differences between observations with different origin according to atmospheric conditions. To be assessed as normal distributed, the day-plot should look random, and no systematic should occur.

The complete approach will be used in both the time averaging window test and the baseline distance test, as a way of initially verifying the collected data sets. If the level of normal distribution in a dataset is assessed as "low", this will be kept in mind when performing the "combined data examination" and examining the results.

5.5.2 Combined data examination (several grouped observations)

When combining and comparing data with different origin, ie. averaging time window or baseline length, figure 5.2 is used as the examination approach.

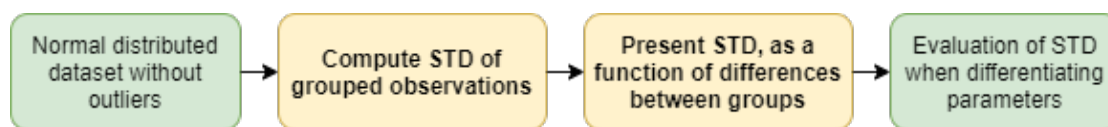


Figure 5.2: Approach for combined data examination. Green boxes symbolizes input. Yellow boxes symbolizes tasks and ways to achieve the output.

It is seen that the first step is to compute the standard deviation of the single grouped data set. The different standard deviations with different origin can afterwards be presented as a function for the difference between the origin. The output will be an evaluation of the presented data.

Test of averaging time window 6

The test of the averaging time window is supposed to add an empirical basis for choosing an appropriate averaging time window setting. Chapter 5.2 on page 24 describes the initial prerequisites of the test design. The following describes how the data collection has been performed in practice, and what considerations the collection has been affected by.

6.1 Data collection

Due to lack of success with RTK-transmission, as presented in section 5.4 on page 26, the data collection for the averaging time test has been fragmented. The collection has been done with two different sets of equipment and in two different locations. The baseline has though been held at approximately the same distance, 750 m.

The data collections have been performed at different days to vary the atmospheric conditions. Every day several "series" have been performed. Every series consist of the following different settings:

- 5 seconds
- 15 seconds
- 30 seconds
- 1 minute (60 seconds)
- 2 minutes (120 seconds)
- 4 minutes (240 seconds)
- 10 minutes (600 seconds)

After every series a minor break was held, which results in a minimum of 25 minutes between the start of every series.

In table 6.1 the different days of observations are listed.

Run no.	Day	Location	No. of series	Base antenna	Rover antenna	Satellite sytems
1	27-02-2021	Aalestrup	7 (one removed)	Leica GS 14	Leica GS14	GPS+GLO
2	07-03-2021	Aalestrup	4	Leica GS 14	Leica GS 14	GPS+GLO
3	16-03-2021	Aalestrup	7	Leica GS 14	Leica GS 14	GPS+GLO
4	13-04-2021	Sabro	5	TAPAS TA11	Leica GS 16	GPS+GLO+GAL+BEI
5	21-04-2021	Sabro	8	TAPAS TA11	Leica GS 16	GPS+GLO+GAL+BEI
6	27-04-2021	Sabro	3	TAPAS TA11	Leica GS 18	GPS+GLO+GAL+BEI
7	03-05-2021	Sabro	3	TAPAS TA11	Leica GS 18	GPS+GLO+GAL+BEI

Table 6.1: Days and prerequisites of data collection

As seen in the table, the data collection has been performed with different antennas, and with different satellite systems. The use of different antennas had to be accepted, due

to practical reasons. For a number of these testings, multi frequent receivers compatible with Galileo and Beidou have not been used, as the equipment was not available. The different antennas have been the only way to achieve several days of data collection, which is assessed to be a more important parameter for the test.

In the following, the characteristics and choices of the data collection in the two locations will be discussed.

6.1.1 Data collection in Aalestrup with Leica GS14

All observations have been collected with a baseline of 775 meters, at figure 6.1 the baseline of the test is visualized.



Figure 6.1: Baseline of test set up in Aalestrup

With the base mounted in radar reflector no. 5 and with the rover mounted in radar reflector no. 6. The threaded mounts on the DRP's entail the absence of centring errors. In figure 6.2 the DRP is seen, with the rover antenna mounted.



Figure 6.2: Rover mounted on DRP no. 6. Viewed from north to south

It is seen that not a completely clear view is obtained by the rover. Some satellite signals may be left out, due to blocked paths.

6.1.2 Data collection in Sabro with Leica GS16/GS18 and corrections from single baseline TAPAS

In Sabro the test setup is relying on the corrections derived from the TAPAS network. A single base station has been located, and the baseline is sought to obtain a distance in the magnitude of 775 m. as used in Aalestrup. The baseline is seen in figure 6.3. And the environment at the rover position is seen in figure 6.4

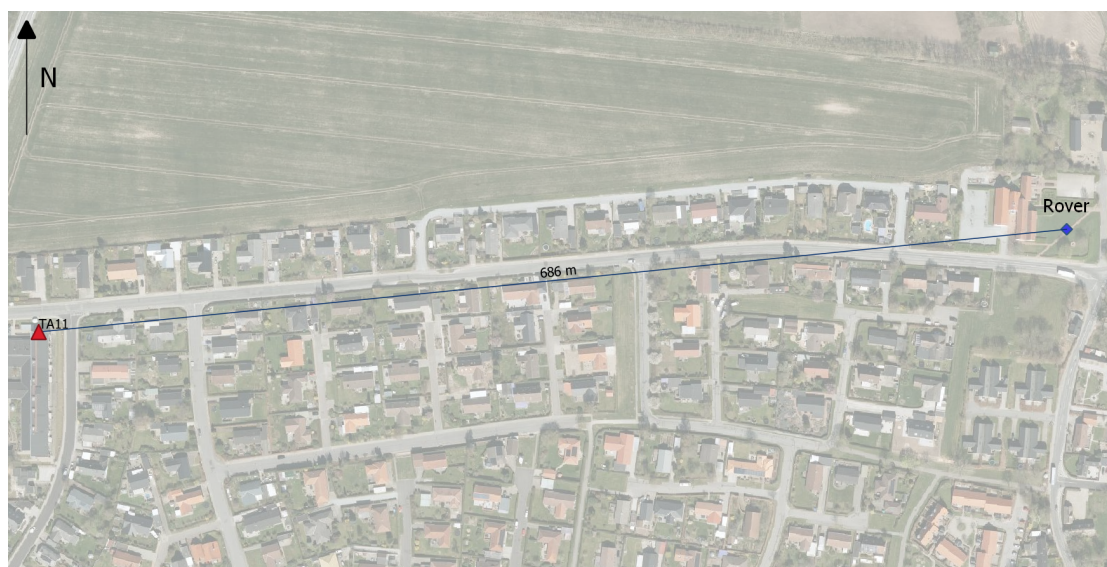


Figure 6.3: Baseline of test set up in Sabro



Figure 6.4: Rover mounted in Sabro. Viewed from north to south.

6.2 Data examination

The data examination is separated into two steps. An individual data examination where the collected data is separated into groups, outliers are detected and the normal distribution within each group is assessed. The second step is combining the groups of data, to conclude tendencies of behaviour when varying the time averaging window.

6.2.1 Individual data examination

The data have been grouped into groups related to the used averaging time window. Furthermore, the groups have been separated into groups of data collected in Aalestrup and data collected in Sabro. A total of $2 * 7 = 14$ groups.

The 14 groups have been examined individually according to the approach for data examination of the individual groups, as presented in section 5.5.1 on page 27. A complete data series, the 7th of the first day in Aalestrup have been removed due to strange and high DCQ-values. Outliers besides the removed series have not been detected. The 14 data sets have been examined as being normally distributed. The test statistics used are though limited due to the small sample size. No major differences in mean values and precision are seen when isolating observations in days of collection. The histograms, normal probability plots, and "day-plots" of the 14 data sets are seen in appendix E on page 117.

6.2.2 Combined data examination

The combined data examination is aiming to compare the different data groups, i.e. data averaging windows, to identify tendencies. When looking at the raw grouped data, seen at figure 6.5 no clear tendencies is seen. The mean value used to calculate the deviations from the mean is a combined mean for all groups of observation. Calculating a separate mean for the different time windows only deviates from the combined mean by a maxi-

mum of 1 mm. So, the mean of even the shortest time windows results in approximately the same as the longest time window.

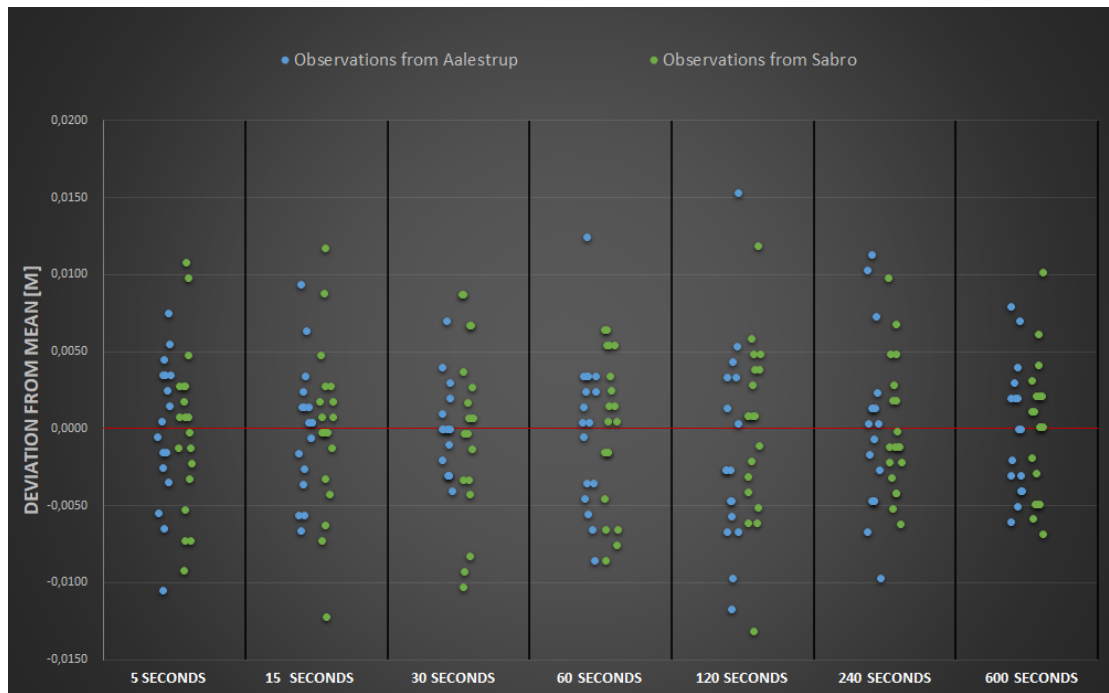


Figure 6.5: Height observations from both Aalestrup and Sabro, grouped in associated time averaging windows

Table 6.2 shows the calculated standard deviations of the different time averaging windows.

Averaging time[s]	σ_H Aalestrup [mm]	σ_H Sabro [mm]	σ_H combined [mm]
5	4.7	5.3	5.0
15	4.2	5.4	4.8
30	2.9	5.6	4.3
60	5.1	4.9	5.0
120	6.6	5.6	6.1
240	5.7	4.3	5.0
600	4.2	4.4	4.3

Table 6.2: Standard deviations of observations from Aalestrup, Sabro and both combined (the non weighted mean value of the two)

On figure 6.6 and 6.7 the computed standard deviations with the belonging 95 % confidence interval are plotted.

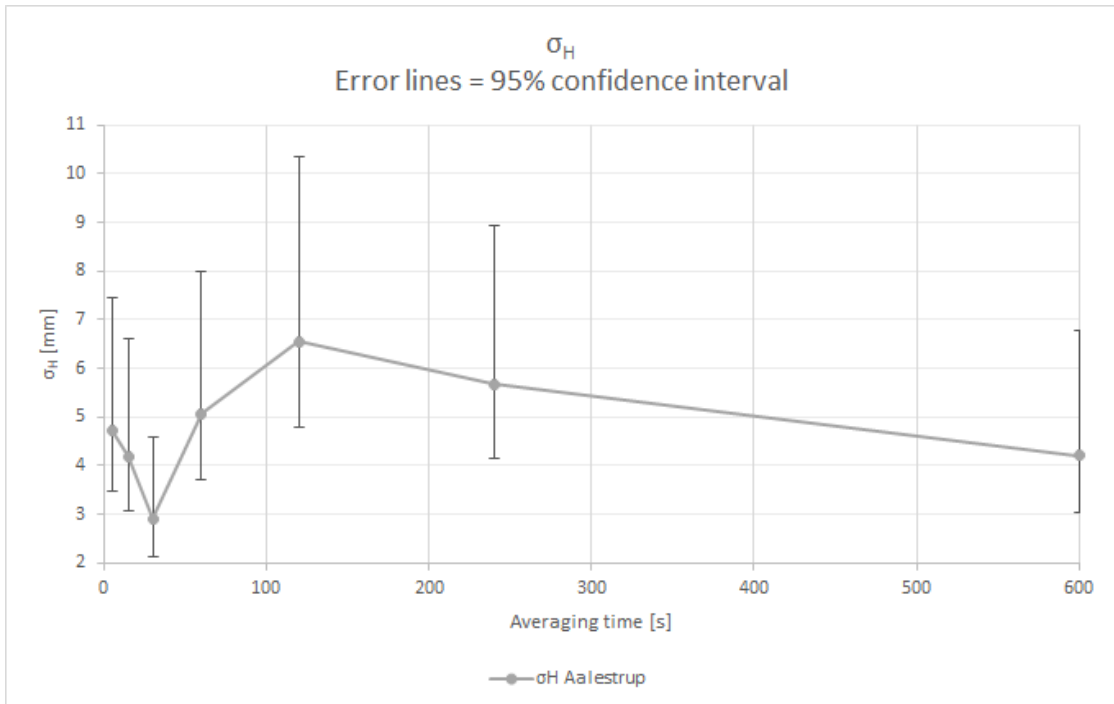


Figure 6.6: σ_H with different time averaging windows. Observations from Aalestrup. Error lines representing 95% confidence.

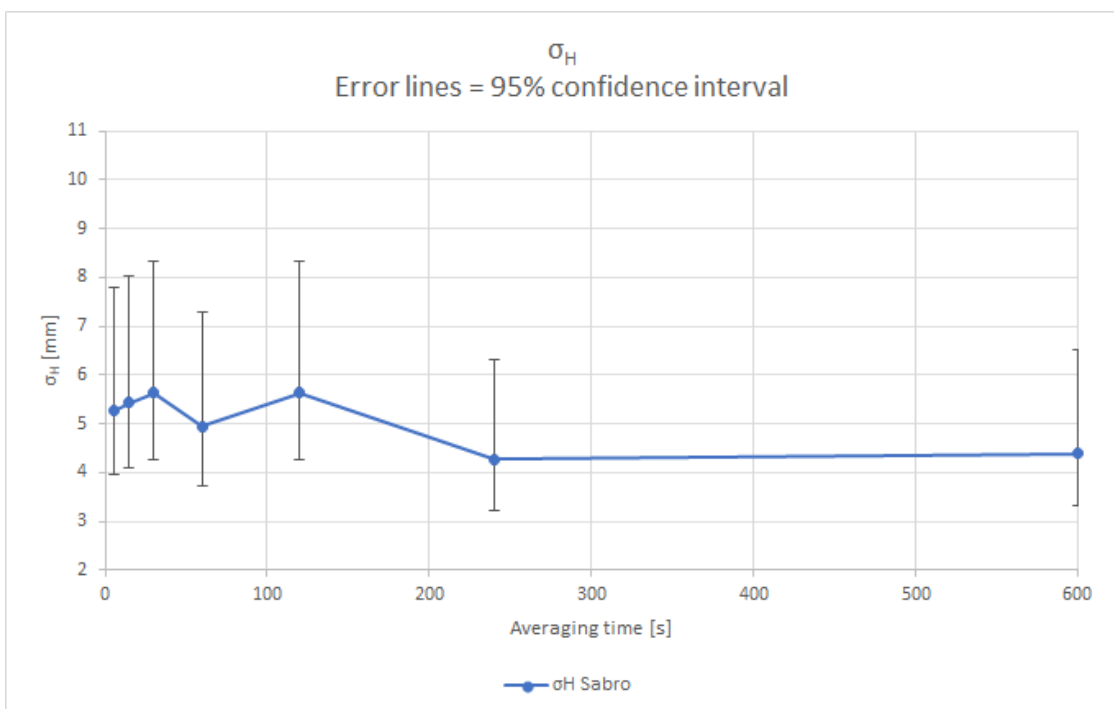


Figure 6.7: σ_H with different time averaging windows. Observations from Sabro. Error lines representing 95% confidence.

When looking at the tendencies on the data collected in Aalestrup it looks like the short averaging time windows perform slightly better than the longer. When looking at the

data from Sabro, it looks like all averaging time windows perform at the same level. F-tests could have been implemented in the assessment, to verify the stated tendencies, and compare the standard deviations quantitatively.

6.3 Conclusion

The time test does show interesting results. No clear conclusion can be stated, on which time-averaging window is most precise. More testing should be done, to narrow down the confidence intervals on the stated precisions.

The choice of selecting an appropriate time-averaging window is to a larger extent a compromise between performance (precision) and labour consumption. The results presented in this chapter do not show performance gains when using long averaging time windows, why a relatively short averaging time window should be used at least for short baselines.

The results are based on a relatively short baseline, approximately 700 meters. It can be assumed that longer baselines would have shown other results, where the longer time averaging windows performs better compared to the short.

For further testing in the project, averaging times of 60 seconds are assessed to be suitable. It could be argued that even shorter time averaging windows seem to result in about the same precision. However, it is assessed that result of this test holds some uncertainty, and to secure comprehensive further examination 60 seconds is chosen. This decision is also based on research, which indicates the effect of a long time averaging window flattens after about 60 seconds.

Baseline distance test

7

This chapter will present the data collection and data examination for the baseline distance test. This test is an important component for the whole project of testing the precision of SRTK with relatively short baselines. The baseline distance test will be based on the prerequisite stated in section 5.3 on page 25.

7.1 Data collection

As mentioned in the test design (section 5.4 on page 26), it has been chosen to use the TAPAS test reference system in the Aarhus region, which allows to receive corrections from a single reference station and uses the four prerequired satellite programmes. The TAPAS network, which in total includes 11 reference stations, has been screened to find a suitable area for testing the predetermined baseline lengths up to about 5 km. A suitable area was found in the smaller town Sabro, where TAPAS reference station TA11 is located.

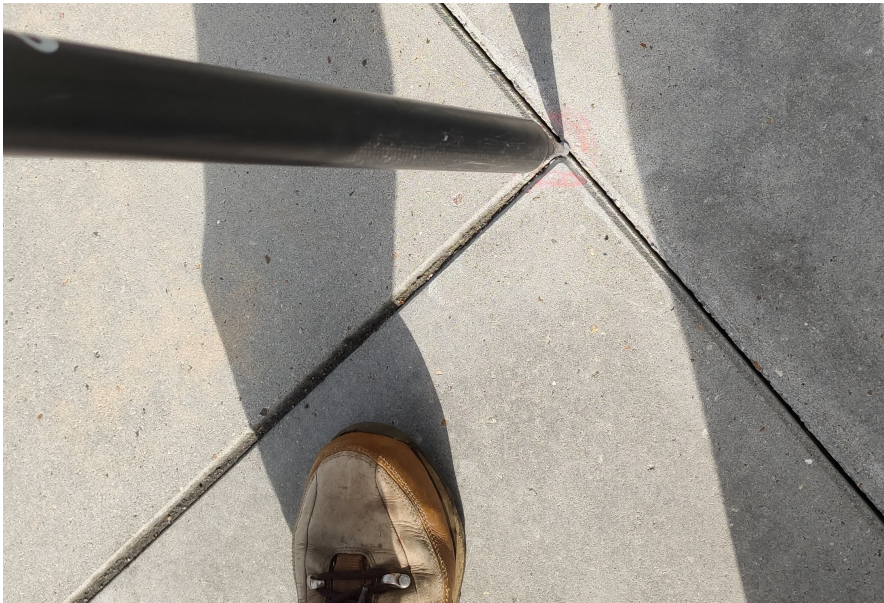


Figure 7.1: Established test point with nail in sidewalk

Test points have been established which result in the six different baselines shown in figure 7.2. Points 1,2,4,5 and 6 have been established with nails in asphalt and sidewalks, point 3 is an official height reference point. An example of an established test point is seen in figure 7.1.

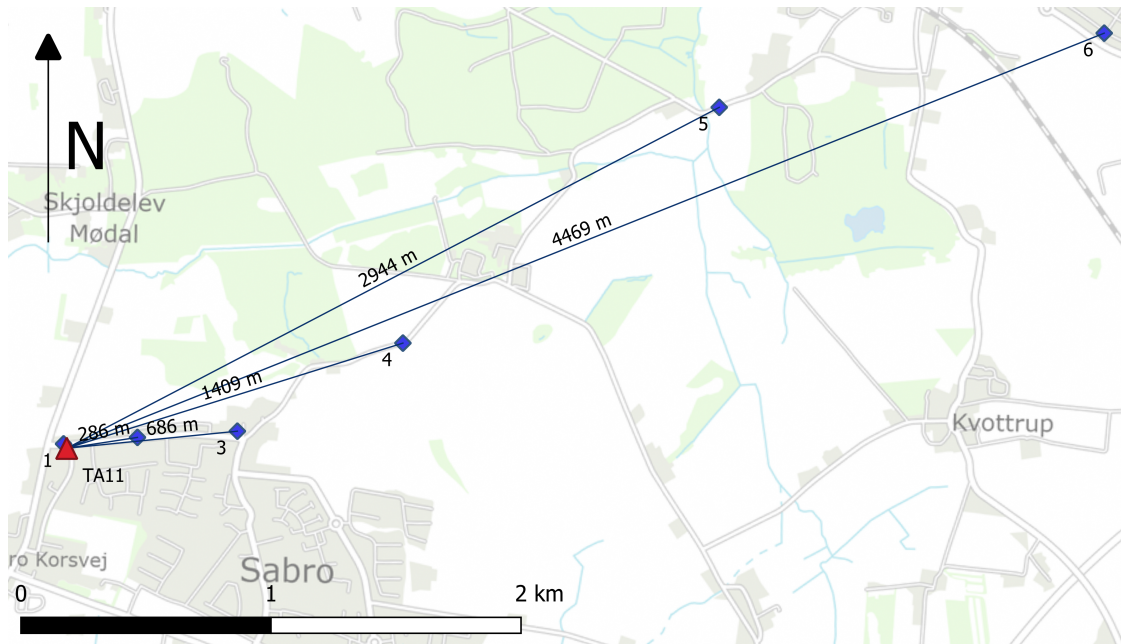


Figure 7.2: Short baselines. Derived by using a static base station (TA11), but different rover points (no. 1-6)

By receiving corrections from different TAPAS reference stations, it is possible to have various baselines length while the rover remains in the same location. By this procedure four relative long baselines have been tested as shown in figure 7.3, where the rover remains at test point 3, while receiving corrections from four difference reference stations.

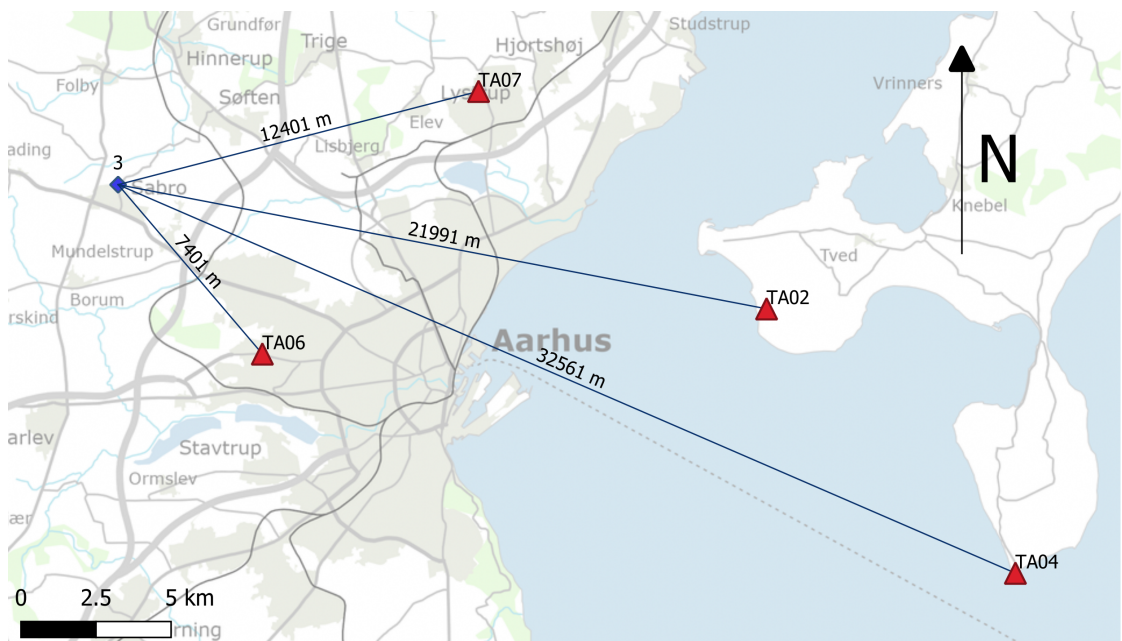


Figure 7.3: Long baselines. Derived by using different base stations, but a static rover point (no. 3)

As visualized the test points and different base stations will represent different baseline lengths and the exact value is listed in table 7.1.

Baseline number	Baseline length [m]	Test point	Base station
1	22	1	TA11
2	286	2	TA11
3	686	3	TA11
4	1.409	4	TA11
5	2.944	5	TA11
6	4.469	6	TA11
7	7.401	3	TA06
8	12.401	3	TA07
9	21.991	3	TA02
10	32.561	3	TA04
11	—	3	Smartnet IMAX

Table 7.1: Table of baselines used in baseline test. Baseline 1-6 is seen at figure 7.2 and baseline 7-10 is seen at figure 7.3.

The observations are collected in series. One series consists of one observation of every baseline number. The averaging time window is defined as 60 seconds, as examined in section 6.3 on page 37. The data collection, the transportation time between test points, and the time used for changing base stations result in about 45 minutes between the start of every series. In an efficient workday, 8-10 series can be collected by one person. Table 7.2 shows the different days and times of collection along with the number of series collected every day.

Run No.	Day	No. of series	Time at start	Time at end	Comments
1	13-04-2021	7	9:30 am	15:00 pm	GS16 used for long baselines
2	15-04-2021	9	8:00 am	15:30 pm	GS16 used for long baselines
3	21-04-2021	11	9:00 am	16:00 pm	
4	27-04-2021	6	8:00 am	15:00 pm	
5	03-05-2021	5	9:00 am	14:30 pm	

Table 7.2: Table of days of observations, used antennas etc.

Independence in atmospheric conditions has been striven for, which is done by spreading the days of the collection as much as possible. Practical reasons and the need of collecting a thorough data set early in the project period do affect the choice of days for collection.

7.2 Data examination

The data examination is separated into an individual data examination and a combined data examination.

7.2.1 Individual data examination

The current section is aiming to examine the collected data for outliers and investigate the level of normal distribution throughout every data set. The examination is carried out by computing normal probability plots, histograms, and "day-plots", and using hypothesis testing as described in section 5.5.1 on page 27.

The collected data consists of 11 independent data sets, derived from 11 different baselines. Every examination is therefore performed individually for every single data set. One outlier was found and removed during the testing with the 3σ -rule and the Grubbs-test.

The histograms normal probability plots and "day-plots" of the 11 grouped data sets are seen in appendix F on page 133. Table 7.3 summaries the assessment of the plots, and the results of the hypothesis tests.

Dataset (baseline)	Histogram		Norm-plot		KS-test		SW-test		Day-plot	
	Accept	Reject	Accept	Reject	Accept	Reject	Accept	Reject	Accept	Reject
22 m	X		X		X		X		X	
286 m		X	X		X			X	X	
686 m	X		X		X		X		X	
1.409 m	X		X		X		X		X	
2.944 m	X			X	X			X	X	
4.469 m	X		X		X		X		X	
7.401 m	X		X		X		X		X	
12.401 m	X		X		X		X		X	
21.991 m	X		X			X		X	X	
32.561 m	X		X		X		X		X	
Smartnet IMAX	X		X			X	X		X	

Table 7.3: Summary of assessed results of initial data examination, according to the level of standard distribution among the different data sets

Baseline 2 (286 m), baseline 5 (2.944 m), baseline 9 (21.991 m), and baseline 11 (Smartnet IMAX) are having difficulties with the level of normal distribution. The Shapiro-Wilk test is rejecting the null-hypothesis in 3 of the data sets, and the histograms seem rather non-bell-shaped. When looking at the normal probability plot though, it seems like the abnormal tails are the reason. The day-plot does not indicate any "bad days". It is decided to continue with the collected data sets, but the not perfect normal distribution will be taken into consideration when assessing the combined data examination.

7.2.2 Combined data examination

The current section is aiming to examine the collected data sets when combined. The aim is to examine the distance-dependent error and how it affects precision. The 10 SRTK data sets with corrections derived from a TAPAS reference station are the basis for determining the distance-dependent error of SRTK. Baseline 11 (Smartnet IMAX RTK service) is a benchmark, which can be used as an independent comparison.

The standard deviations for the 10 different baselines are listed in table 7.4 and visualized at figure 7.4. The standard deviation varies from 2.4 mm to 16.3 mm, and overall

increasing the baseline length result in a higher standard deviation as expected. The standard deviation for Smartnet IMAX is 8.7 mm, which is on a level with the baselines of 4500 m, 7400 m, and 12400 m.

Baseline	Length [m]	Samples	Std H [m]
1	22	38	0.0025
2	286	38	0.0024
3	686	38	0.0043
4	1.409	38	0.0047
5	2.944	37	0.0056
6	4.469	38	0.0080
7	7.401	35	0.0079
8	12.401	36	0.0094
9	21.991	35	0.0131
10	32.561	34	0.0163
11	IMAX	36	0.0087

Table 7.4: Standard deviation for the 10 different baseline lengths and Smartnet VRS. Not dimensionally correct x-axis.

The 10 standard deviations of the SRTK baselines have been compared with the standard deviation of the IMAX, to decide at which baseline distances the SRTK performs better, similar, and worse. A two-sided F-test has been performed, with a significance of 95%. The results is seen in table 7.5.

Baseline length [m]	22	286	686	1.409	2.944	4.469	7.401	12.401	21.991	32.561
Is STD of SRTK equal to Leica IMAX STD?	No	No	No	No	No	Yes	Yes	Yes	No	No

Table 7.5: Results of two sided F-test. H_0 : No difference in variances between Leica IMAX STD and 10 different SRTK STD at 95% significance.

It is seen that baseline 1 to 5 is obtaining better precision than the IMAX. Baseline 6,7 and 8 are obtaining equal precision as IMAX. Baseline 9 and 10 are obtaining worse precision than IMAX.

Figure 7.4 visualizes a relatively clear picture of the standard deviation increasing corresponding to the increasing baseline length. This increase almost seems like a linear function, but it is noticeable that the proportion of the x-axis is not equivalent to the baseline lengths. The standard deviation increases about 5-6 mm from 22 m to 4469 m, but in the same magnitude for 12401 m to 32561 m, wherefore the effect of increasing the baseline length is reduced at the long baselines.



Figure 7.4: Standard deviation for the 10 different baseline lengths

The results show minor exceptions at 286 m and 7401 m where the longer baseline does not result in a higher standard deviation. In theory, the 286 m baseline should result in a higher standard deviation than the 22 m baseline, but it is at the same level decreasing from 2.5 mm to 2.4 mm. It is assumed that variations of the nearby conditions and environment of the test points are the explanation. The increase of the standard deviation from 286 m to 686 m is also noticeable, why it is possible that the test point at 686 m baseline is affected by slightly poorer conditions for GNSS survey.

Another unexpected result is the minor decrease of the standard deviation from 8.0 mm to 7.9 mm when increasing the baseline length considerably from 4469 m to 7401 m. The test point for 4469 m is the last of the short baselines and 7401 m categorized as a long baseline, which means these points are tested using different reference stations. It is probable, that using this other reference station results in a lower standard deviation, but there is no immediate explanation as the baseline length is increased by about 3 km. The results for the rest of the long baseline, all with different reference stations, are as expected where the standard deviation increases relative to the baseline length. At figure 7.5 the standard deviations for the 6 short baselines are visualized. On this graph, the standard deviations are plotted with the correct values of the baseline length on the x-axis. The graph also includes a line computed by weighted linear regression of the 6 points.

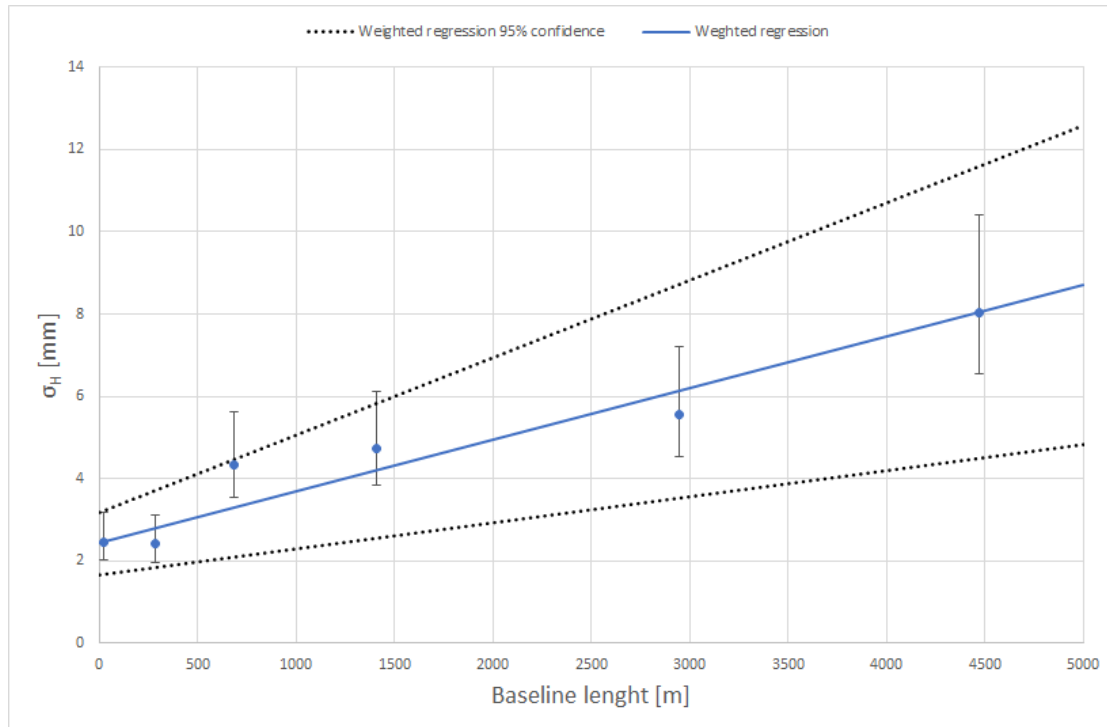


Figure 7.5: Standard deviation for baseline 1-6 (short baselines). Error lines representing 95% confidence. Linear regression weighted with $\frac{1}{\sigma_{\sigma_H}^2}$. $R^2 = 0.88$

	Lower 95%	Coefficient	Upper 95%
Slope [mm/km]	<i>0.63</i>	1.26	<i>1.88</i>
y-axis intercept [mm]	<i>1.66</i>	2.43	<i>3.19</i>

Table 7.6: Short baselines. Coefficients of weighted linear regression, with 95% confidence interval. Regression weighted with $\frac{1}{\sigma_{\sigma_H}^2}$

For some of the points, this linear regression seems like a rough assumption for a model of the standard deviation's relation to the baseline length, but as stated earlier the individual results are affected by local variations in the conditions for GNSS survey. By this linear regression, the graph's starting point is a standard deviation of approximately 2.4 mm at baseline length 0. Afterwards, the standard deviation increases by about 1.3 mm per kilometre baseline, and through this examination, it is concluded that the distance-dependent error will be in this magnitude for baseline lengths up to 5 km. The statistic uncertainty is though significant. The ppm can be anywhere between 0.6 and 1.9 mm/km, with a 95% confidence.

At figure 7.6 the standard deviation for all 10 baselines is visualized. The earlier showed linear relation between the standard deviation and the baseline length, does not continue when adding the 4 long baselines. For these 4 long baselines, with lengths between 7.4 and 32.5 km, the standard deviation increases only about 0.3 mm per kilometre, which is about a third of the increase when compared to the short baselines up to 4.5 km.

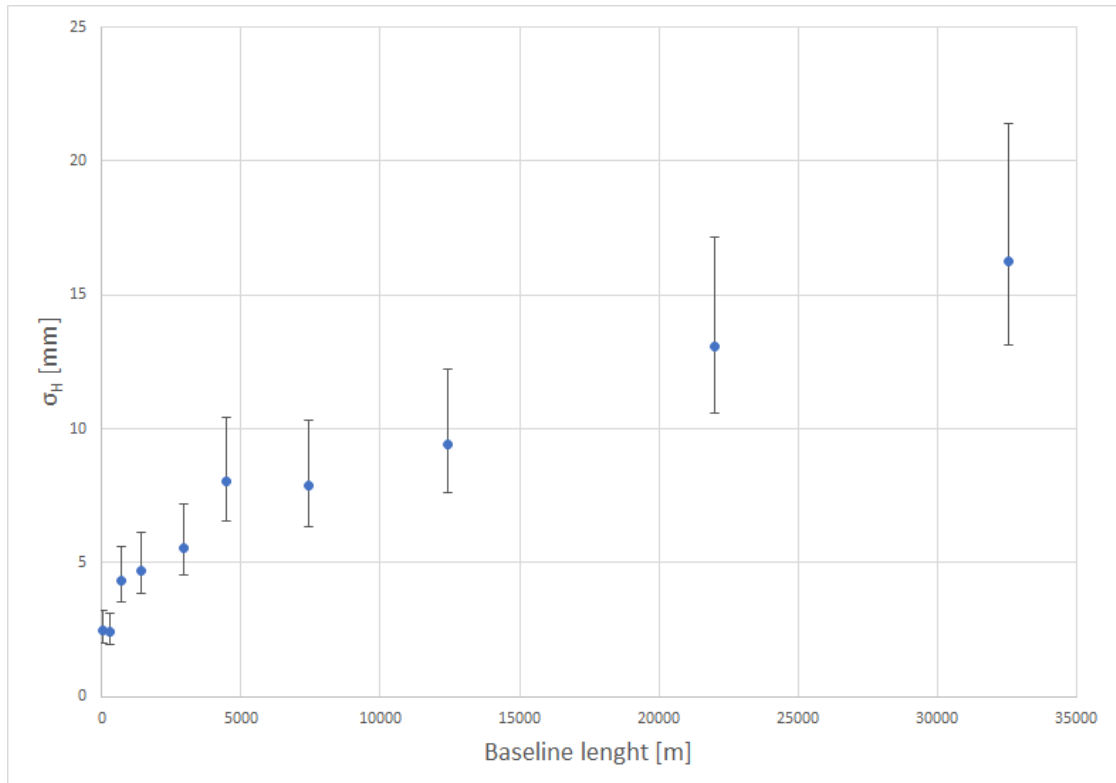


Figure 7.6: Standard deviation for baseline 1-10 (All baselines). Error lines representing 95% confidence.

A linear relation can be spotted between the four longest baselines. Figure 7.7 on the facing page shows the weighted linear regression between the four points, and table 7.7 on the next page shows the coefficients.

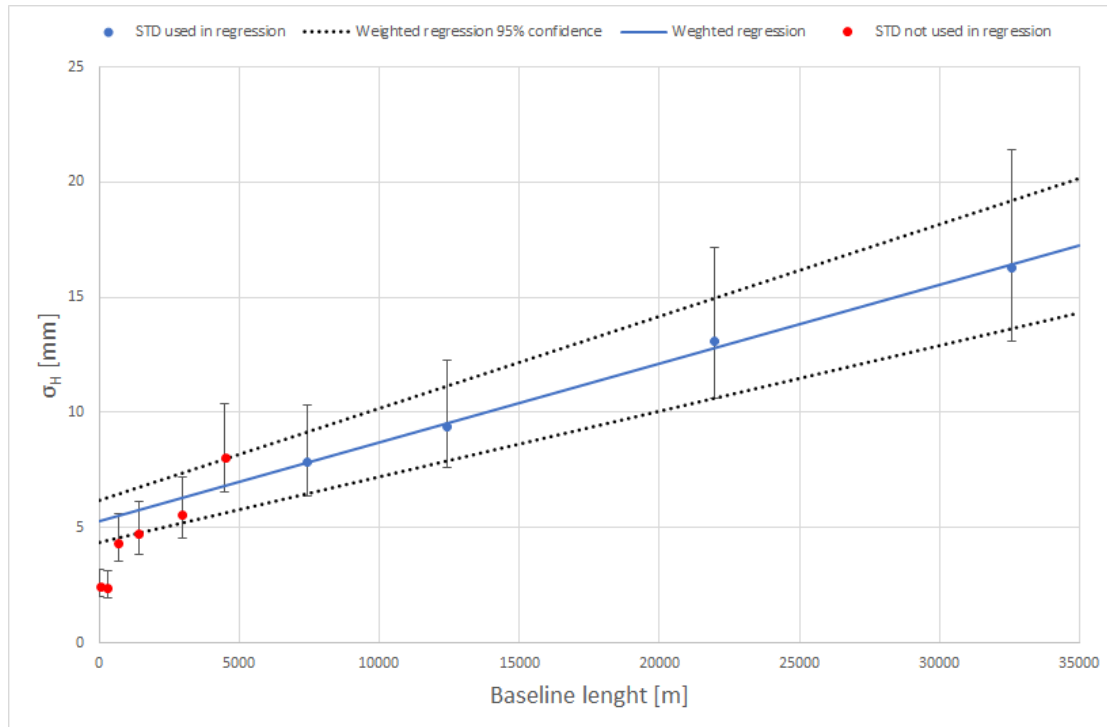


Figure 7.7: Standard deviation for baseline 7-10 (long baselines). Error lines representing 95% confidence. Linear regression weighted with $\frac{1}{\sigma_{\sigma_H}^2}$. $R^2 = 0.99$

	Lower 95%	Coefficient	Upper 95%
Slope [mm/km]	<i>0.28</i>	0.34	<i>0.40</i>
y-axis intercept [mm]	<i>4.39</i>	5.31	<i>6.22</i>

Table 7.7: Long baselines. Coefficients of weighted linear regression, with 95% confidence interval. Regression weighted with $\frac{1}{\sigma_{\sigma_H}^2}$

The regression of the 4 points is very precise, and it is possible to verify the coefficients with a high degree of confidence, one has to observe that only two over determinations are used though. It can be concluded that the distance-dependent error does not behave linearly. At short distances, it is more aggressive and steep, and at some point, maybe at about 5 km, a less steep distance dependency is seen.

Assuming the observations are normally distributed 95 % will be within $\pm 1.96 * \sigma$. At table 7.8, this density of the normal distribution has been used to classify the different baselines into a certain level of precision. Baseline 1 and 2 are distinguished by having significantly better precision where 95 % of the observation will be within ± 5 mm. The next level of precision, ± 10 mm, will include baseline 3, 4, and 5, or in other words baseline lengths up to about 2900 m. The third level of precision includes baselines 6, 7, 8, and Smartnet IMAX where the 95 % will be within ± 15 -20 mm. Lastly, the two longest baselines are classified with the poorest level of precision which is more than ± 20 mm.

Baseline	Length	Std H [m]	2σ [mm]	95 %
1	22 m	0.0025	5	±5 mm
2	286 m	0.0024	5	
3	686 m	0.0043	9	±10 mm
4	1409 m	0.0047	9	
5	2944 m	0.0056	11	
6	4469 m	0.0080	16	±15-20 mm
7	7401 m	0.0079	16	
8	12401 m	0.0094	19	
9	21991 m	0.0131	26	±>20 mm
10	32561 m	0.0163	33	
11	IMAX	0.0087	17	±15-20 mm

Table 7.8: Classified level of precision

In figure 7.8 the distribution of each observation is visualized as the deviation from the mean value of the individual test point. The mentioned levels of precision should be recognized in the figure, where for example 95 % of the observations should be within ± 5 mm for baseline 1 and 2. For baseline 1, two of the observations deviate slightly more than the 5 mm and these are theoretically part of the last 5 % with higher deviation. Baseline 3, 4, and 5, which are classified ± 10 mm, look very similar at this visualization with almost no extreme values and deviation up to 10 mm.

For baseline 6 with the length of 4469 m, the number of extreme values seems to increase and continue when looking at the longer baselines. These extreme values will have a significant effect on the estimated standard deviation, but also an important factor if considering the reliability. Baseline 6 has a limited number of extreme values, but the deviation of these are at the same level as baseline 7, and baseline 8 which is more than twice the length. Again, the Smartnet IMAX looks like baseline 6, 7, and 8, also affected by a couple of extreme values. For baseline 9 (22.0 km) the observations are generally more deviated, while baseline 10 (32.6 km) also includes some significant extreme values.

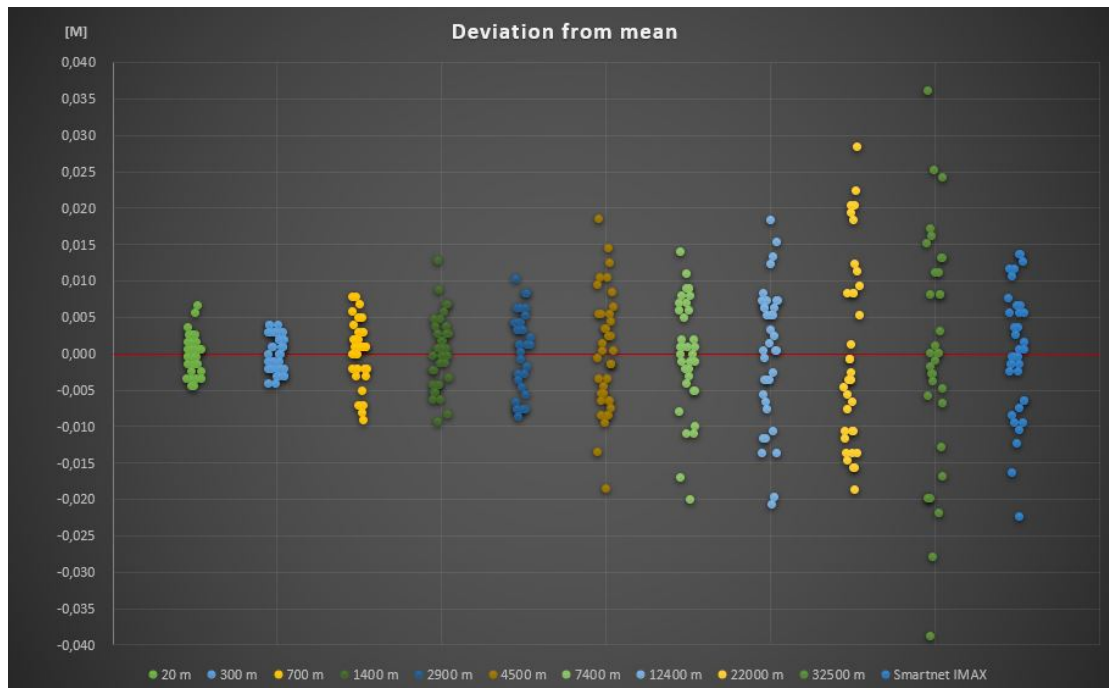


Figure 7.8: Deviation from mean value - The 10 baselines + Smartnet IMAX

The following chapter is concluding on the distance test, as well as the entire Part I.

Conclusion - Part I - Precision of SRTK 8

The current chapter is aiming to conclude on research question one; "*What is the vertical precision of SRTK?*"

Two significant parameters affecting the precision have initially been identified; *the data averaging window* and *the baseline distance*. The two parameters have been isolated in two different tests. The test of data averaging window led to surprising results, compared to the initial hypothesis that longer averaging time windows result in higher precision. No tendencies are seen that can support and confirm the hypothesis. Maybe the lack of effect is caused by a relatively short baseline.

When isolating the baseline distances effect on precision, more clear results are seen. It can be concluded that the random distance-dependent error of SRTK, when measured with a 60-second time-averaging window, can be stated in the range of $2.4mm + 1.3mm/km$ for short-range baselines (0-4.5 km.) and $5.3mm + 0.3mm/km$ for long baselines (7.4-32.6 km.). Baselines in between (4.5-7.4 km.) are assumably a mix of the stated precisions.

Baselines up to 2.944 km. performs statistically significantly more precisely than the Leica IMAX network RTK solution. Baselines up to 12.4 km perform equally compared to the Leica IMAX network RTK solution. Longer baselines perform worse.

The stated conclusions are not general in all conditions and all parts of the world. The stated precisions are also only applicable when measuring with a Leica GS16/GS18, in nearly perfect conditions, with a cut off angle of 10° , enabled for all GNSS programs (GPS, GLONASS, Galileo, and BeiDou) and with RTK corrections derived from the high-end base stations used by TAPAS. Multipathing environment, other hardware, etc. will assumably affect the random errors.

Part II

Accuracy of SRTK in interaction with the DRP

Introduction to examination of accuracy of SRTK in interaction with the DRP

9

The current chapter is introducing part II, where the accuracy of SRTK is being examined. The part is answering research question 2; "*What is the vertical accuracy of SRTK in interaction with the DRP?*" The accuracy is, as described in chapter 3.1.1 on page 11, a measure for how systematic errors (trueness) and random errors (precision) affects the total error (accuracy). The aim for this part is to examine the *trueness* and combine it with the precision as examined in part I.

The relation; $H_{orthometric} = h_{ellipsoid} - N_{geoid}$ is central in the examination. To examine trueness of orthometric heights of relative GNSS it is necessary to examine the trueness of the two components; $h_{ellipsoid}$ and N_{geoid} . The third component, used as a reference value, is; $H_{orthometric}$.

The three different components used in this part origins from;

- $H_{orthometric}$ derived from geometric levelling in relation to trusted reference points. Performed by both the project group and SDFE
- $h_{ellipsoid}$ derived from previous data collection (part I) and from static GNSS performed by SDFE
- N_{geoid} derived from geoid models interpolated in the point of interest. Two different geoid models are used separately

9.1 Orthometric heights

The orthometric heights used as a reference, when assessing the trueness of SRTK are not perfect. The heights have been geometrically levelled with high precision and reliability in relation to trusted reference points. Some net tensions will be expected, as the levelling has not been performed at the same time. An approximate accuracy of the reference orthometric heights can be 1-2 mm (1σ).

9.2 Ellipsoidal heights

The ellipsoidal height data used is the same as in part I. In short, the dataset consists of 10 different SRTK baseline distances, with every baseline measured between 34 and 38 times (after removing outliers), collected at 5 independent days during one month. The complete description of how the data is collected is seen in section 7.1 on page 39. The

ellipsoidal height used is the mean of the independent observations, which results in 10 different mean ellipsoidal heights, as seen in table 9.1.

#	Baseline distance [m]	h_{mean} [m]	σ_h [mm]	No. of observations	σ_{mean} [mm]
1	22	125.276	2.5	38	0.4
2	286	130.136	2.4	38	0.4
3	686	132.503	4.3	38	0.7
4	1409	114.968	4.7	38	0.8
5	2944	79.527	5.6	37	0.9
6	4469	85.287	8.0	38	1.3
7	7401	132.505	7.9	35	1.3
8	12401	132.508	9.4	36	1.6
9	21991	132.514	13.1	35	2.2
10	32561	132.520	16.3	34	2.8

Table 9.1: Table of h_{mean} and σ_{mean} of 10 baselines

The stated σ_{mean} is a measure of the uncertainty of the h_{mean} , as a product of the number of independent observations and their standard deviation. The uncertainty needs to be taken into considerations at the assessments where the h_{mean} is used.

In the examination, ellipsoidal heights of 11 TAPAS base stations are also used. These ellipsoidal heights are derived from state of the art static post-processed GNSS, why the accuracy of these are very high, probably less than 1 mm (1σ). The static GNSS data collection and data processing has been performed by SDFE.

9.3 Geoid heights

In Denmark, the geoid DVR90 is usually used. SDFE (Agency for Data Supply and Efficiency), who are responsible for DVR90, strives to make a model of the geoid accurate in a magnitude of 5 mm [SDFE, 2017]. For the moment the present geoid model DVR90 (dvr90g2013.01) is described to have an accuracy of 1-2 cm [Keller and Forsberg, 2020]. The geoid model DVR90 is based on measurements of gravitational acceleration, which is fitted with GNSS-observations and levelling surveys. DVR90 is in reference to the global reference system by 13 permanent GNSS receivers, distributed throughout the country. The DVR90 geoid is implemented by approximately 3000 height references, which are levelled with high precision. Even more height references exist, approximately 67000, though they are levelled with lower precision and in a lower frequency. [SDFE, 2021a].

Different geoid models, organized in regular grids of approximately 1x1 km, can be used when calculating orthometric heights by observed ellipsoidal heights. Geoid heights in different planar points can be interpolated, by different software applications. The present official geoid model, "dvr90g2013.01" [SDFE, 2012], is implemented in various GNSS equipment used in Denmark. A newer, but not final, version has been made available by SDFE, for use in this project. This geoid model should be capable of reaching higher levels of accuracy, than the present.

Assessment of accuracy and precision of geoid models

10

The current chapter is examining the two different geoid models mentioned in section 9.3 on the facing page. The two models will be examined and compared in terms of accuracy and precision. The present version is called geoid model 2013 (N_{2013}) and the new version is called geoid model 2021 (N_{2021}). The examination of accuracy is both performed at a regional and a local level, where the examination of precision is only performed at a local level.

To be able to quantify the magnitude of accuracy and precision of different geoid models an empirical approach has been used. As described earlier there is a clear context between ellipsoidal heights, orthometric heights and geoid heights (originating from the used geoid model). With this context in mind, and with the known ellipsoidal height and orthometric height of a planar point, the observed geoid height (N_{obs}) can be calculated. This height can be used as a reference, and be compared to the geoid height originating from various geoid models.

10.1 Regional examination

The 11 TAPAS base stations, seen in figure 10.1 are equipped with an ellipsoidal height derived with state of the art post-processed static GNSS, and an orthometric height derived from high precision levelling in reference to acknowledged and physically stable height reference points [SDFE, 2021b].

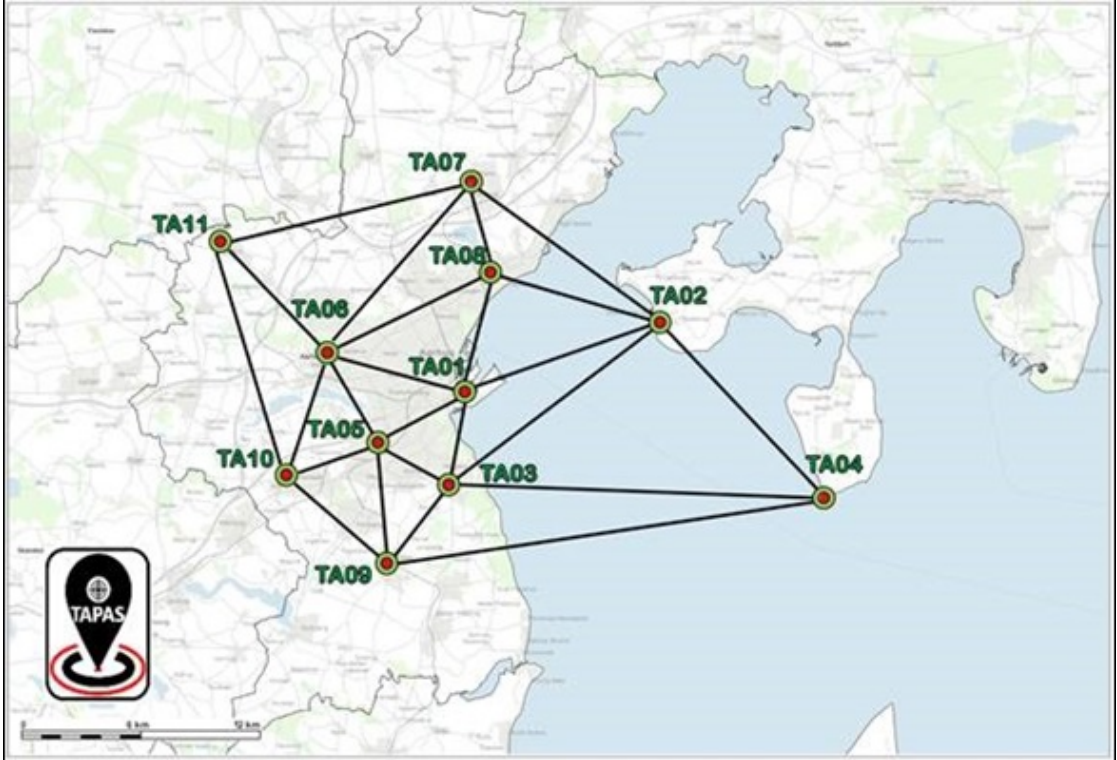


Figure 10.1: Map of TAPAS base stations

In table 10.1 the ellipsoidal heights and orthometric heights (DVR90) are listed. The N_{obs} , which is the observed geoid height is also listed as a reference for the geoid heights derived from the models. The geoid heights derived from the official 2013DVR90 geoid and from the 2021 version, which is a preliminary model aiming for obtaining 5 mm accuracy, are also listed for the 11 points.

TAPAS Basestation	h_{obs}	H_{obs}	N_{obs}	N_{2013}	N_{2021}	$N_{2013} - N_{2021}$	$N_{obs} - N_{2013}$	$N_{obs} - N_{2021}$
TA01	45.003	6.012	38.991	38.992	38.989	0.003	-0.001	0.002
TA02	53.093	14.477	38.616	38.616	38.610	0.006	0.000	0.006
TA03	139.220	100.131	39.089	39.086	39.083	0.003	0.003	0.006
TA04	45.351	6.873	38.478	38.477	38.472	0.005	0.001	0.006
TA05	70.118	30.956	39.162	39.165	39.165	0.000	-0.003	-0.003
TA06	107.078	67.887	39.191	39.183	39.186	-0.003	0.008	0.005
TA07	102.368	63.587	38.781	38.785	38.788	-0.003	-0.004	-0.007
TA08	49.689	10.851	38.838	38.848	38.846	0.002	-0.010	-0.008
TA09	96.756	57.555	39.201	39.207	39.205	0.002	-0.006	-0.004
TA10	130.291	90.970	39.321	39.320	39.322	-0.002	0.001	-0.001
TA11	132.426	93.161	39.265	39.266	39.274	-0.008	-0.001	-0.009
Mean						0.0005	-0.0011	-0.0006
STD						0.0041	0.0047	0.0059

Table 10.1: Regional geoid heights (N) comparison between observed geoid heights ($h_{ellips} - H_{ortho}$) [SDFE, 2021c]. 2013 geoid model [SDFE, 2012]. 2021 geoid model [SDFE, 2021b]. All units in meter. Red colours symbolize extreme values ($> \pm 0.007mm$)

The three different geoid heights have been compared, mean values and standard deviations have been computed. It is assessed that no systematic errors can be seen, as the mean values are very close to 0. The STD of $N_{obs} - N_{2013}$ and $N_{obs} - N_{2021}$, where the N_{obs} is used as a reference for accuracy assessment, are close to each other with 4,7 mm and 5,9 mm. When performing a two-sided F-test with a significance level of 95% the three standard deviations can be considered to be equal (mainly due to the low number of samples).

It is assessed that the two examined geoid models are not perfect. They are assessed to have the same level of accuracy, in the magnitude of 5 mm at 1σ , when the N_{obs} is considered as without errors. No bias of the geoid models is seen, why the 5 mm accuracy is only derived by the precision of the models. The examination can only be considered as applicable in the area of the sample points ie. within the TAPAS network.

10.2 Local examination

A more local investigation has been performed, to investigate not only the accuracy but also the precision of the geoid models. Levelled absolute orthometric heights have been collected of four different points within 1400 meters. The levelling have been performed with a Leica LS15 ($0.3 \frac{mm}{\sqrt{km}}$). The levelling has been performed as seen in figure 10.2.

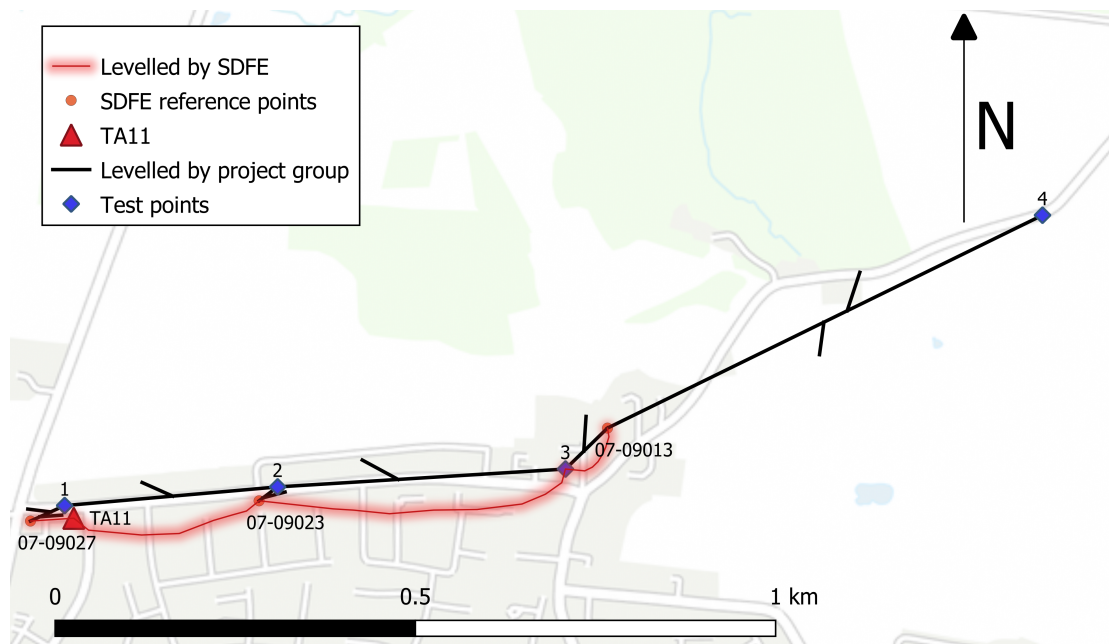


Figure 10.2: Map of geometric levelling of test points in Sabro.

DVR90 orthometric heights (with 5 decimals) of point 07-09027, 07-09023 and 07-09013 levelled by SDFE in 2019, and verified to be the best DVR90 reference in the area, have been used in the calculation of the height of the 4 test points [SDFE, 2021b]. The final orthometric heights of the 4 test points are seen in table 10.2.

	Point 1	Point 2	Point 3	Point 4
Orthometric height, DVR90 [m]	86.0087	90.8780	93.2574	75.7516

Table 10.2: Levelled orthometric heights of 4 test points

Observed ellipsoidal heights and the comparison with the two geoid models are listed in table 10.3.

Point	h [m]	H [m]	N_{obs}	N_{2013}	N_{2021}	$N_{2013} - N_{2021}$	$N_{obs} - N_{2013}$	$N_{obs} - N_{2021}$
1	125.276	86.009	39.267	39.266	39.274	-0.008	0.001	-0.007
2	130.136	90.878	39.258	39.256	39.264	-0.008	0.002	-0.006
3	132.503	93.257	39.245	39.243	39.251	-0.008	0.002	-0.006
4	114.968	75.752	39.216	39.215	39.222	-0.007	0.001	-0.006
					Mean	-0.0077	0.0016	-0.0061
					STD	0.0005	0.0006	0.0005

Table 10.3: Local geoid heights (N) comparison between observed geoid heights ($h_{ellips} - H_{ortho}$). 2013 geoid model. 2021 model. All units in meter.

When looking at the third row when seen from the right, $N_{2013} - N_{2021}$, it is clear that there is a systematic deviation between the two geoid models at about 8 mm. When looking at the $N_{obs} - N_{2013}$ which computes the absolute deviation between the 2013 geoid model and the reference N_{obs} it is seen that the deviations within the four points do not vary by more than 2 mm. The same is seen when examining the $N_{obs} - N_{2021}$, though a systematic error of about 6 mm is seen. Levelling is all about relative height differences, why the relative precision between one geoid height compared to another in the area of interest is more important than the absolute value of it.

10.3 Height differences

In this section, orthometric height differences determined by GNSS are compared to differences determined by geometric levelling. The basis for this comparison is point 1-4 from the distance test, which has been supplemented by a geometric levelling as described in section 10.2 on the preceding page. Table 10.4 presents the results of the analysis, where the geometric levelling is seen in the second column. In the first column is the difference of the determined ellipsoidal heights seen, which are the mean values from the distance test. Column three and four contain the differences of geoid model N_{2013} and N_{2021} , which is the computed difference of the values of for example N_{2013} for point 1 and 2.

The orthometric height is calculated $H_{orthometric} = h_{ellips} - N_{geoid}$, which mean the orthometric height difference is calculated:

$$\Delta H_{orthometric} = \Delta h_{ellips} - \Delta N_{geoid}$$

	Δh_{ellips} [m]	Levelled dif. [m]	ΔN_{2013} [m]	ΔN_{2021} [m]	ΔH (N_{2013})	Dif. [mm]	ΔH (N_{2021})	Dif. [mm]
Pt 1-2	4.8602	4.8694	-0.0100	-0.0100	4.8702	0.9	4.8702	0.9
Pt 1-3	7.2269	7.2488	-0.0230	-0.0230	7.2499	1.1	7.2499	1.1
Pt 1-4	-10.3081	-10.2571	-0.0510	-0.0520	-10.2571	-0.1	-10.2561	0.9
Pt 2-3	2.3667	2.3794	-0.0130	-0.0130	2.3797	0.3	2.3797	0.3
Pt 3-4	-17.5350	-17.5058	-0.0280	-0.0290	-17.5070	-1.2	-17.5060	-0.2

Table 10.4: Height differences between levelled height difference and ΔH . Light blue rows symbolizes heights and differences derived from geoid model 2013, and darker blue rows from geoid model 2021

In the table, ΔH is calculated using both geoid N_{2013} and N_{2021} , and this value can be compared to the levelled height difference. For easier comparison, the difference between the geometric levelling and ΔH is listed in the column to the right in [mm].

Figure 10.4 and 10.3 is a visualization of the levelled height difference compared with delta H derived from N_{2013} and N_{2021} . Both figures, and the exact values in the table, shows a similar picture where the values of ΔH are very close to the levelled height differences. The largest deviations are about 1 mm, and there is no direct link between the deviation and the distance between the two points. At this magnitude, the precision is considered to be about the same level as the reference levelling.

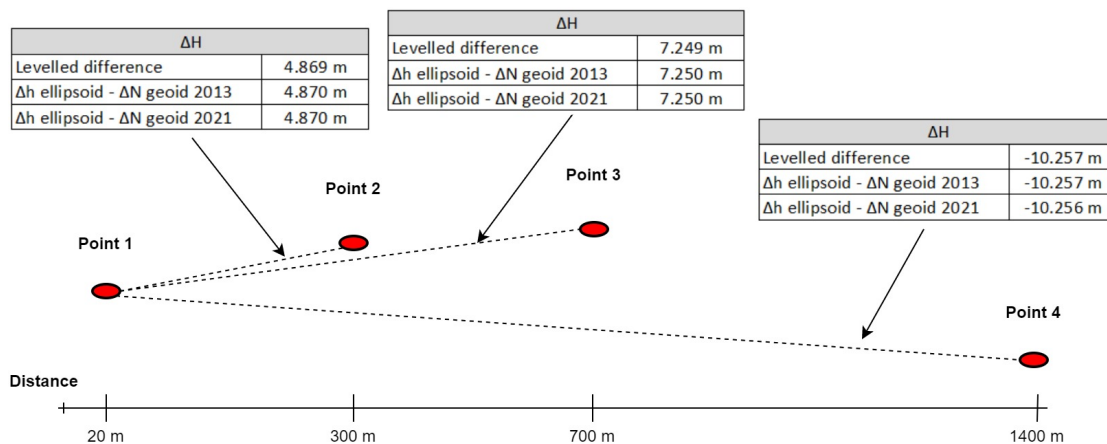


Figure 10.3: Orthometric height difference between point 1 and the other points

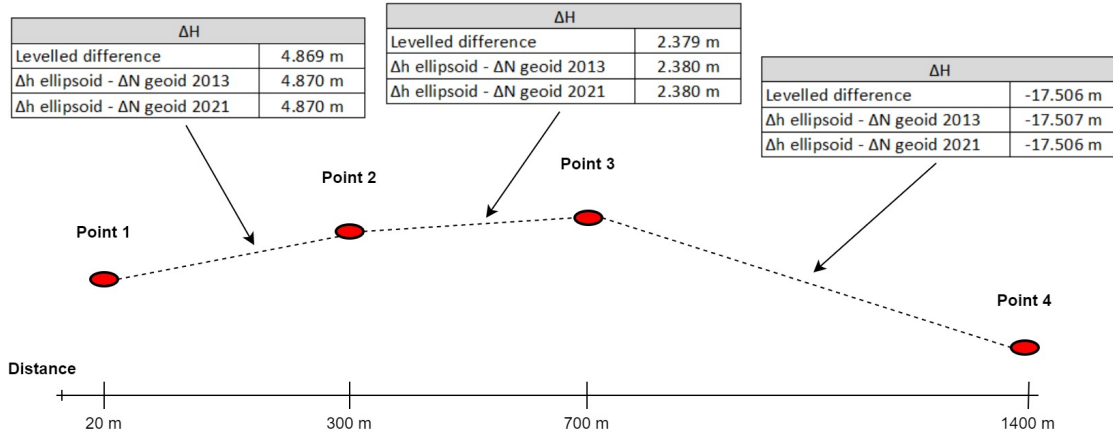


Figure 10.4: Orthometric height difference between point 1, 2, 3 and 4

The absolute orthometric height of each point determined by GNSS might not obtain millimetre accuracy, but this analysis concludes that the relative accuracy between the test points is in a magnitude of about ± 1 mm. This relative accuracy between the test points could more correctly be considered the precision of levelling performed by GNSS. This method of determining height differences is directly comparable to the traditional method of geometric levelling, which is also relative and needs to be related to a certain reference point, to obtain an absolute orthometric height.

The result of this analysis is obtained by isolating the error contribution to the geoid model. The ellipsoidal heights are mean values of 38 measurements wherefore the error contribution from GNSS precision is limited. Systematic errors of the reference frame and of how accurate the geoid model is fitted to this frame are eliminated as all measurement will be affected by the same errors. Figure 10.5 was initially shown in the project introduction to illustrate the error contribution of these two matters; GNSS precision and accuracy of the reference. As stated, by measuring relative height differences with a larger number of GNSS observations these errors are eliminated or limited.

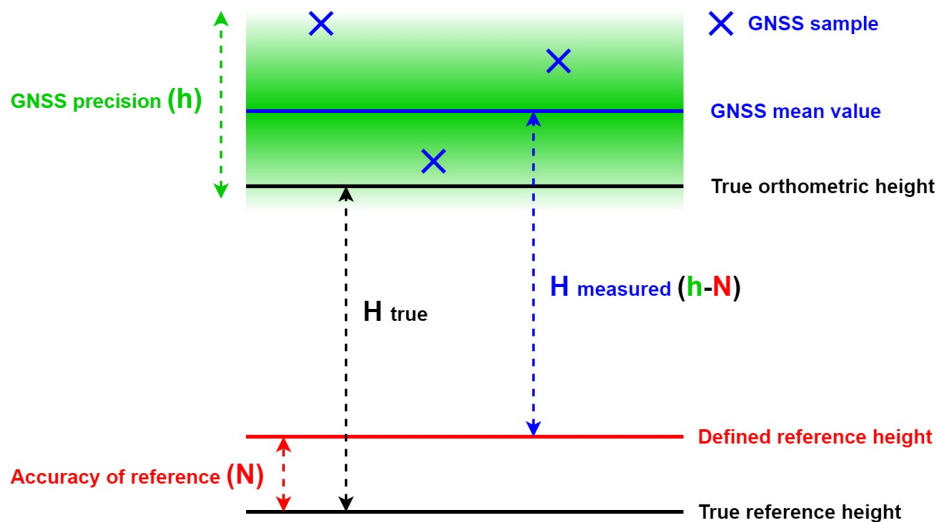


Figure 10.5: Determining factors N and h - Accuracy of N and precision of h

The precision of the geoid model itself will be a factor, but for this relatively small area, the effect seems limited and ignorable. Both geoid models seem to have about the same precision. A prerequisite of the assessment is that the geoid heights used only consists of decimals in the range of mm. Sub-mm geoid heights could have increased the precision even more.

It can be concluded that the precision of the geoid height does not contribute to the precision of an orthometric height difference between two points measured by SRTK GNSS, within a distance of approximately 1500 m. It can also be concluded that the only error contribution comes from the SRTK GNSS observations. The precision of a height difference can therefore be calculated, when knowing the basic error and distance-dependent error of one GNSS observation, and the baseline distances to the two points. An example is computed in the following equations.

The laws of error propagation tells us:

$$\sigma_{\Delta H}^2 = \sigma_{H_1}^2 + \sigma_{H_2}^2 \quad (10.1)$$

$$\sigma_{\Delta H}^2 = (\sigma_{basic} + \sigma_{dist} * dist_1)^2 + (\sigma_{basic} + \sigma_{dist} * dist_2)^2 \quad (10.2)$$

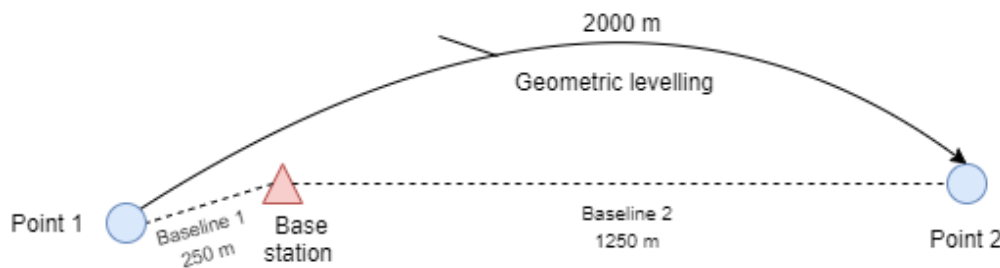


Figure 10.6: Sketch of two points "levelled" with SRTK and with geometric levelling.

When point 1 is measured with a baseline distance of 250 m. and point 2 is measured with a baseline distance of 1250 m, as seen in figure 10.6. And GNSS measurements can be described as concluded in section 8 on page 51, with a basic error of 2.4 mm and a distance dependent error of 1.3 mm/km, propagation to the height difference will be:

$$\sigma_{\Delta H} = \sqrt{\left(2.4mm + 1.3 \frac{mm}{km} * 0.25km\right)^2 + \left(2.4mm + 1.3 \frac{mm}{km} * 1.25km\right)^2} = 4.9mm \quad (10.3)$$

Different combinations of baseline distances of the two points will result in the precisions of height differences stated in appendix G on page 145. A visualization of the precisions,

when using different baseline distances at the two points measured points is seen at figure 10.7

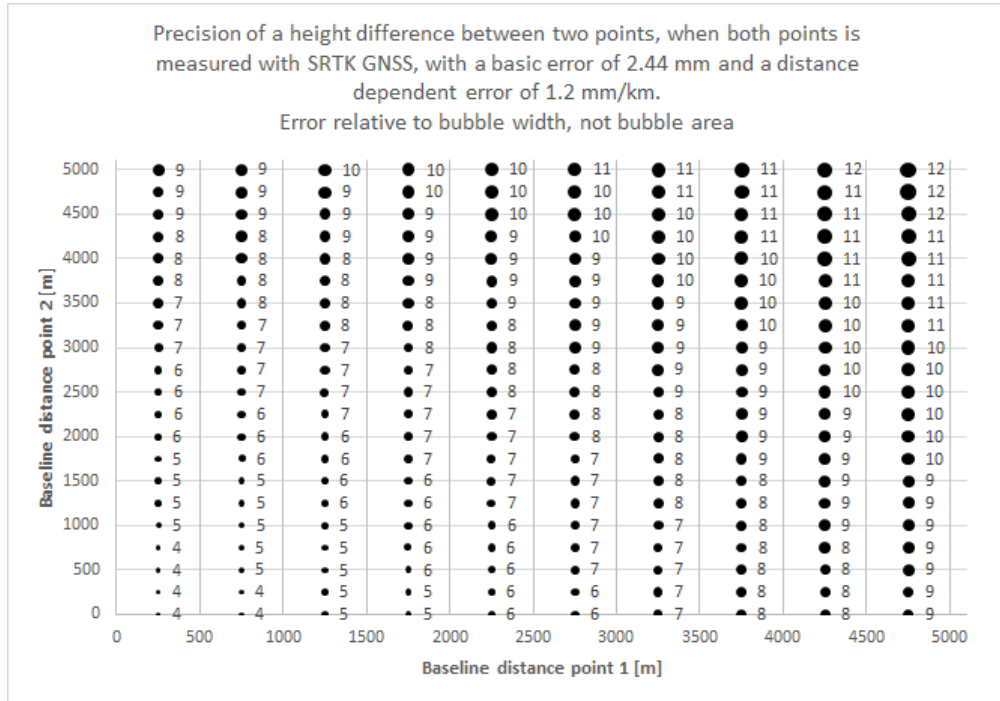


Figure 10.7: Precisions of height differences between two points [mm]

The stated error propagations are only applicable if the precision of the geoid model is assumed as not in a contributing magnitude, which only has been verified at distances up to approximately 1500 m. The GNSS-error contribution has though been confirmed up to about 4500 m.

Using classical geometric single run levelling at the distances used in equation 10.3 (1500 m), with a low-end digital level, Leica Sprinter 50 ($2 \frac{mm}{\sqrt{km}}$, at double run), results in a precision of 4.0 mm. When taken into account that levelling a distance as a direct line is not always an option, why an assumed 33% extra levelling is needed, as seen in figure 10.6. The precision of "SRTK-levelling" of 4.9 mm compared to classical geometric levelling with a precision of 4.0 mm seems competitive in precision, and superior in labour consumption.

If better precisions are needed, several independent measurements can be collected at different points. Precisions can be improved by \sqrt{N} when collecting N independent observations. As an example, with 3 independent observations at both points, the baseline distances used in equation 10.3 would result in a precision of 2,9 mm.

Accuracy (Trueness) of SRTK

11

The following chapter analyses the trueness, and thereby the accuracy of the SRTK. As presented in figure 3.3 in the method, accuracy is a product of precision and trueness. The precision of SRTK was examined in part I of this project, and as presented in chapter 9 on page 55 heights derived from SRTK are in this part mean values. Though these values are not perfect, choosing the mean value should in theory eliminate the random error contribution from the precision of SRTK. If the error contribution from precision is eliminated the accuracy is determined by the trueness, and therefore this examination equals trueness and accuracy.

11.1 Ellipsoidal heights

Accurate ellipsoidal heights are a key parameter for obtaining accurate orthometric heights. Earlier examinations show that the precision of measured heights worsens when increasing baseline length. When looking at the mean value of the observed ellipsoidal heights interesting contexts can be seen. Figure 11.1 and table 11.1 shows the mean observed ellipsoidal height measured at reference point 98-07-00804 in Sabro, with corrections from 5 different base stations in the Aarhus region (optionally see figure 7.3), with different baseline lengths.

TAPAS Basestation	Baseline length [m]	$H_{base} - H_{rover}$	h_{obs}	h_{ref}	$h_{obs} - h_{ref}$
TA11	686	-2 m	132,503	132,499	0,004
TA06	7401	-27 m	132,505	132,499	0,006
TA07	12401	-32 m	132,508	132,499	0,009
TA02	21991	-81 m	132,514	132,499	0,015
TA04	32561	-88 m	132,504	132,499	0,021

Table 11.1: Mean absolute ellipsoidal heights measured at reference point with corrections from different base stations (with different baseline length and orthometric height)

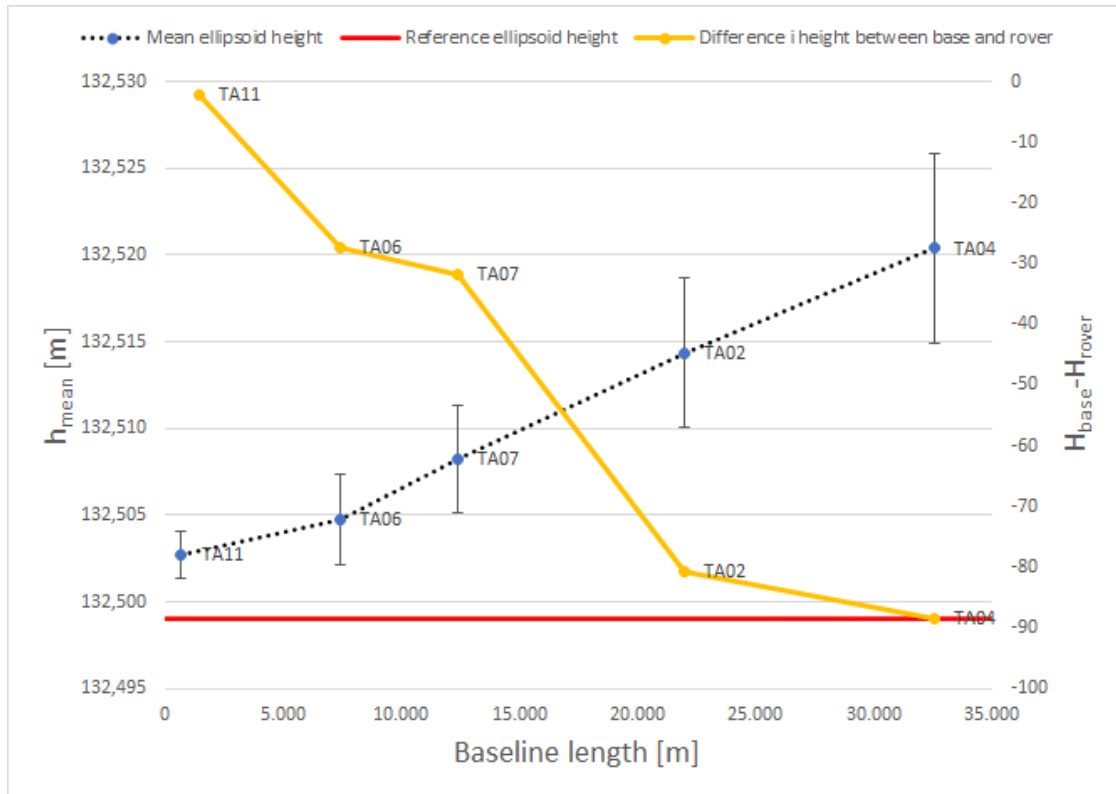


Figure 11.1: Mean absolute ellipsoidal heights measured at reference point with corrections from different base stations (with different baseline length and orthometric height). Error lines representing 95% confidence.

All of the observed mean ellipsoidal heights are higher than the reference ellipsoidal height, which is derived by static post-processed GNSS. It could be a tendency that longer baseline length leads to systematically wrong RTK-corrections, leading to higher observed ellipsoidal heights. No theories explain this phenomenon. A more plausible tendency is that the difference in orthometric height between base and rover, and therefore the difference in tropospheric delay bias, is the cause. Figure 11.1 shows how the orthometric heights of the base stations and the observed ellipsoidal heights are showing inverse proportionality. A lower base station, compared to the rover position, entails a higher observed ellipsoidal height. The results presented in this section shows bias in the magnitude of up to 20 mm with a difference in orthometric height of base and rover of up to 90 m. Figure 11.2 shows the bias as a function of the difference in orthometric height, with the coefficients listed in table 11.2. The bias can be stated at approximately 1 mm pr. 5 m difference in orthometric height between base and rover, but with a significant amount of uncertainty due to the confidence intervals.

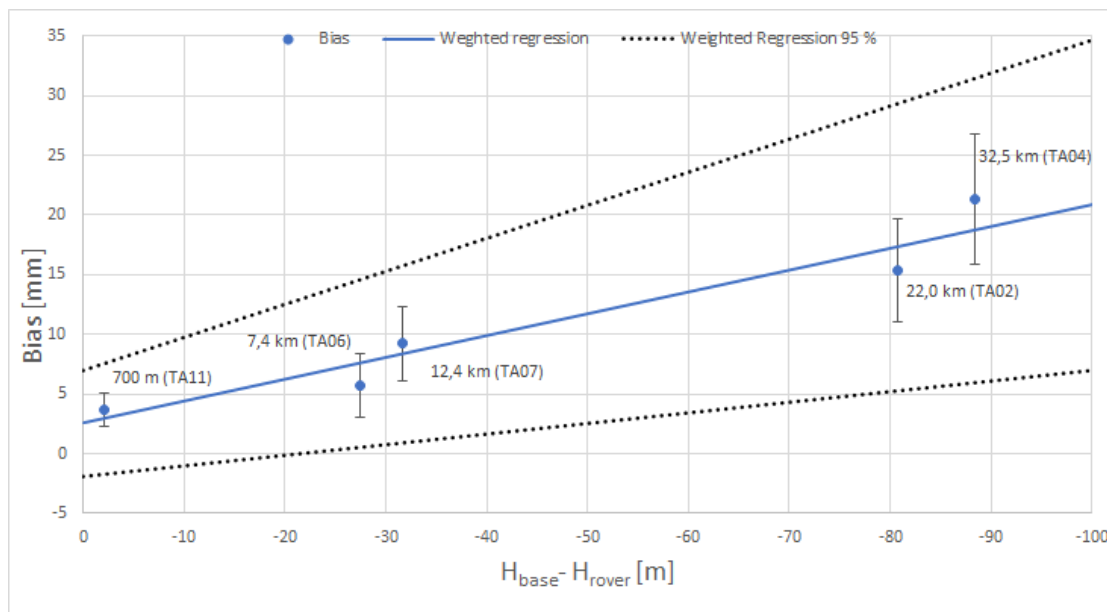


Figure 11.2: Mean bias plotted as a function of base station orthometric height relative to rover receiver. Error lines representing 95% confidence. Linear regression weighted with $\frac{1}{\sigma_h^2}$. $R^2 = 0.92$

	Lower 95%	Coefficient	Upper 95%
Slope [mm/mΔH]	-0.09	-0.18	-0.28
y-axis intercept [mm]	-1.92	2.55	7.04

Table 11.2: Bias of ellipsoidal heights as a function of the height difference between base and rover. Coefficients of weighted linear regression, with 95% confidence interval. Regression weighted with $\frac{1}{\sigma_h^2}$

Tropospheric delay bias is a known error source when performing relative GNSS, why several models for eliminating the bias have been developed. Leica Geosystems does not publish the used model in various specification lists, as it is assumable a market secret. Modelling tropospheric delays are done on every measured pseudorange from every satellite observed. Given between 25 and 35 satellites, which is used in the current examination, the direct difference in pseudorange correction, ϵ_{tropo} , can not be translated directly to a difference in ellipsoidal height. If all satellites are located in zenith, a bias in pseudorange propagates directly to a bias in ellipsoidal height, in a 1:1 relation. The direct influence when having a larger number of satellites, also placed further down the horizon, is uncertain, but shorter pseudoranges will always result in a higher orthometric height since all satellites are placed above the measured point.

When performing relative, GNSS a difference in tropospheric delay must be expected. The difference is mostly caused by different orthometric heights of the base and rover. If the different heights are not taken into account, the corrections delivered to the rover will be affected by a bias. The differences of pseudorange correction, according to tropospheric delay, have been calculated, to examine the magnitude of the correction. Saastamoinen

tropospheric delay model has been used with the following parameters:

- Temperature: *5 degrees celsius*
- Atmospheric pressure: *1013.25 mb*
- Relative humidity: *50 %*
- Orthometric height of base receiver *50 m*
- Orthometric height of rover receiver *51 m*

Different elevation angles have been used in the calculations, as this is the most important parameter. The results are seen in table 11.3 and graphically at figure 11.3

Elevation angle [°]	5	10	15	20	25	30	35	40	45	50	55	60	65	70	75	80	85	90
$\epsilon_{rover} - \epsilon_{base}$ [mm]	3.1	1.8	1.2	0.9	0.7	0.6	0.6	0.5	0.4	0.4	0.4	0.4	0.3	0.3	0.3	0.3	0.3	0.3

Table 11.3: Difference in tropospheric delay with base receiver in 50 m height and rover receiver in 51 m height. [Hofmann-Wellenhof et al., 2008,p. 135]

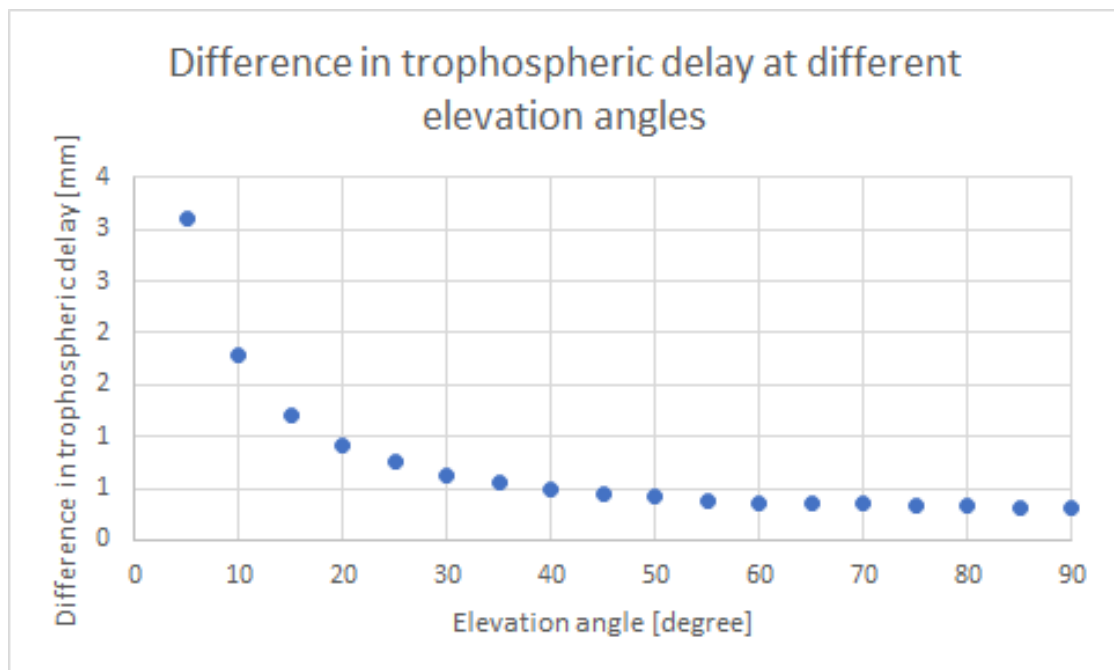


Figure 11.3: Saastamoinen tropospheric delay model. Differences between delay of base height of 50 m and rover height of 51 m. Computed for different elevation angles. [Hofmann-Wellenhof et al., 2008,p. 135]

It is seen that the difference in tropospheric delay is in the magnitude of 2 mm per 5 m height difference when elevation angles are above 30°. It is assumed that the average elevation angle in most cases is in the range of 30° to 60°, where the computed differences are about 0.4-0.6 mm per meter. This is double or triple of the bias discovered in the previous of 0.18 mm per meter (Table 11.2). This examination does not prove a direct link, but as assessed, the magnitude of the bias can be caused by the difference of height between base and rover. It can not be explained why the Leica GS16/GS18 is not better

at determining and correcting the tropospheric delay bias caused by differences in orthometric heights of base and rover, as modelling the errors should be possible to a greater extent than examined.

It can be concluded that when performing SRTK with a Leica GS16/GS18 it is important to have approximately the same orthometric height in both base and rover receiver. Otherwise, tropospheric delay biases will occur. The bias should be reduced by raising the cut off angle, though it can cause other problems.

11.2 Orthometric heights

In this section, the absolute orthometric heights derived from ellipsoid heights measured by SRTK GNSS and the geoid model N_{2013} and N_{2021} , are compared to the absolute height determined by geometric levelling of test point 1-4. Table 11.4 presents the results where the ellipsoidal heights are mean values from the distance test. H is the derived orthometric height; ellipsoidal height minus the value from the respective geoid model ($H = h - N$). The differences between the derived orthometric height and the levelled height are presented in millimetres. Figure 11.4 is a visualization of the same results.

	Baseline length	Levelled orthometric height [m]	H [m] (N2013)	Dif. [mm]	H [m] (N2021)	Dif. [mm]
Pt 1	22 m	86.0087	86.0098	1.2	86.0018	-6.8
Pt 2	286 m	90.8780	90.8801	2.1	90.8721	-5.9
Pt 3	686 m	93.2574	93.2597	2.3	93.2517	-5.7
Pt 4	1409 m	75.7516	75.7527	1.1	75.7457	-5.9

Table 11.4: Absolute orthometric heights of test point 1-4

The four orthometric heights derived from N_{2013} deviate by 1.1-2.3 mm from the levelled heights, which is considered to be an impressive result for the heights determined by RTK GNSS. The result suggests a systematic error as the derived heights all are too high compared to the levelled reference height. The levelled reference heights and the height of the GNSS reference station are not parts of a perfect or flawless system, which can hold an offset error.

In chapter 10 on page 57 it was concluded that the two geoid models have about the same precision, but in this analysis, the absolute orthometric heights derived from the N_{2021} geoid model deviate significantly more from the levelled reference height. However, figure 11.4 makes clear that this is a systematic error as all heights are about 6-7 mm under the reference height. The precision of the geoid model itself seems acceptable, also concluded earlier, but in this case, the geoid model is not fitted well in the test area. The results can be considered as expected as the N_{2013} geoid is fitted to a reference point used as test point 3 and therefore holds a bias, while the N_{2021} is not fitted to nearby reference points.

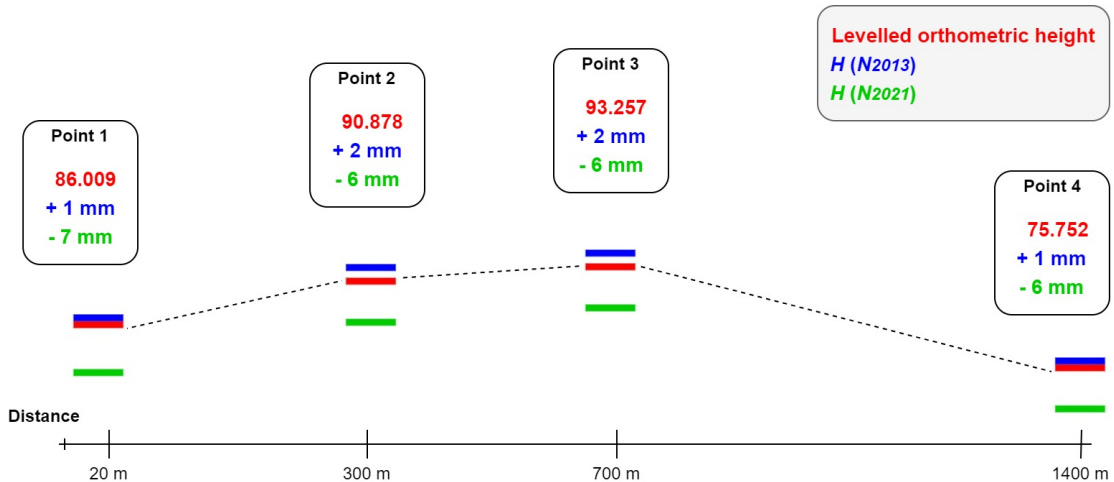


Figure 11.4: Absolute orthometric heights for test point 1-4

11.2.1 Correction of SRTK-setup to obtain absolute orthometric heights

This situation with the geoid model having high precision, but a systematic error in the absolute height can be modified by adjusting the reference height of the reference station. In the test scenario, RTK corrections are based on the reference stations ellipsoidal height. If this reference height is modified so is the ellipsoidal height of the GNSS rover and eventually the orthometric height. Table 11.5 shows data concerning the reference station TA11 used in this test. The reference ellipsoidal height is 132.426 m, but SDFE has also performed geometric levelling of the station related to the nearby reference points. If this orthometric height is joined with the N_{2021} geoid a new ellipsoidal height can be calculated. As seen at the table this new ellipsoidal height deviates 7 mm from the used ellipsoidal reference height.

TA11 reference station	[m]
Ellipsoidal height	132.426
Levelled orthometric height (H)	93.159
N_{2021}	39.274
New modified ellipsoidal height	
$h = H + N$	132.433
Adjustment	0.007

Table 11.5: Adjustment of reference height

Figure 11.5 visualizes how modifying the reference height at the base station will adjust the height of the GNSS rover, where the black illustrates the adjusted ellipsoidal heights. A modified ellipsoidal height will subsequently have a direct effect on the orthometric height, which will be equally adjusted. The green marks illustrate the N_{2021} , where a 7 mm adjustment will position the derived height much closer to the levelled reference height with a deviation up to about 1 mm.

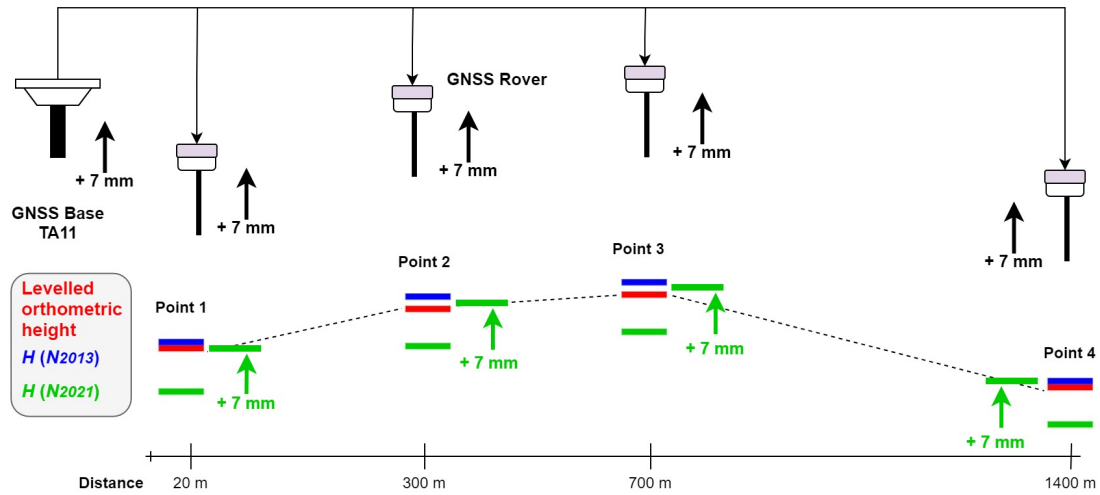


Figure 11.5: Adjusting the geoid model by correct reference height

In practice adjusting the height of the reference station is not a direct option for the test setup, why this subsequent manual adjustment is necessary. However, when using an SRTK set up the base station is given a reference height and this local adjustment is made possible. This reference height would naturally be based on a levelled orthometric height, as for the example presented above.

Conclusion - Part II - Accuracy of SRTK

12

The current chapter is aiming to answer research question 2; *What is the vertical accuracy of SRTK in interaction with the DRP?*

The accuracy of an orthometric height measured by GNSS is depending on the accuracy of the measured ellipsoidal height and the accuracy of the used geoid model. The two parameters have been separated in the analysis. It can be concluded that the geoid models are not perfectly fitted, i.e. systematic biases occur. The bias can be in the magnitude of 10 mm, which results in orthometric heights with a bias of 10 mm if used directly. Within a defined and limited area, with about 1500 m between planar points, the bias of the geoid model can be interpreted as constant. When calculating the height difference between two points, within 1500 m, the precision of the height difference is only depending on the precision of the height of the two points. 1500 m. can be "levelled" by SRTK with a precision of about 5 mm (1σ) for height differences measured once per point.

"Correcting" the height of a base station to compensate for the bias of the geoid model is possible to obtain orthometric heights without bias. The correction is done by knowing the orthometric height of the base station, which entails the possibility of eliminating bias from the fitting of the geoid model. When using a base station with corrected height, the accuracy of the SRTK observations is only depending on the precision of the observation, as no noticeable bias will occur. At short baselines up to 5,000 m, the accuracy can be stated to be $2.4 \text{ mm} + 1.3 \text{ mm/km}$. The corrected base solution has been verified with distances up to 1500 m. Increasing the number of independent observations is a rational way of increasing the accuracy. Table 12.1 show the accuracies at different baseline lengths and with a different number of independent observations.

Sample size	Baseline length			
	1 km	2 km	3 km	4 km
1	7,2	9,7	12,1	14,6
2	5,1	6,8	8,6	10,3
3	4,2	5,6	7,0	8,4
4	3,6	4,8	6,1	7,3

Table 12.1: Accuracy [mm] (95% significance) at different baseline lengths and with different number of independent observations. No contribution from geoid model included.

The ellipsoidal height does suffer from systematic biases, depending on the relation between the orthometric height of the base and rover. The difference in tropospheric delay bias is supposedly affecting the observed ellipsoidal height in a magnitude of about 1 mm pr. 5 m height difference. Which demands the base station is placed at approximately the same height as the survey area. Otherwise better tropospheric delay models need to be implemented in the GNSS equipment, to correct the bias.

Part III

Applicability and potential

Applicability of using SRTK with DRPs

13

Part III of the project is answering the research question 3; "*How is SRTK in interaction with the DRP applicable, and what is the potential?*". The present chapter is aiming to assess the applicability, while chapter 14 on page 81 is assessing the potential. An overall answer to research question 3 is presented in chapter 15 on page 85.

When assessing the applicability of the SRTK in relation to DRPs it is essential to present the procedures for using the technologies in relation. The current chapter is listing the prerequisites of using SRTK in relation to DRPs. The prerequisites are about hardware, software, and procedures. An assessment of the performance of the SRTK in relation to DRPs compared to more conventional methods is also carried out, to assess the level of applicability of the technology.

The concept of the DRP was initially presented in the introduction, section 1.1 on page 3. Additional information about the DRP and basics of the underlying radar technology can be found in appendix A on page 99.

13.1 Procedure for setting up base station at the DRP

When setting up the base station at a DRP it is important to have an approved orthometric height of the point, and an approximate planar coordinate set. Every error in the height and coordinates will propagate directly to the rover.

The orthometric height of the DRP is the tool for handling the bias in the geoid model. Equipping a DRP with an accurate and approved orthometric height is a difficult task. It must be done by traditional levelling techniques. In some areas, it can be difficult to find accurate and stable reference points when performing the levelling.

The advantage of the DRP is that the levelling only needs to be done once. After the initial levelling, it is possible to correct the orthometric height, as time goes by and land subsidence or elevation causes changes in the height.

13.2 RTK correction transmitting method

Transmitting the RTK corrections from the base to the rover is essential. In general 3 technologies can be used:

- VHF/UHF-radio
- GSM-call
- Internet (online server)
 - With sim card with a static IP-address
 - With sim card with a dynamic IP-address, and a dynamic DNS service provider

To choose between the three is a question about convenience and hardware/software support. Radio transmitting is beneficial on short distances, though it requires internal/external radios and antennas. GSM-call transmitting is requiring a GSM-modem, and a suitable sim card. In practice, most sim-cards do not offer the right specifications to make the transmission though. Transmitting corrections from the base to the rover via the internet requires a Dynamic DNS service, which changes the dynamic IP address of the uploading sim-card, to a static domain, which the rover can stream the corrections from. Otherwise, a static IP address on the base is needed, to let the rover stream corrections.

The last option (transmitting via the internet) is chosen to be the most reliable and convenient. An advantage of corrections over the internet is the possibility to connect up to 10 rovers and receive corrections from the same base. The transmitting is not limited by distance, as long as the internet connection is established. The choice between a static IP address or a dynamic DNS service is typically a matter of a compromise between convenience and price. A static IP address on the base is "plug-and-play", but typically more expensive than a dynamic DNS service.

13.2.1 Difficulties with RTK transmission

In the current project, difficulties with obtaining proper RTK transmission from the base (Leica GS16) to the rover (Leica GS18) occurred. The ineffective transmission method was "transmission over the internet" in cooperation with a dynamic DNS service (DynDNS.com). After several support calls to Leica, it was concluded that the difficulties were caused by a bug in the operating system of the equipment. The bug should be fixed in future software updates, if it is not fixed one of the other RTK transmitting methods could be tried. Other manufacturers of GNSS receivers than Leica have not been tested.

13.3 Procedures for RTK corrections from DRP base station

In general, using a rover with RTK corrections from a base station positioned in a DRP is no different than using corrections from any other base station or network solutions.

When using the GNSS rover and performing measurements or stakeouts of heights it is essential to have a basic knowledge of the technology of relative GNSS. The users need to be aware that the reliability of one single measurement is very limited. Outliers do occur, as a consequence of wrong integer ambiguities. The outliers can be detected when performing at least two independent measurements. Several measurements are also increasing the precision and thereby the accuracy of the mean value.

The testing in the project showed very little advantage regarding increased measuring time or the averaging time window. Even the averaging time window of 10 minutes showed no significant improvement compared the only 5 or 15 seconds. It is the impression that independent measurements, with a new satellite constellation, will have a much

larger positive effect regarding precision and reliability than increasing the measuring time.

It is discovered that differences in height of base and rover can cause a bias in the calculated orthometric height at the rover position (1 mm pr. 5 m height difference). Therefore it is not recommended to work with a bigger height difference, than the tolerance of the task can cope with.

13.4 Performance of SRTK in relation to DRP's

The performance of a height determination method can be defined by various parameters. In the current section, the performance is identified by the *consumption of time and additional costs* and the *precision and trueness of the determination*.

SRTK is competing against conventional methods when the task is either determination of absolute orthometric heights or determination of relative differences in orthometric heights. The most used conventional methods are;

- GNSS with RTK corrections from a network service (NRTK)
- Geometric levelling

In the following, the performance of the bullets above will be compared to the performance of SRTK in relation to DRP's. In the comparison, it is assumed that the DRP is already established, and equipped with an absolute orthometric height.

SRTK vs. NRTK

SRTK is a little more costly than NRTK, as a result of the need of setting up an extra GNSS antenna. On the other hand, it is significantly more accurate when determining orthometric heights and relative differences between orthometric heights, when short baselines are used (<5km). At longer baselines, NRTK might be superior. In general, the NRTK is more versatile and a more "plug and play" solution, but also a solution where it can be difficult to know what you get. By establishing the base by yourself, you will have knowledge about baseline length and reference height, which is essential when making predictions about the output.

SRTK vs. geometric levelling

SRTK are obtaining precisions comparable with low-end levelling equipment, but with a significantly lower workload. Geometric levelling requires at least two persons, where SRTK only requires one. Precisions of high-end geometric levelling are superior to SRTK. Two GNSS antennas are more expensive than a levelling instrument. It is easier to perform several occupations of the points of interest with SRTK, with levelling a whole new run that needs to be performed. Assumably the SRTK does not perform well in a multipathing environment, where geometric levelling does not suffer precision-wise.

The applicability is present, when assessing SRTK in relation to DRP's, though both pros and cons can be stated when compared to conventional methods. In the following chapter, specific tasks are presented where the SRTK shows promising potentials.

Potential for SRTK in interaction with the DRP 14

The present chapter is assessing the potential of the DRP in general and in interaction with SRTK. The *potential* differs from the *applicability* as potential demands a demand for the technology. The current chapter is assessing possible demands and various tasks, to discuss the level of potential.

14.1 Satellite data and radar reflectors

Despite the Sentinel program is relatively new, the potential usage of satellite data is widely acknowledged. The joint publication “Danish uses of Copernicus” presents 50 user stories with different usage of Sentinel data [SDFE et al., 2021]. The purposes can be monitoring floods or coastal dynamics, or detection of specific vegetation, but also several different purposes regarding heights. These purposes include screening for land subsidence, detection of changes of buildings or sewer systems, or monitoring the effect of building activity. Figure 14.1 shows an example where Geopartner has used Insar radar data for detection of land subsidence.

In general, the majority of the purposes regard land subsidence, water, or climate changes. In Denmark, all of these are topics of immediate interest, for good reason when considering the low elevation and porous underground. Like many other countries, the biggest cities, and therefore a large part of the societal values, are placed in coastal areas with higher risks regarding climate changes and rising sea levels.



Figure 14.1: Screening for land subsidence in Thyborøn, Denmark - by Geopartner [Vognsen et al., 2020]

Radar reflectors

According to Geopartner, the reflector secures a strong and explicit return of the radar signal, which can be used to calibrate the signal from the surrounding natural objects. This will offer higher precision of the monitored natural objects. The reflector can also be placed directly on for example buildings or water level gauges for monitoring. [Inspections, 2021] Radar reflectors are an interesting and relevant product for all areas with increased risk of land subsidence such as coastal areas, harbours, or constructions close to the water, sewer systems, or areas with underground extraction or storage [Vognsen, 2021]. It is assumed that the present interest in construction or land subsidence, climate changes, and satellite data in general, is a basis for expansion potential for radar reflectors.

14.2 The dynamic reference point

The idea of using the reflectors as a dynamic reference point can be considered as a link between the radar technology and physical reference points. In this regard also a link to the absolute reference system, DVR90. The ability to stake out accurate heights does not seem to be a hot topic when compared to the immediate interest in relative monitoring and detection. However, if there is a potential of expanding the usage of radar reflectors and possibly build up actual reflector networks, the cost of the extended purpose as a DRP is minor. There might be a cost related to geometric levelling to provide an orthometric height when establishing the DRP, but if the reflector was to be established anyway the additional cost is limited. Maintenance costs in the following years will benefit from the continuous and free radar data.

Reference system

According to SDFE, the strategy for the Danish height reference system DVR90 is to continue maintenance of local reference points by levelling. SDFE also considers the possibility of reducing the amount of levelling in areas where the need for updated reference points is limited. According to the strategic publication, SDFE is examining the need for a new height reference system and declares it is possible after 2025 when having a larger series of data from permanent GNSS stations. [SDFE, 2017]

A height reference system with reliable and available physical reference points is an extensive assignment with continuous cost. To make the reference network available in every part of the country, there are today about 67,000 local height reference points in Denmark [SDFE, 2021a], which requires a considerable amount of work to maintain. However, regular maintenance is necessary to sustain a reliable and accurate network due to subsidence or damaged points. Many of these local points are levelled decades ago why regular maintenance is deficient.

DRP's as part of the reference system

It is assessed that the DRP has the potential to be a part of a future height reference system with its ability of low-cost maintenance and continuously updated reference heights.

The process of calculating precise relative movements of the DRP is not necessarily simple and must be based on larger data series, but it is assumed that upscaling of this process has the potential of significant cost reductions. Radar images cover a width of 250 km, and it is assumed that a larger number of DRP's potentially could be calculated as a part of a joint process. Compared to levelling, where every point must be visited physically with no possibility of large-scale cost reduction, this is a major advantage.

Large-scale potential

It seems reasonable to assume that radar technology and possibly DRP's will be used as high-class reference points in the future. It is more questionable if the technology can be extended to a larger network of reference points and thereby function as local reference points. Geopartner considers the major cities, harbour areas, or critical coastlines the natural customers in Denmark for a DRP solution. Regarding the major cities, even a few DRP's could provide an accurate and reliable reference for a large number of tasks and applications due to continues urban development nearby. Many of the harbour areas in danish cities undergo intensive urban development as well. These areas in the cities are attractive, but also at high risk land subsidence when large buildings are placed close to the sea or fjords. This results in the potential of monitoring buildings and harbour areas for subsidence using radar reflectors. Outside the urban areas, critical coastlines such as dams and protective installations at the Danish west coast. Geopartner has developed different radar reflectors with consideration to the cost because a cheaper product is easier to sell and more likely to be a widespread solution.

14.3 Potential of SRTK in interaction with the DRP

As presented, there is a larger catalogue of potential usage of radar reflectors and radar technology in general for monitoring or detection. The exact usage of the radar reflector as a "dynamic reference point" regards the ability to determine or stake out absolute orthometric heights. SRTK in interaction with the DRP can be considered as a derived purpose, and the additional cost for this purpose is almost not present. The DRP is established with a mount for the GNSS antenna, which needs to be provided with an offset value. Afterwards, there is no additional cost regarding the SRTK.

The DRP has excellent potential regarding the supply and utility industry for the registration of supply lines. Also, the construction phase will benefit from this solution, where especially the construction of sewer systems is completely dependent on accurate orthometric heights. Climate adaption or water protection is also a current issue with the demand for accurate heights. For both the utility industry and climate issues the requirement is often an accuracy of 1 cm (95%). The current reference system can be challenging when accommodating these requirements, where for example accurate heights in harbour areas can be almost impossible. [Vognsen, 2021] The requirement for 1 cm accuracy could be met by a DRP and SRTK solution for baselines up to about 2 km. Repeated and independent measurement can improve precision, and thereby potentially increase the baseline length and still meet the requirement.

The process of doing geometric levelling is very resource-demanding, and if SRTK could replace some of the tasks it would be a major advantage. One employee and an SRTK solution have the potential of much higher performance than two employees doing geometric levelling. Regarding the resources, SRTK has great potential, and it will probably be a relevant solution for numerous tasks, where the requirement is accuracy of about 1 cm. Compared to levelling, a fast SRTK solution can also be more convenient regarding bad weather, which can be challenging when levelling. SRTK will also be convenient regarding hostile terrain where levelling is difficult or the ability to stake out a height for a pole in the water. [Vognsen, 2021]

Conclusion - Part III - Applicability and potential

15

The current chapter is answering research question 3; *"How is SRTK in interaction with the DRP applicable, and what is the potential?"*

For SRTK two GNSS receivers are needed, which can be costly compared to levels. However, the setup will benefit from the potential of only one employee doing more work than two employees could do with levelling. The SRTK setup relatively simple, but for this project, there have been transmission problems for the used equipment. These problems are to be fixed by the manufacturer and it is assessed that SRTK can work efficiently when startup troubles have been solved. However, SRTK will not be as convenient as NRTK.

It is assessed that Denmark is a country with significant potential for using radar technology as a piece of efficient equipment to monitor vertical movement. The soft and porous underground combined with long coastlines makes land subsidence and protection against climate changes a topic of immediate interest. Radar reflectors can improve the effectiveness of radar data by giving a more precise output or by monitoring objects or areas which otherwise were not possible. Coastal areas, harbours, large constructions, or areas with increased risk of land subsidence could benefit from radar reflectors.

Radar reflectors can work as dynamic reference points (DRP) and will benefit from a high accuracy and relatively easy and inexpensive maintenance. It is assessed that DRPs has the potential of being a part of a future height reference system in Denmark, where larger cities and coastal areas are assessed to be the most obvious fields for application. DRPs are established with mounts for GNSS antenna and can be used for SRTK with no additional cost.

In practice today, geometric levelling is an expensive procedure, and in some cases, it can be difficult to meet customer requirements of for example 1 cm accuracy because of unreliable reference points. The DRP can deliver high accuracy and reliability as a reference point, and SRTK has the potential for significant cost reductions compared to levelling.

Part IV

Main conclusion, discussion and perspectives

The current chapter is answering the problem statement;

What are the capabilities of single-baseline RTK in interaction with the “dynamic reference point”?

The word *capabilities* have been divided in different parameters; *precision*, *accuracy* and *applicability and potential*, all in relation to the determination of orthometric heights.

The *precision* of one SRTK observation (with a time-averaging window of 60 sec.) in optimal conditions can be described with a basic error of 2.4 mm and a distance-dependent error of 1.3 *mm/km*, with baselines up to 5 km. With longer baselines, up to 32.6 km the precision have been examined to be 5.3 mm + 0.3 *mm/km*. Assessment of the time averaging window showed no notable improvement in precision for longer time windows. Same assessment showed that time averaging windows shorter than 60 seconds, likewise results in no notable difference in the precision.

The *accuracy* of an orthometric height determined by GNSS is depending on the accuracy of the used geoid model and the accuracy of the measured ellipsoidal height. The term accuracy relies on the terms *precision* and *trueness*. Two geoid models have been examined, none of them is perfect in terms of trueness, where deviations in the magnitude of a cm can be seen. Both geoid models are though showing a high degree of precision, at least within a horizontal distance of 1,500 m, where the numeric bias is constant. When using a DRP, equipped with an accurate orthometric height as a base station, the bias mentioned above can be neglected, as they are corrected by the DRP. When assuming the DRP is the "true" orthometric height, an SRTK setup with the base station in a DRP can obtain absolute accuracy in magnitudes equal to the precision, 2.4 mm + 1.3 *mm/km*, within short distances - in test scenario with baseline lengths up to 1500 m.

In the project test scenario, the ellipsoidal heights suffer from a systematic lack of trueness, which assumable is caused by the difference in orthometric height of the base and rover. It is assumed that the bias is caused by incorrect modelling of differences in tropospheric delay biases in the rover. If the modelling can not be improved, it is necessary to keep a close relationship between the orthometric height of the base and rover.

According to the *applicability* of the technology, it can be stated that SRTK is significantly less time-consuming than conventional methods (geometric levelling) but less accurate. It is assessed that SRTK in interaction with the DRP obtains reasonable accuracy, which is applicable in surveying workflows. When using the DRP and having knowledge about the baseline length it is possible to have more specific anticipation about the output's level of precision and accuracy. This can enable a series of tasks to be measured by SRTK and the DRP, which were not possible for NRTK.

When discussing the *potential* of the DRP in general and specifically the SRTK in inter-

action to a DRP, the need for accurate orthometric heights can be stated to be increasing. The DRP itself can be used as a subsidence monitoring technology, with higher precision than when only using the reflection of natural objects. The DRP will also have the potential for being a part of a future height reference system, with continuously updated reference heights. Using the DRPs for SRTK is a derived purpose with very limited additional cost, and combined with the potential of the DRP it is assessed that the solution has a relevant potential. Tasks such as registration of utility supply lines, where accuracy requirements of 1 cm (95%) are common, will be a relevant market for the technology. A DRP and an SRTK setup can potentially deliver the required accuracy within a radius of about 2 km by performing one measurement and about 4 km performing two independent measurements. For numerous tasks, this will be a basis for a significantly lower workload than the conventional method; geometric levelling.

The conclusions are stated with various disclaims. The capabilities of SRTK in relation to DRP's will vary if used under different conditions, with different hardware or in locations where the geoid model might not hold the same level of precision.

Discussion 17

Current chapter present a discussion about the projects test methods related to the conclusions. The subject of the base rover setup, general precision of the geoid model, and the test conditions have been found relevant.

No testing of actual base and rover setup

To test the performance of SRTK, the preferred test method was a base and rover setup where regular survey GNSS receivers were used. This was a natural choice as this would be the realistic setup when using the DRPs. However, software and transmission problems made this assessment impossible, or at least very difficult to carry out for the project testing. This resulted in an alternative test approach were permanent, but single reference stations at the test facility TAPAS were used.

This test approach will to some extent be deficient regarding knowledge about how the actual SRTK and DRP setup will perform. It is assumed that concluded level of precision will be nearly identical with a manual base and rover setup. Regarding the accuracy, the manual base setup would allow the opportunity to modify the reference height and thereby fit the geoid model, which was not possible with the alternative test setup. This issue was assessed and simulated in the project and should work in practice without further consideration. Initially, it was also the intention to use a test area with a larger network of high precision levelled reference points. Due to resources and ability, it has not been possible for the project group to perform levelling to the same extend. SDFE has provided information about reference points and earlier levelling in the used test area, which can partly compensate for this matter.

Overall a base and rover setup would have been a more realistic, and therefore better test solution. However, the chosen alternative test solution is assessed to give a comprehensive conclusion about SRTK precision and the distance-dependent error. Positively, the test facility TAPAS allows easy testing of longer baselines and larger-scale assessment of the geoid model.

General precision of the geoid model

The project aims to examine the SRTK and DRP method as a general solution for orthometric height determination in Denmark. The precision of the ellipsoidal heights is universal and assessed to be valid in general for SRTK measurement under similar conditions. Due to the geoid model, it is difficult to assume that the same level of accuracy can be obtained everywhere. However, the concept of the DRP allows fitting the geoid in that specific point. The accuracy then comes down to how precise the geoid model is, and in test scenarios within a limited distance to the DRP. It is known that the geoid model has lower precision in coastal areas, but apart from that, it is assumed the geoid will have a very limited effect on the accuracy over short distances [SDFE, 2021b] [Vognsen, 2021].

Optimal or realistic test conditions

The testing of SRTK in the project is performed under conditions, which can be considered optimal. This has intentionally been the aim for the testing for better isolation of the distance-dependent error. Various test points were located relatively close to smaller buildings or a tree, but overall, the conditions should be close to optimal. However, optimal conditions are not always available, which is a well known disadvantage for GNSS. Naturally, the result from this project is not obtainable at every task due to various GNSS conditions. It can be discussed if the project should test under more challenging surroundings and conditions to provide a conclusion on a more general and realistic precision and accuracy. For this project, it has been prioritized to collect a larger number of data, including data from several days of data collection to have variation in satellite constellation and weather conditions. This is a comprehensive approach, and if this had to be extended by more test scenarios with various surroundings, it is assessed to be too resource-demanding for this project.

One of the key potentials for the DRP and SRTK is however larger cities, where few DRP's potentially could be the basis for larger output due to extensive usage nearby. However, the urban environment is also a well-known challenge for GNSS. Multipath and fewer satellites result in the dense urban environment being very unsuitable for the GNSS survey. The modern multi-frequency receivers used in this project should in theory be more robust regarding multipathing, but as mentioned this is not tested. It is assessed that the dense urban environment will lower the precision, and since this is a field of potential it can be argued that tests under these conditions should be performed.

Perspectives 18

In the essence of this thesis, the assumed causations regarding SRTK and the DRP were confirmed. Short baselines result in high precision, and by correcting the bias in the geoid model by the DRP high accuracy is also possible. In the end significantly more accurate orthometric heights than NRTK, but not quite the precision like geometric levelling. Again, the expected outcome by a solution in between NRTK and levelling, when it comes to precision, but also when considering the workload. It is easy to imagine numerous tasks where the SRTK and DRP solution would be suitable, but the DRPs are not there yet.

It can seem unrealistic to believe that a larger network of DRPs covering the majority of Denmark will be here anytime soon. The expenses to such a network would simply be too high compared to the immediate profits. For many tasks, the absolute accuracy is not relevant, and when it is, surveyors seem to manage it just fine. But in a more long-term perspective, the possible social economy profit might be there by having a more accurate official height reference system to base different services and sectors upon. This social or governmental interest for investing in height reference infrastructure could be a derived consequence of interest in protection against climate changes.

A more realistic scenario is private or public-private partnerships to be investors in DRP solutions. Utility companies, large production or energy facilities, or harbours could be realistic stakeholders. Either due to the vast need for accurate orthometric heights or because a whole facility could benefit from just one DRP. Public interest could more likely come from the municipality of larger cities where the possible benefit would be significant from even a few DRPs. As an example, the whole city community of Aalborg could be covered by about 5-6 DRPs if the requirement is a maximum baseline length of approximately 2 km. Aalborg has about 140,000 residents and the area is known for the high occurrence of subsidence and unreliable reference points due to soft underground. It is relatively easy to imagine the potential if the fourth largest city in Denmark with all its urban development, subsidence, and flood risk can benefit from just 5-6 DRPs.

However, as mentioned in the discussion, a dense urban environment and GNSS survey is not a desirable combination. Multipath and a general basis of fewer satellites due to the limited view will affect the precision - also when using SRTK. If the urban areas are core stakeholders for DRP investment, further studies of the performance of SRTK in this environment should be carried out. It is essential to know what to expect from SRTK in this environment, but also knowledge about how to prevent significant influence by the well-known urban challenge. New multi-frequent receivers should be more resistant to multipath and could be a requirement in the urban environment. Studies of how a higher cut-off angle affects precision could also be interesting. The higher cut-off angle should increase the resistance against multipath as well, and today's high number of available satellites makes this a relevant approach.

Bibliography

- Emardson et al., 01 2010.** Ragne Emardson, Per Jarlemark, Jan Johansson, Sten Bergstrand, Martin Lidberg and Bo Jonsson. *Measurement Accuracy in Network-RTK*. Bollettino Geod. Sci. Affini, 2010.
- European Union, 2020.** European Union. *Homepage Copernicus*. <https://www.copernicus.eu/en>, 2020. Visited: 02-03-2021.
- GeoTeam A/S, 2021.** GeoTeam A/S. *GPSnet, Network RTK*. http://produkter.geoteam.dk/Produktblade/GPSnet/GPSnet_landmaaling.pdf, 2021. Visited: 08-01-2021.
- Grubbs, 02 1969.** Frank E. Grubbs. *Procedures for Detecting Outlying Observations in Samples*. Technometrics, 11, 21, 1969.
- Hofmann-Wellenhof et al., 2008.** Bernhard Hofmann-Wellenhof, Herbert Lichtenegger and Elmar Wasle. *GNSS – Global Navigation Satellite Systems*. ISBN: 978-3-211-73017-1, eBook. Springer-Verlag Wien, 2008.
- Inspections, 2021.** Geopartner Inspections. *Radarreflektorer*. <https://geopartner-inspections.com/services/opmaaling/geodaetisk-opmaaling/radarreflektorer/>, 2021. Visited: 25-05-2021.
- Janssen et al., 02 2012.** Volker Janssen, Joel Haasdyk and Simon Mcelroy. *Real-time GNSS field procedures: Maximising gain and minimising pain*. Position, 57, 24–27, 2012.
- Keller and Forsberg, 2020.** Kristian Keller and René Forsberg. *En ny nøjagtig geoid – til et GNSS-baseret højdesystem*. GEOFORUM PERSPEKTIV, 37, 6, 2020.
- Leica Geosystems, 2021a.** Leica Geosystems. *Leica GS18I GNSS Antenna - Data Sheet*. https://leica-geosystems.com/-/media/files/leicageosystems/products/datasheets/leica_gs18i_ds.ashx?la=da&hash=F864CBE724FA04F778FB1325A4E6307A, 2021a. Visited: 08-01-2021.
- Leica Geosystems, 2021b.** Leica Geosystems. *Leica SmartNet, Network RTK*. <https://hxgnsmartnet.com/da/services/netvaerks-rtk>, 2021b. Visited: 08-01-2021.
- Luo et al., 2017.** Xiaoguang Luo, Jun Chen and Bernhard Richter. *How Galileo benefits high-precision RTK*. GPS World, August 2017, s. 22–28, 2017.
- Maciuk, 06 2018.** Kamil Maciuk. *Advantages of combined GNSS processing involving a limited number of visible satellites*. Scientific Journal of Silesian University of Technology. Series Transport, 98, 2018. doi: 10.20858/sjsutst.2018.98.9.
- Menditto et al., 2007.** Antonio Menditto, Marina Patriarca and Bertil Magnusson. *Understanding the meaning of accuracy, trueness and precision*. Accreditation and Quality Assurance, January 2007, 2007.

- Mohd Razali and Yap, 01 2011.** Nornadiah Mohd Razali and Bee Yap. *Power Comparisons of Shapiro-Wilk, Kolmogorov-Smirnov, Lilliefors and Anderson-Darling Tests*. J. Stat. Model. Analytics, 2, 2011.
- Olynik et al., 2002.** Michael Olynik et al. *Temporal characteristics of GPS error sources and their impact on relative positioning*. University of Calgary: Calgary, Canada, 2002.
- PennState, 2021a.** PennState. *GEOG 862: GPS and GNSS for Geospatial Professionals - Relative Positioning*.
<https://www.e-education.psu.edu/geog862/node/1725>, 2021a. Visited: 09-02-2021.
- PennState, 2021b.** PennState. *GEOG 862: GPS and GNSS for Geospatial Professionals - User Equivalent Range Error*.
<https://www.e-education.psu.edu/geog862/node/1713>, 2021b. Visited: 18-03-2021.
- SDFE, 2012.** SDFE. *DKGEOID12A*.
https://www.isgeoid.polimi.it/Geoid/Europe/Denmark/denmark12A_g.html, 2012. Visited: 31-03-2021.
- SDFE, 2021a.** SDFE. *Nationale referencenet i Danmark, Grønland og Færøerne*.
<https://sdfe.dk/saadan-arbejder-vi-med-data/geodaesi-og-referencenet/nationale-referencenet-i-danmark-groenland-og-faeroerne/>, 2021a. Visited: 09-02-2021.
- SDFE, 2020.** SDFE. *C17 Thyborøn By og Havn - Klima, kloak og sætninger*.
https://sdfe.dk/media/2920029/monitorering-af-infrastruktur-og-landbevaegelser-fra-satellit_2020.pdf, 2020. Visited: 02-03-2021.
- SDFE, 2021b.** SDFE. *Interviews with Kristian Keller, Geodesist*, 2021b. Interviews held in the spring of 2021.
- SDFE, 11 2017.** SDFE. *Strategi for Danmarks geodætiske infrastruktur 2015–2025*. Geomatics Notes 4, 36, 10, 2017.
- SDFE, 2021c.** SDFE. *Valdemar - Archive of the danish reference points*.
<https://valdemar.kortforsyningen.dk/>, 2021c. Visited: 31-03-2021.
- SDFE et al., 2021.** SDFE, SFU and DTU Space. *Danish uses of Copernicus - 50 user stories based on earth observations*.
https://sdfe.dk/media/6611/copernicus-eng_digital.pdf, 2021. Visited: 25-05-2021.
- Skoffer and Larsen, 2019.** Esben Kudsk Skoffer and Peter Dietz Larsen. *TAPAS - A new RTK standard?* [https://projekter.aau.dk/projekter/da/studentthesis/tapas--a-new-rtk-standard\(692dc8d8-27a5-4181-bf6f-5ef3a0d09e3f\).html](https://projekter.aau.dk/projekter/da/studentthesis/tapas--a-new-rtk-standard(692dc8d8-27a5-4181-bf6f-5ef3a0d09e3f).html), 2019. Visited: 08-03-2021.

Trimble, 2021. Trimble. *GNSS Planning Online*. <https://www.gnssplanning.com/>, 2021. Visited: 08-01-2021.

Trimble Inc., 2021. Trimble Inc. *Critical factors affecting RTK accuracy*. https://www.trimble.com/OEM_ReceiverHelp/V4.44/en/PositionModes_CriticalFactorsRTK.html?fbclid=IwAR1fdmHRk-DMiFFKwF0cy06sJ5tfuEmqWSfdbj30_ITz6kXJp8minQosYfU, 2021. Visited: 31-03-2021.

Vognsen, 2021. Karsten Vognsen. *Interviews with Karsten Vognsen, Chief Advisor, Geopartner*, 2021. Presentations handed out and interviews held in the spring of 2021.

Vognsen et al., 2020. Karsten Vognsen, Niels Broge, Henrik Brændskov Larsen, Søren Holst, Carlo Sass Sørensen and Per Knudsen. *C17 Thyborøn By og Havn - Klima, kloak og sætninger*. https://geopartner-inspections.com/wp-content/uploads/sites/2/2020/06/thyborn-rapport-final_-12062020.pdf, 2020. Visited: 02-03-2021.

Understanding the dynamic reference point

The technology behind the dynamic reference point consists of different elements. The foundation of the continuous relative measurements is the data sets originating from the Sentinel 1 programme. Furthermore, the physical reflector applies the opportunity to track one unique point's vertical movement. In the following the Sentinel programme, and the concept of the dynamic reference point is presented.

A.1 Sentinel 1

The European Unions earth monitoring programme is called Copernicus. The programme aims to deliver different services to the member countries and their citizens, especially by using remote sensing technologies. One of the aims is to deliver radar images, which can be used to compute relative vertical movements of the surface. The Sentinel satellite programme is part of the Copernicus programme. One part of the Sentinel constellation, the satellites Sentinel 1A and 1B delivers radar images, free of charge. The images spatial resolution is 5x20 m. Every 6 days one of the two satellites passes Denmark, which they will continue to do until 2030. [European Union, 2020][SDFE, 2020]

A.2 Dynamic reference point - concept

The concept of the "dynamic reference point" is based on a radar reflector as seen in figure A.1 on the next page and A.2 on the following page. The radar reflector is metal plates forming a half cube, which direction is adjusted for optimal reflection of the electromagnetic waves from the Sentinel 1 radar satellites.

Figure A.1: **D**ynamic **R**eference **P**ointFigure A.2: Height reference point of **DRP**

The reflector returns a strong and definite signal, and by knowledge of wavelength and propagation time, vertical changes of the reflector are detected. The Sentinel satellite passes by every sixth day, and with a long series of data precise vertical changes can be detected, within a magnitude of for example mm/year. The radar reflector works as a link and converter between the relative radar data, and the levelled height at the ground. [Vognsen et al., 2020]

The reflector itself is mounted on an iron pole, which is firmly secured at a concrete foundation or similar. The physical reference point for levelling is mounted at the iron pole as shown in figure A.2. The continuous satellite monitoring of the reflector offers two major advantages for this reference point compared to a classical reference point without monitoring. Firstly, the radar data makes maintenance of the reference point an easy and low-cost task. The reference point could easily be checked for example once a year to secure that the reference point has not been damaged or affected by land subsidence. Secondly, the radar data can be used for directly updating the reference point without the need for any levelling at the ground. Through a continuous data series, it can be detected if a reference point is stable or affected by vertical changes. An unstable reference point can then be given a new reference height every year, every third year, or whatever is assessed to be suitable. This continuous monitoring, checking, and especially the updating possibility is what makes it a dynamic reference point (DRP). Two different time series is seen at figure A.5 and A.6



Figure A.3: Map of position of Radar Reflector *LVS4* [Vognsen, 2021]

Figure A.4: Map of position of Radar Reflector *LVS6* [Vognsen, 2021]

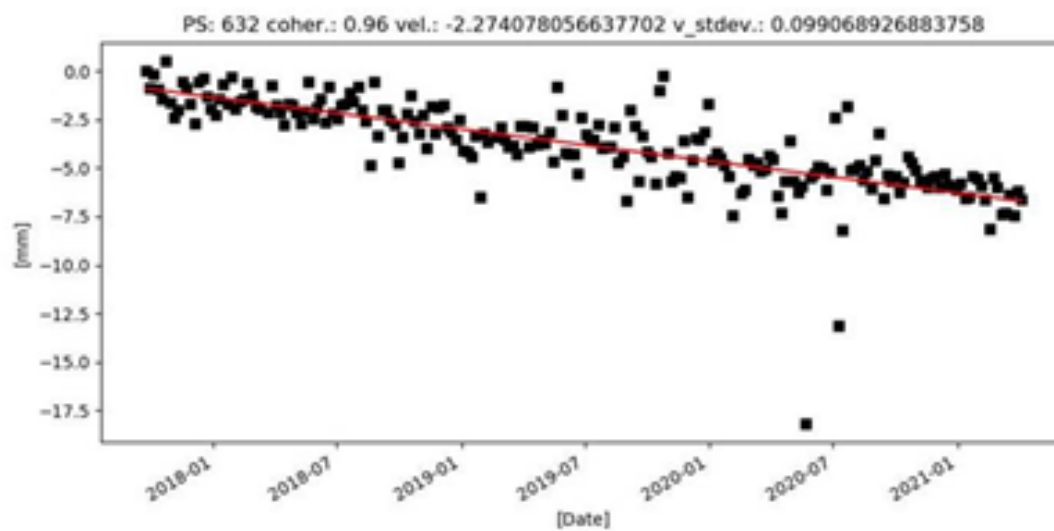


Figure A.5: Time series of Radar Reflector *LVS4* [Vognsen, 2021]

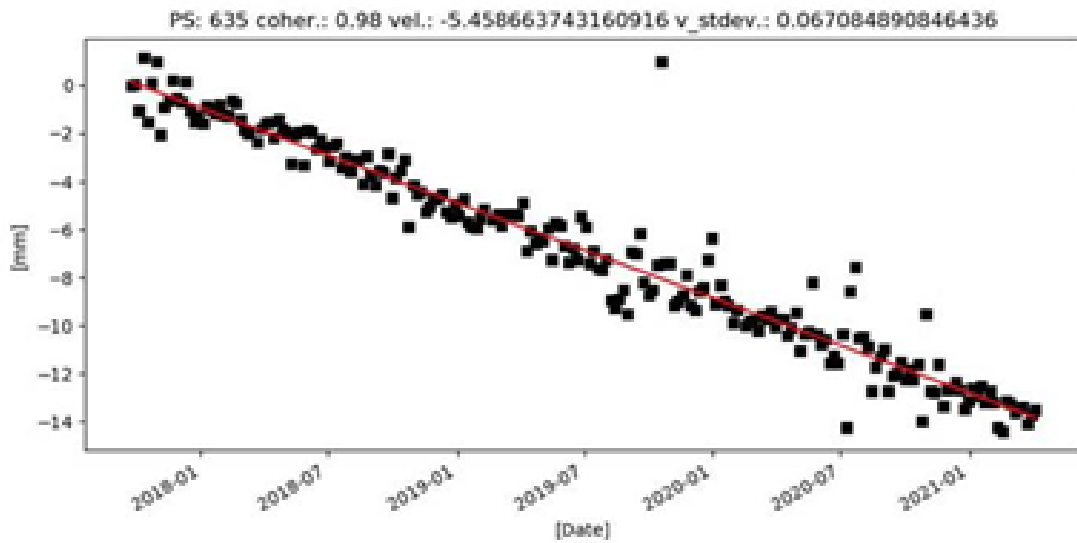


Figure A.6: Time series of Radar Reflector *LVS6* [Vognsen, 2021]

Furthermore, the DRP is prepared for GNSS survey by having a threaded bolt mounted at the top suitable for a GNSS antenna. When the DRP is established, the offset between the reference point the antenna bolt is measured and both of them can afterwards be monitored through data from the reflector. Vertical relative changes can also be calculated of observed "natural reflectors" by InSAR-data. Though the natural reflectors reflect signals with more noise, as seen in figure A.7. Figure A.7 shows the difference between the natura reflection of a concrete pillar, and when a radar reflector was mounted on top of it.

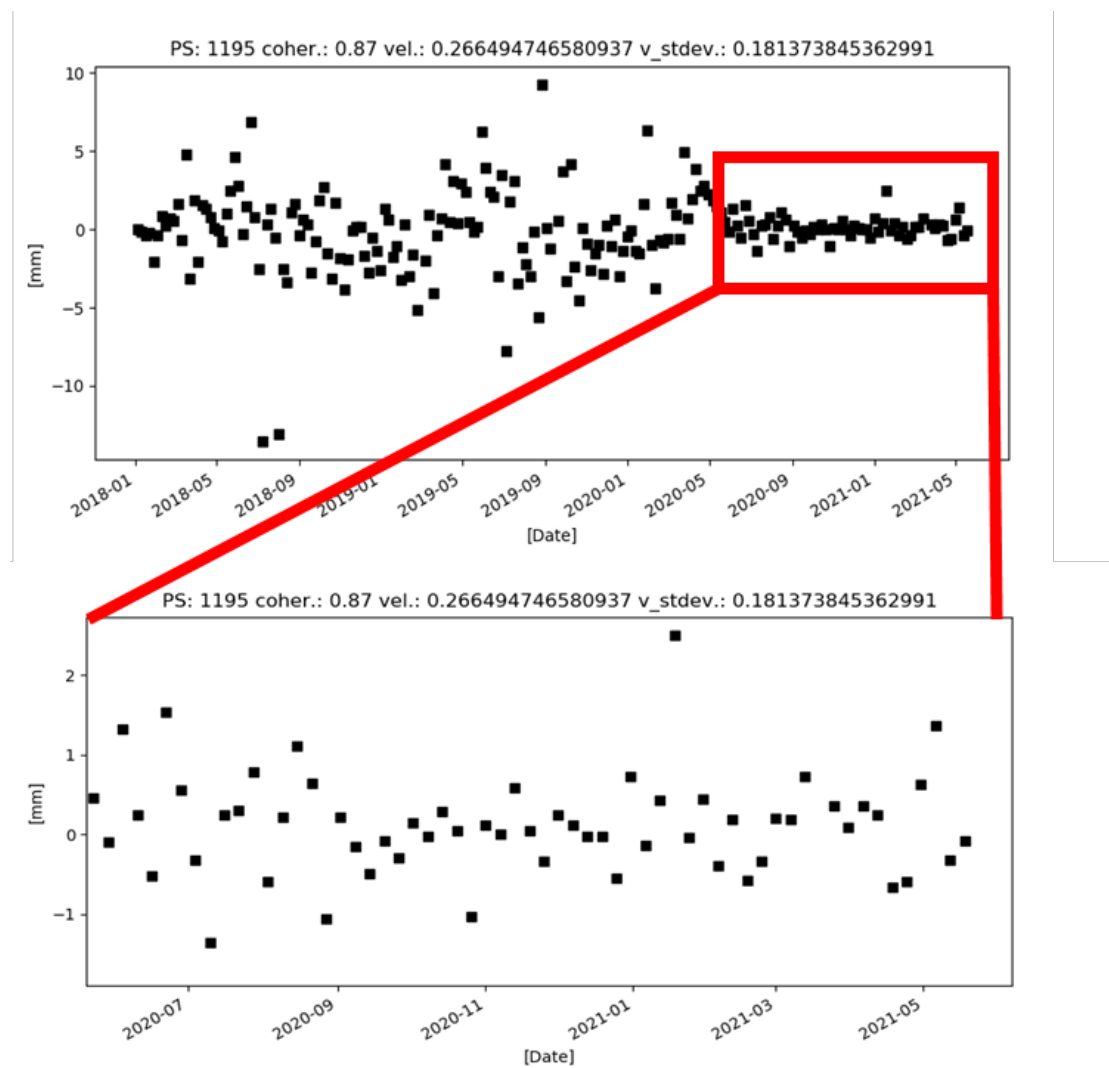


Figure A.7: Difference in noise between natural reflectors and radar reflector [Vognsen, 2021]

More images of the radar reflektor, with a GNSS antenna mounted is seen at figure A.8, A.9, A.10 and A.11



Figure A.8: Photo of radar reflector



Figure A.9: Photo of radar reflector



Figure A.10: Photo of radar reflector



Figure A.11: Photo of radar reflector

Accuracy of RTK GNSS B

The current appendix shows an empiric experience about the orthometric height accuracy of RTK GNSS in Thyborøn, Denmark. The experienced accuracy is probably worse than general, as the geoid model is known for having problems in coastal areas.

[Vognsen, 2021]

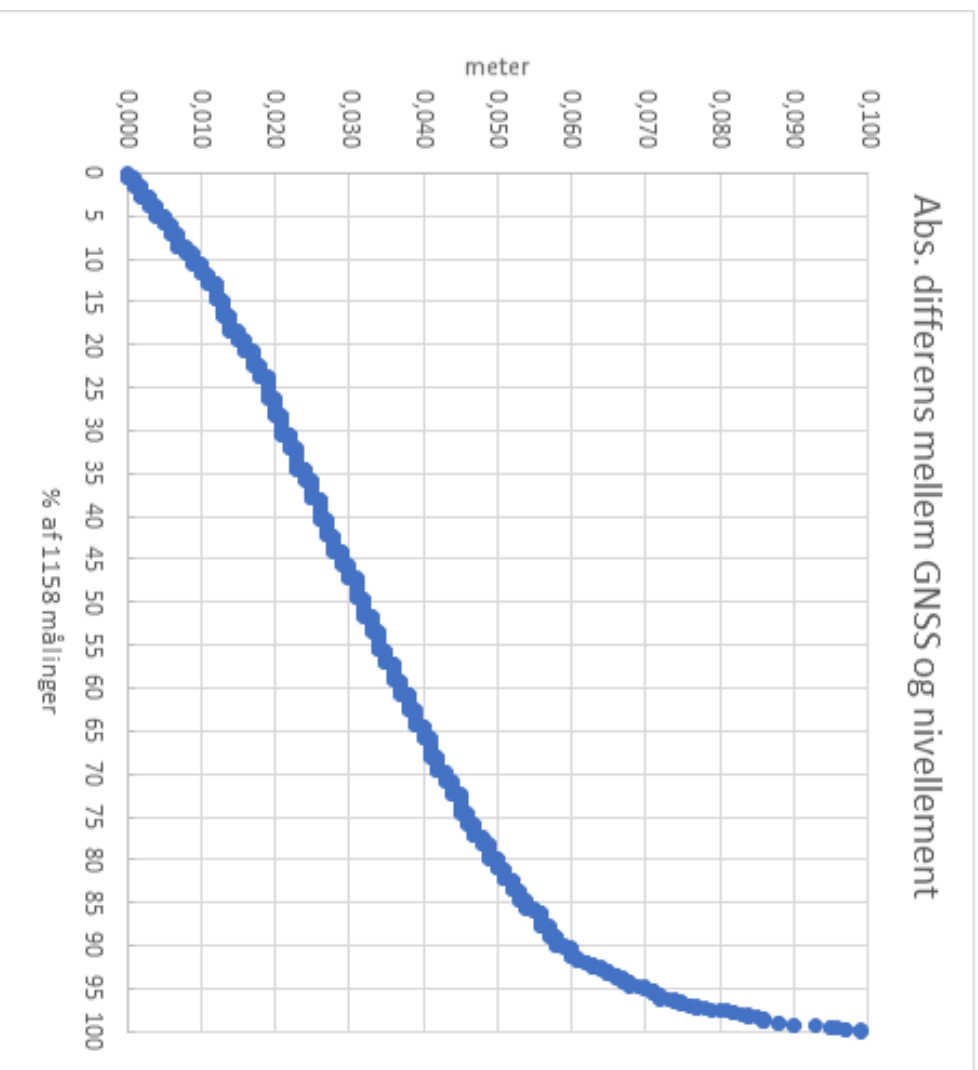
Brøndmålingen



- Fikspunktmåling
- GPS 1189 dæksler
- Nivelleret til 1193 dæksler
- Nedstik i 1137 brønde



GPS nøjagtighed



Beregnet i forhold til
den nivellerede kote
på dækslerne:

R95 = 70 mm

Absolute positioning



An absolute position of a GNSS receiver can be calculated by simultaneously measuring the distance to a minimum of four satellites as illustrated in figure C.1. A minimum of four satellites is to determine the 3D position of the receiver and at the same time calculating a clock error.

The distances to the GNSS satellites are determined by an information code to send out through a radio wave signal from the satellites, including satellite identification, position, time etc. The GNSS receiver is a receiver only receiving the information and, on that basis determining an absolute position.

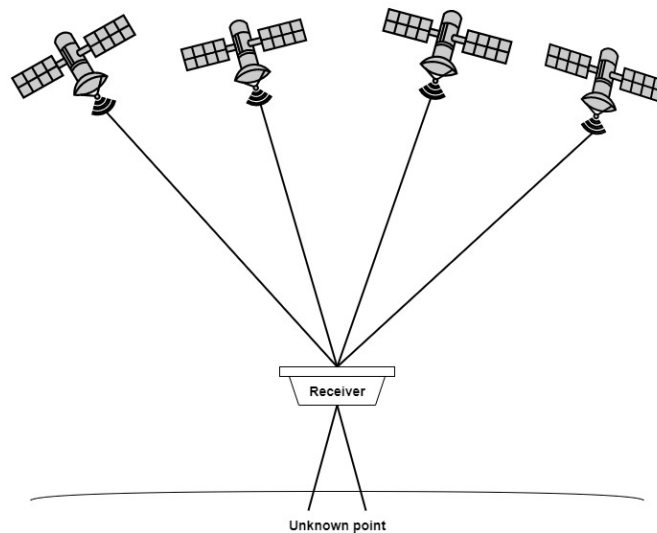


Figure C.1: Principle for absolute GNSS positioning

Due to the uncertainty of the distance to the satellites and the geometry of the satellite constellation, it can generally be presumed that adding more satellite distances to the calculation can improve the accuracy of the determined position of the receiver. Nevertheless, the accuracy of absolute positioning is limited, where high-end receivers can determine positions accurate within a few meters. To achieve higher accuracy the sources of error in the calculation have to be attended to.

C.1 Error sources

The accuracy of an absolute position of a GNSS receiver mainly depends on the precision of the distances and the satellite geometry. The distance precision is affected by error contribution from atmospheric signal delay and imperfect clocks and satellite orbit, which can be defined as “user equivalent range error” [PennState, 2021b]. UERE combines the contribution of the error from satellite clocks, orbit errors, ionospheric delays,

tropospheric delays, receiver noise and multipath. In other words, the UERE is the difference between the true distance and the measured distance as shown in figure C.2. As the absolute position depends entirely on the determined distances the UERE will affect the position accuracy. Calculation models can be set up to limit the error influence, but the accuracy is not suitable for surveying purposes.

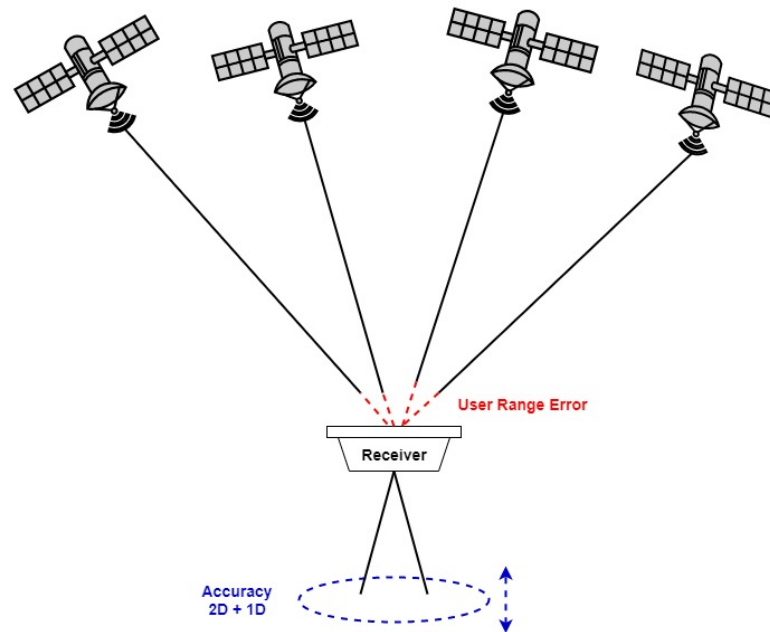


Figure C.2: "User equivalent range error" and accuracy

The calculation of the absolute 3D position is a triangulation based on the distances on a minimum of four satellites. This triangulation can suffer from poor geometry if the satellites are placed in roughly the same direction, and not widely spread out. An increasing number of available satellites improves the opportunity of better satellite geometry, and higher accuracy when the position is calculated with the use of far more than four satellites. The available GNSS programs and new opportunities are presented in section 4.3 on page 21.

**Number of satellites,
DOP-values and elevation
of satellites** D

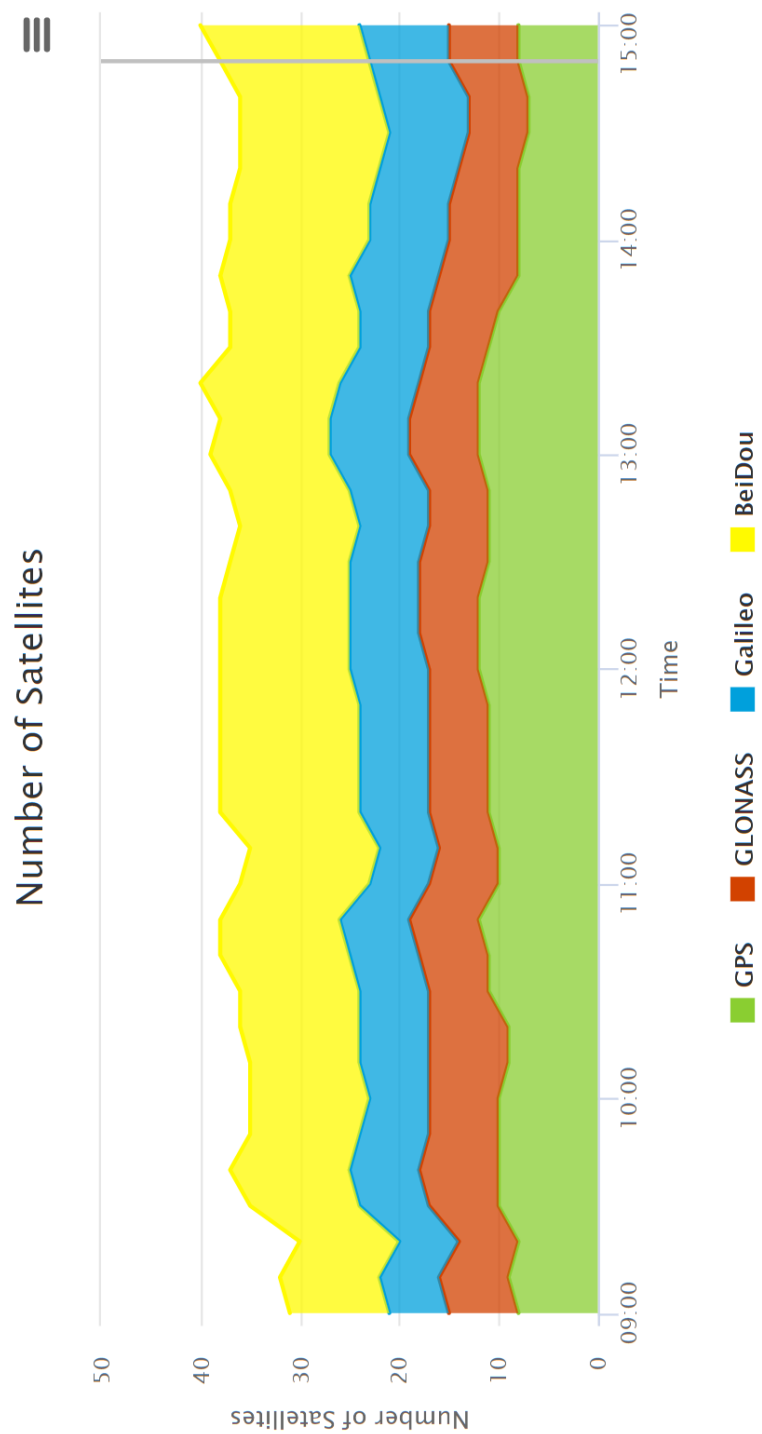


Figure D.1: Number of available satellites in Central Jutland during a random day, with an elevation cut off of 10° [Trimble, 2021]

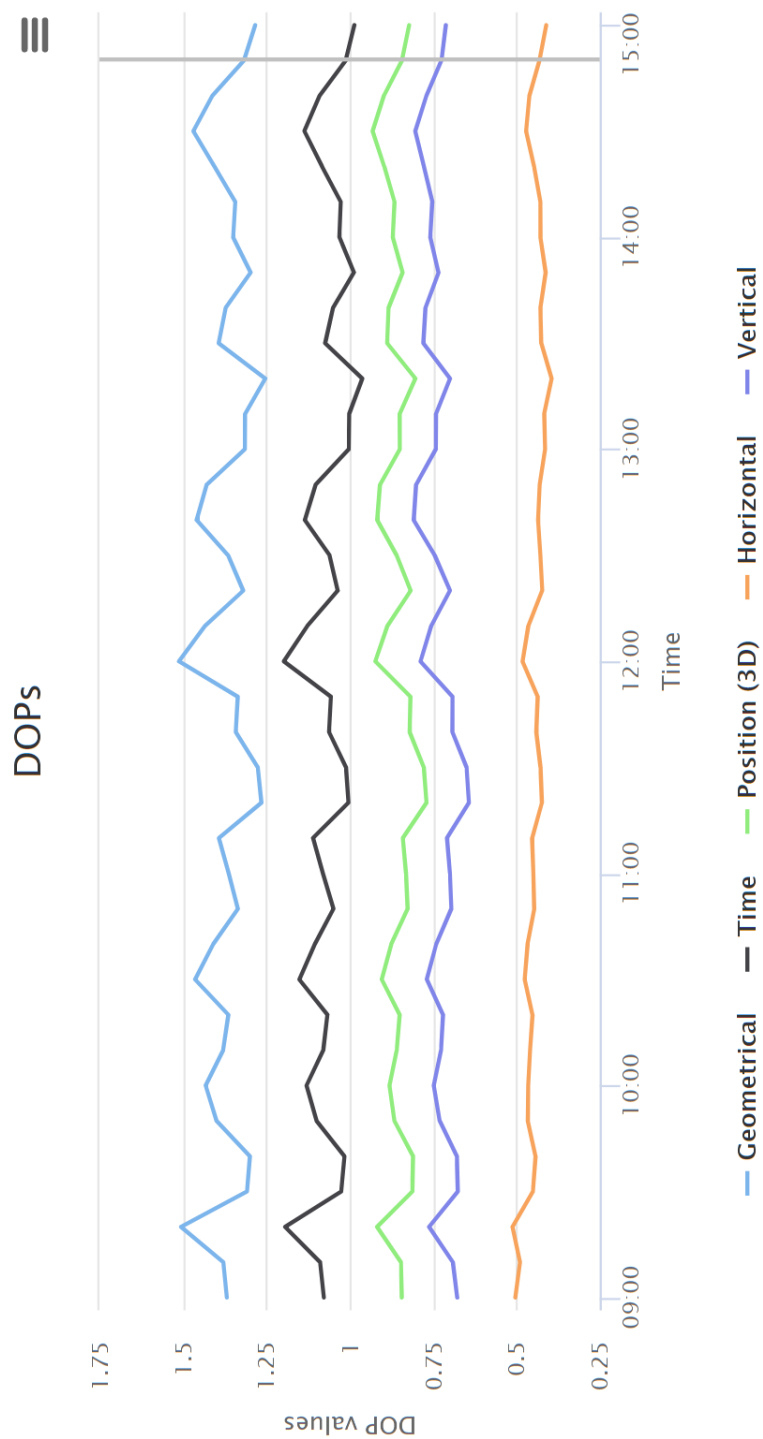


Figure D.2: DOP-values of available satellites in Central Jutland during a random day, with an elevation cut off of 10° [Trimble, 2021]

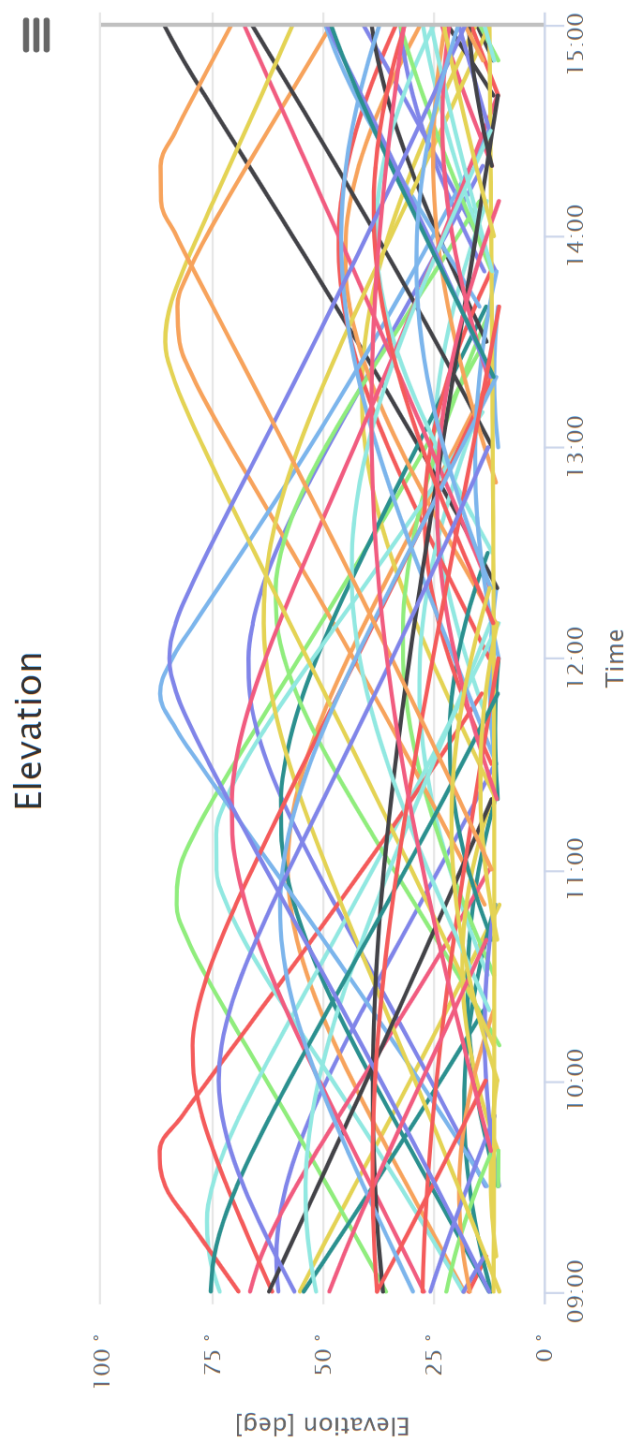


Figure D.3: Elevation of satellites in Central Jutland during a random day, with an elevation cut off of 10°[Trimble, 2021]

**Individual data
examination of test of
averaging time window** E

E.1 Data collected in Aalestrup

Time averaging window of 5 seconds, Aalestrup

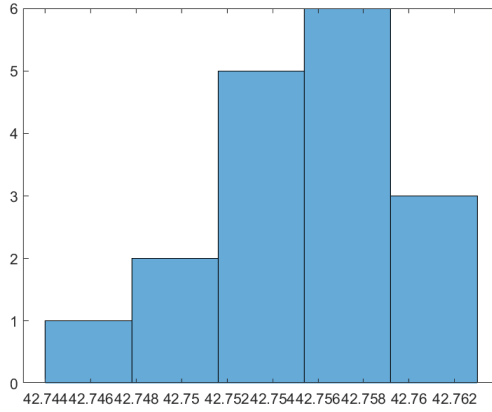


Figure E.1: Histogram - 5 seconds

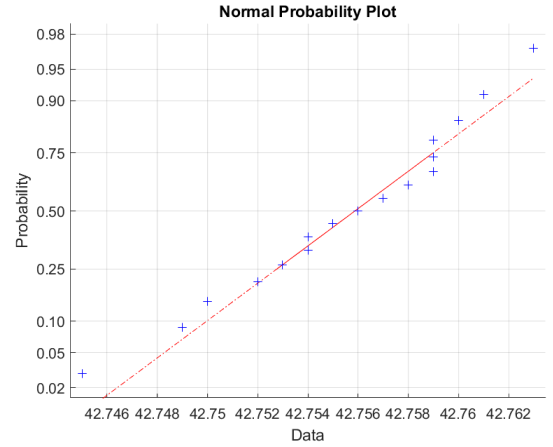


Figure E.2: Norm plot - 5 seconds

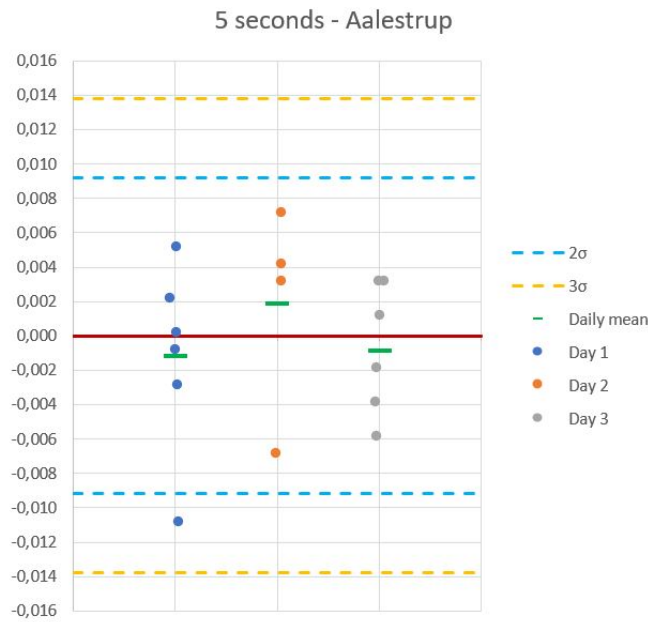


Figure E.3: Plots of observations from different days of collection. 5 second averaging time window

	Accepted	Rejected
Kolmogorov-Smirnov test	X	
Shapiro-Wilk test	X	

Table E.1: Hypothesis testing for normal distribution. H_0 : Normal distributed sample at $\alpha = 0.05$

Time averaging window of 15 seconds, Aalestrup

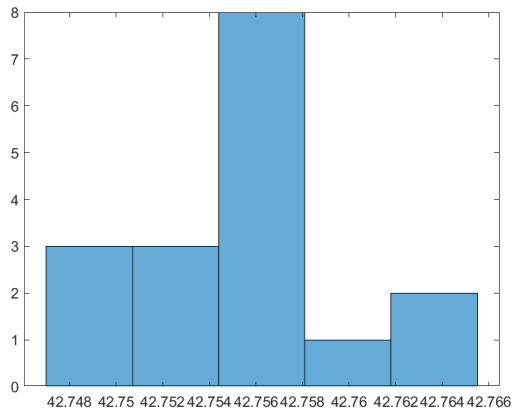


Figure E.4: Histogram - 15 seconds

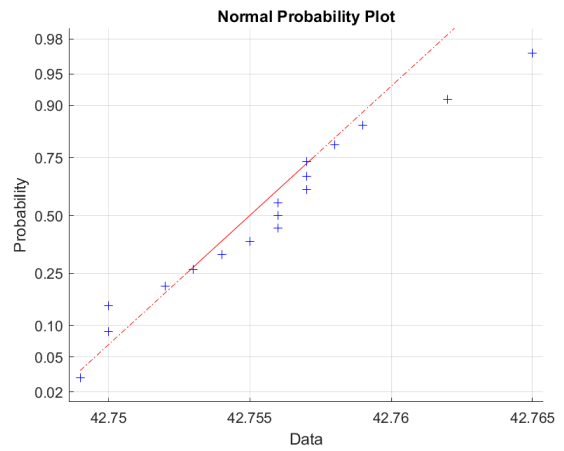


Figure E.5: Norm plot - 15 seconds

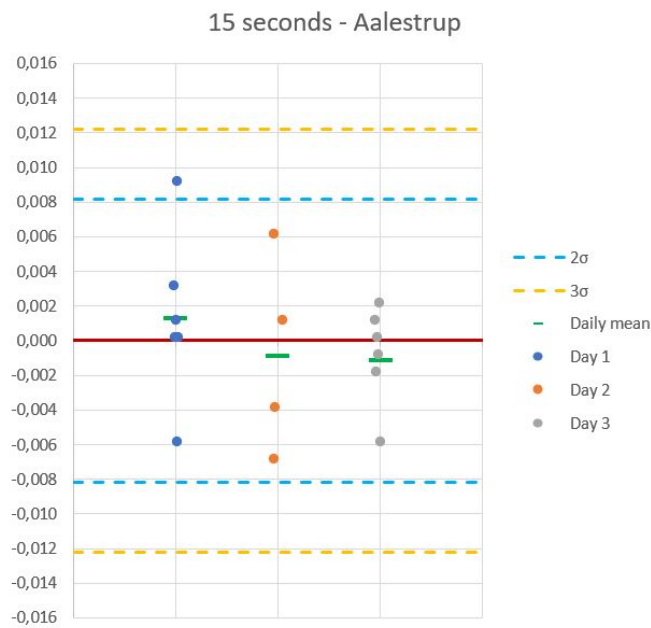


Figure E.6: Plots of observations from different days of collection. 15 second averaging time window

	Accepted	Rejected
Kolmogorov-Smirnov test	X	
Shapiro-Wilk test	X	

Table E.2: Hypothesis testing for normal distribution. H_0 : Normal distributed sample at $\alpha = 0.05$

Time averaging window of 30 seconds, Aalestrup

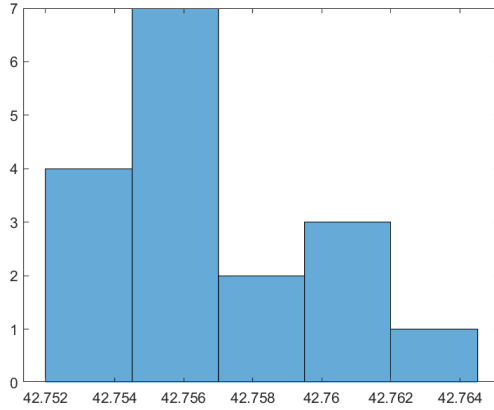


Figure E.7: Histogram - 30 seconds

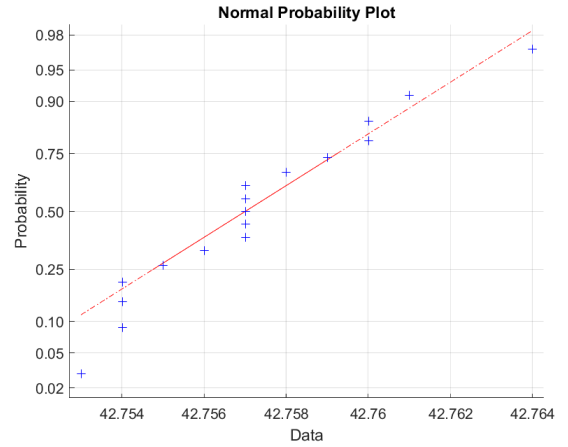


Figure E.8: Norm plot - 30 seconds

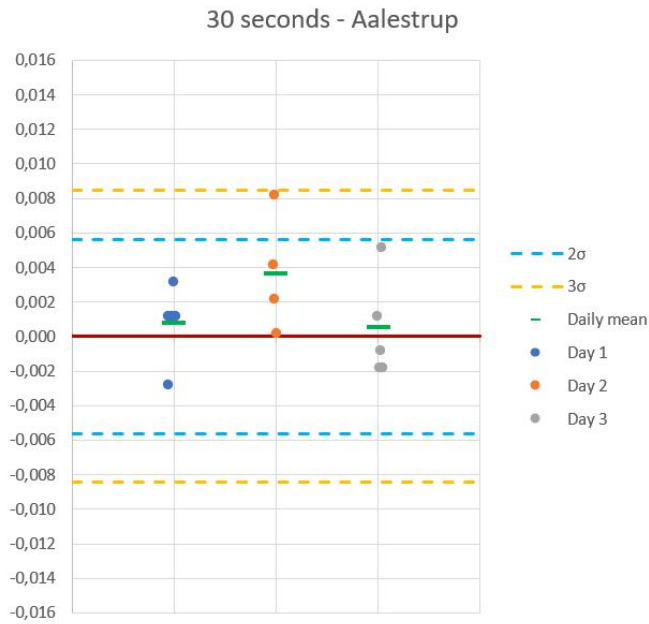


Figure E.9: Plots of observations from different days of collection. 30 second averaging time window

	Accepted	Rejected
Kolmogorov-Smirnov test	X	
Shapiro-Wilk test	X	

Table E.3: Hypothesis testing for normal distribution. H_0 : Normal distributed sample at $\alpha = 0.05$

Time averaging window of 60 seconds, Aalestrup

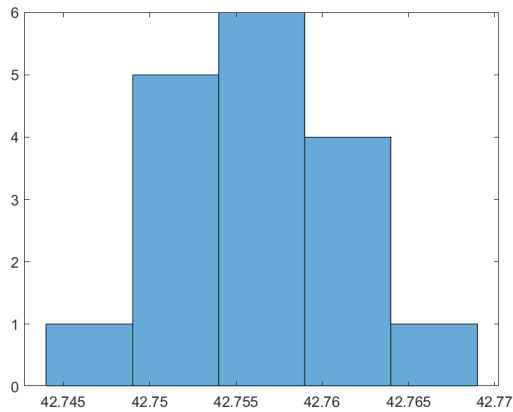


Figure E.10: Histogram - 60 seconds

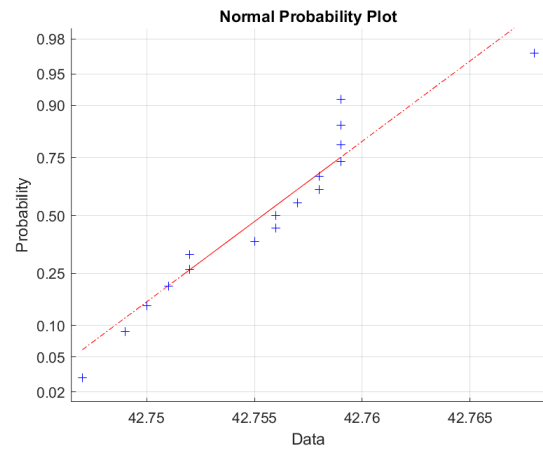


Figure E.11: Norm plot - 60 seconds

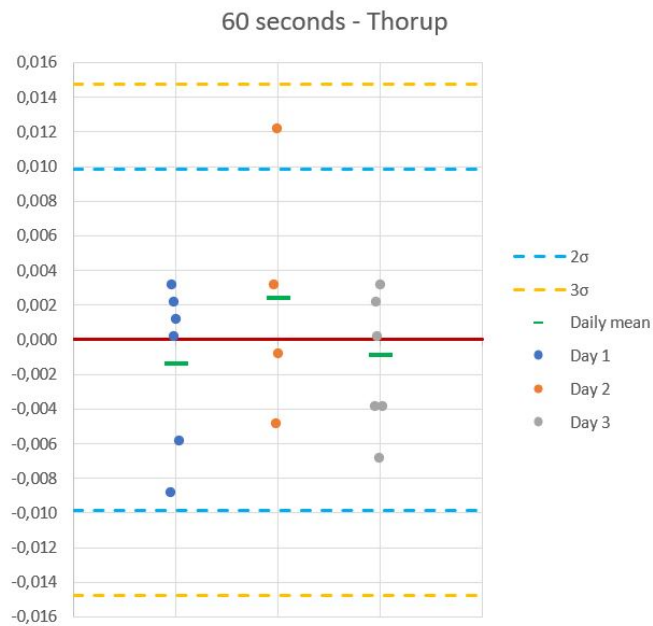


Figure E.12: Plots of observations from different days of collection. 60 second averaging time window

	Accepted	Rejected
Kolmogorov-Smirnov test	X	
Shapiro-Wilk test	X	

Table E.4: Hypothesis testing for normal distribution. H_0 : Normal distributed sample at $\alpha = 0.05$

Time averaging window of 120 seconds, Aalestrup

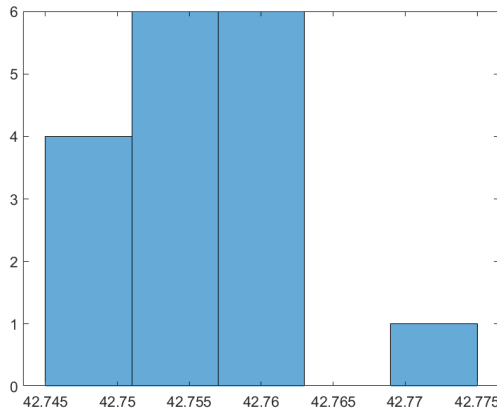


Figure E.13: Histogram - 120 seconds

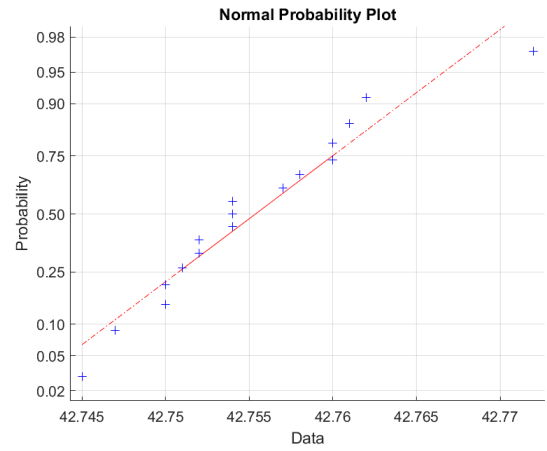


Figure E.14: Norm plot - 120 seconds

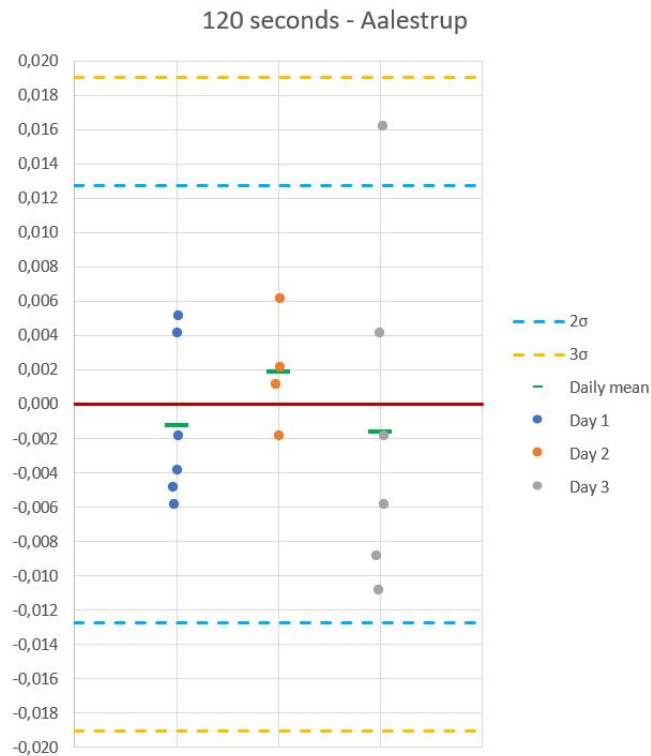


Figure E.15: Plots of observations from different days of collection. 120 second averaging time window

	Accepted	Rejected
Kolmogorov-Smirnov test	X	
Shapiro-Wilk test	X	

Table E.5: Hypothesis testing for normal distribution. H_0 : Normal distributed sample at $\alpha = 0.05$

Time averaging window of 240 seconds, Aalestrup

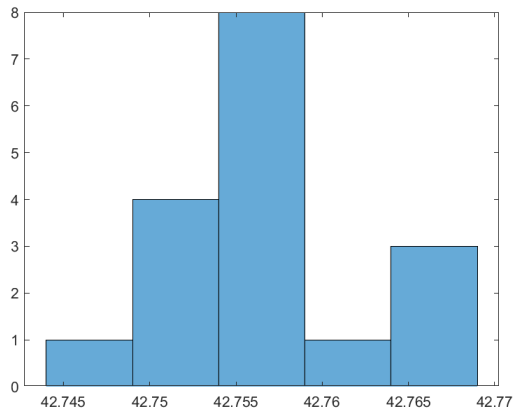


Figure E.16: Histogram - 240 seconds

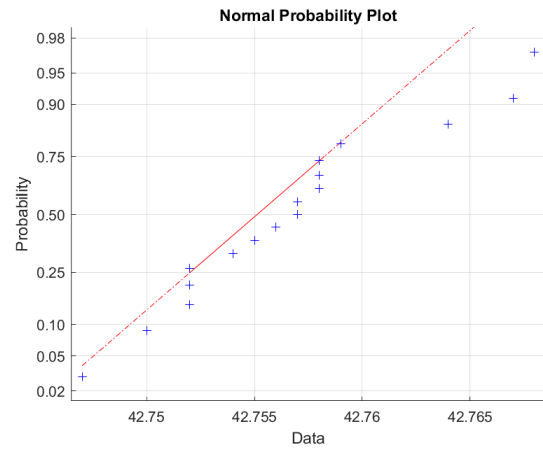


Figure E.17: Norm plot - 240 seconds

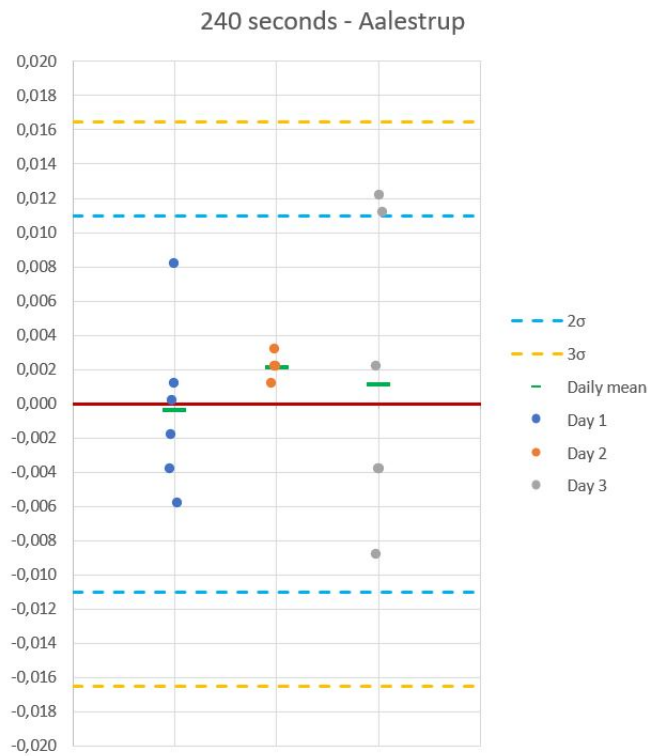


Figure E.18: Plots of observations from different days of collection. 240 second averaging time window

	Accepted	Rejected
Kolmogorov-Smirnov test	X	
Shapiro-Wilk test	X	

Table E.6: Hypothesis testing for normal distribution. H_0 : Normal distributed sample at $\alpha = 0.05$

Time averaging window of 600 seconds, Aalestrup

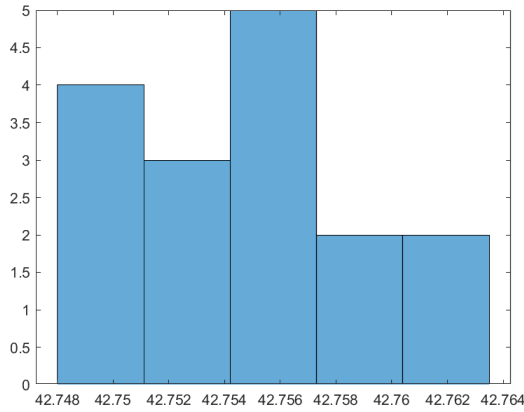


Figure E.19: Histogram - 600 seconds

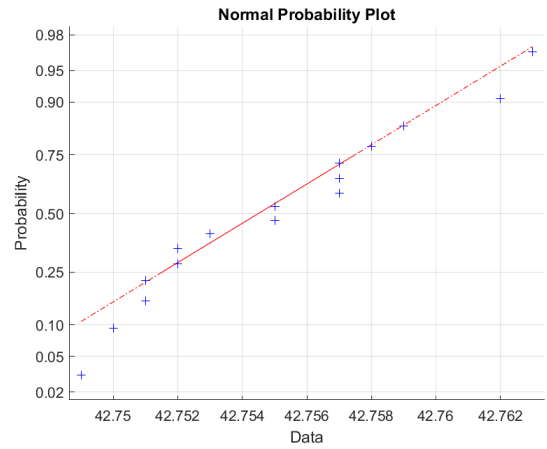


Figure E.20: Norm plot - 600 seconds

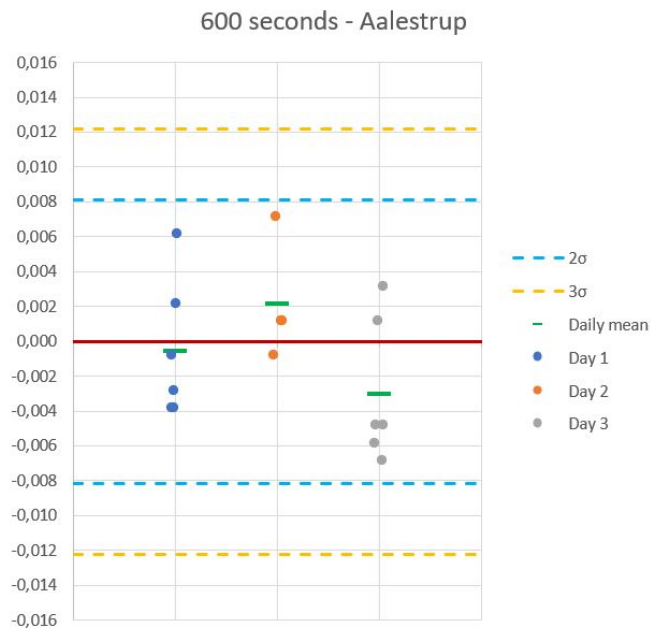


Figure E.21: Plots of observations from different days of collection. 600 second averaging time window

	Accepted	Rejected
Kolmogorov-Smirnov test	X	
Shapiro-Wilk test	X	

Table E.7: Hypothesis testing for normal distribution. H_0 : Normal distributed sample at $\alpha = 0.05$

E.2 Data collected in Sabro

Time averaging window of 5 seconds, Sabro

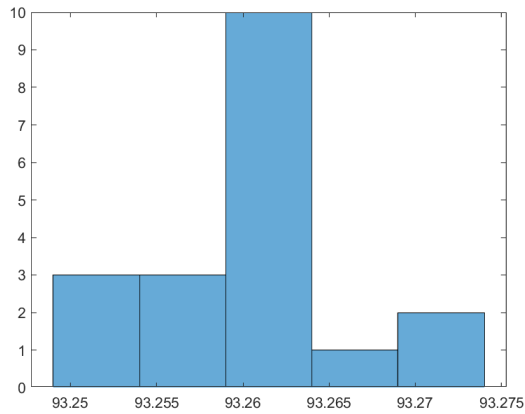


Figure E.22: Histogram - 5 seconds

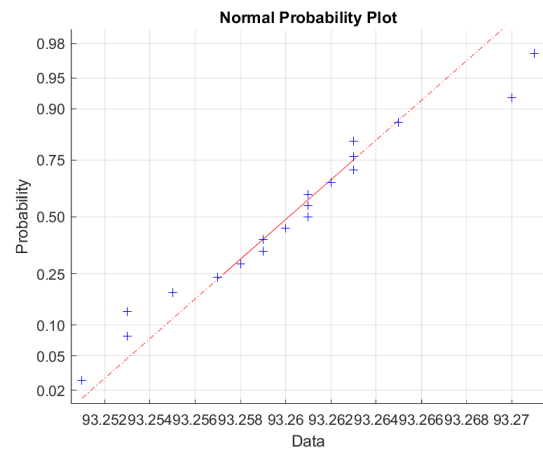


Figure E.23: Norm plot - 5 seconds

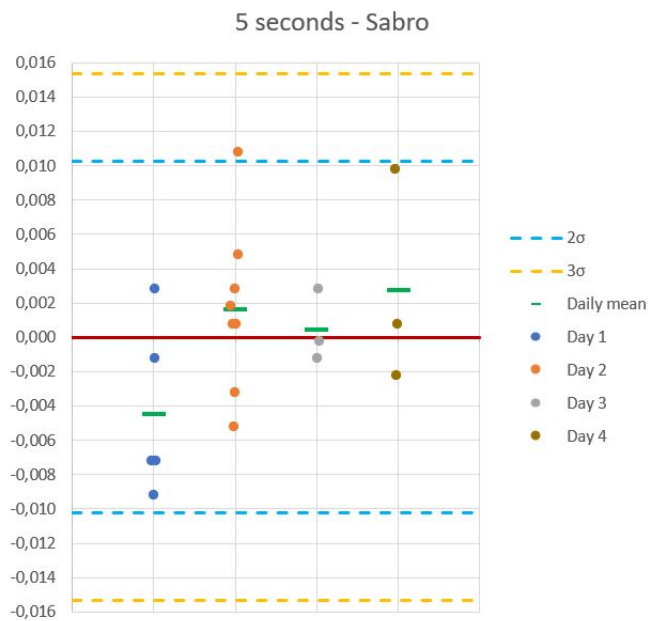


Figure E.24: Plots of observations from different days of collection. 5 second averaging time window

	Accepted	Rejected
Kolmogorov-Smirnov test	X	
Shapiro-Wilk test	X	

Table E.8: Hypothesis testing for normal distribution. H_0 : Normal distributed sample at $\alpha = 0.05$

Time averaging window of 15 seconds, Sabro

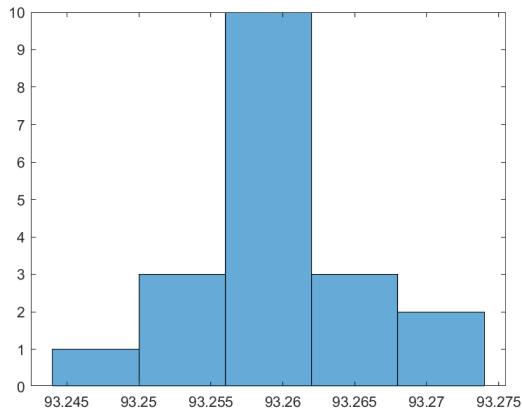


Figure E.25: Histogram - 15 seconds

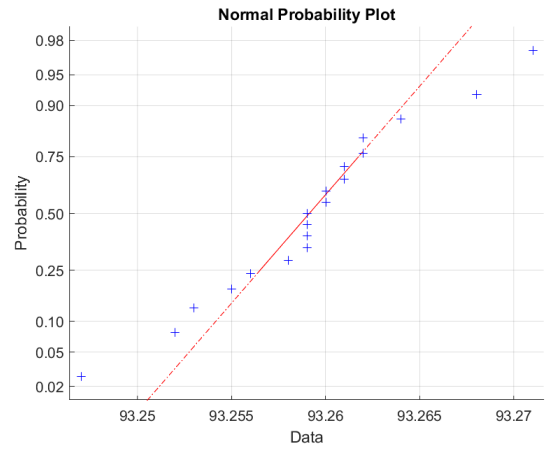


Figure E.26: Norm plot - 15 seconds

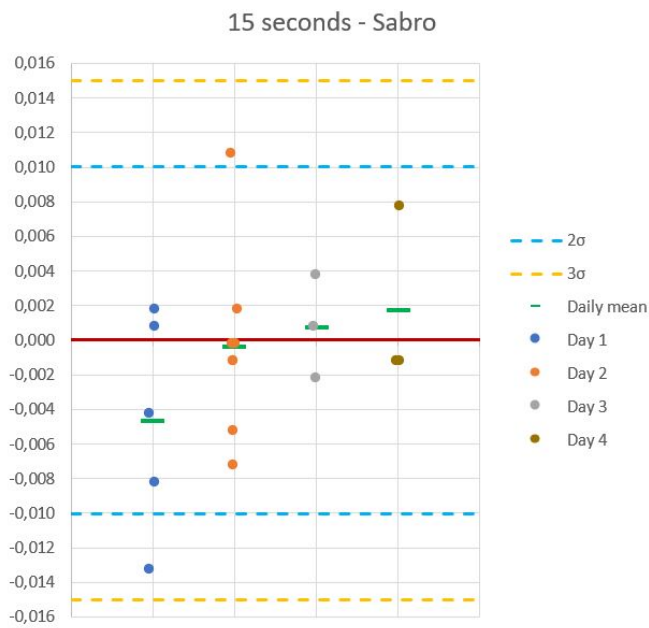


Figure E.27: Plots of observations from different days of collection. 15 second averaging time window

	Accepted	Rejected
Kolmogorov-Smirnov test	X	
Shapiro-Wilk test	X	

Table E.9: Hypothesis testing for normal distribution. H_0 : Normal distributed sample at $\alpha = 0.05$

Time averaging window of 30 seconds, Sabro

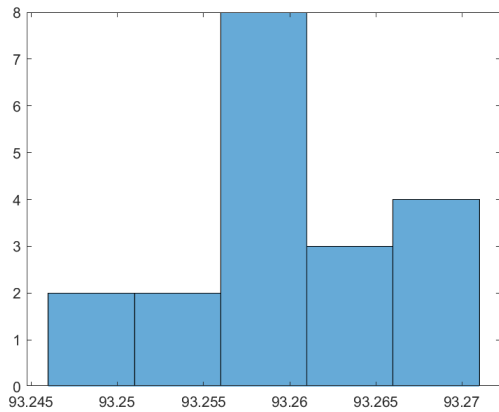


Figure E.28: Histogram - 30 seconds

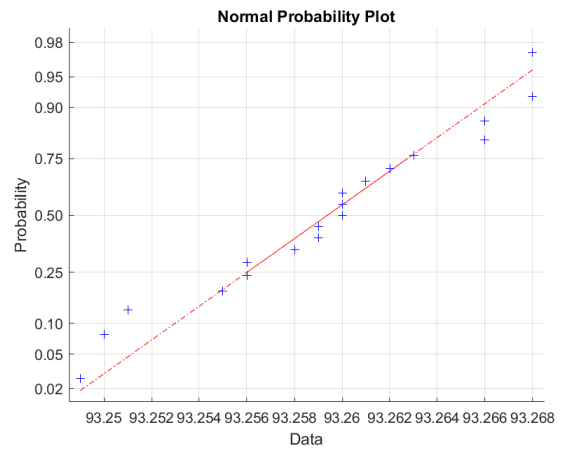


Figure E.29: Norm plot - 30 seconds

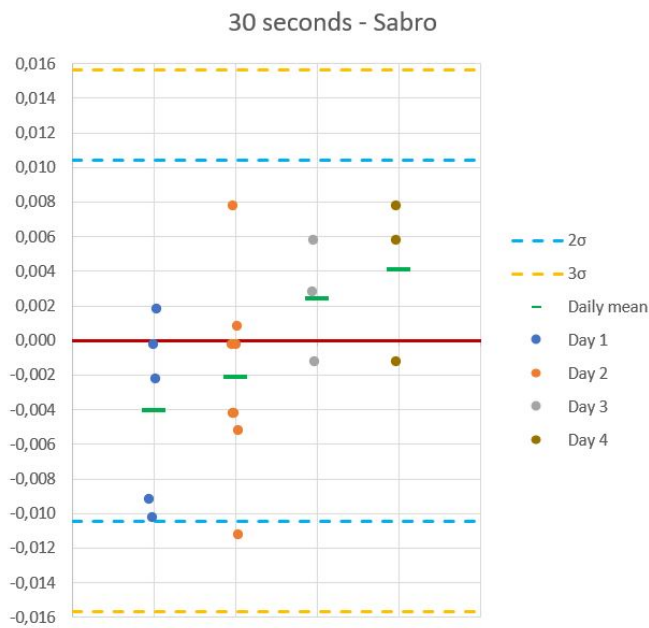


Figure E.30: Plots of observations from different days of collection. 30 second averaging time window

	Accepted	Rejected
Kolmogorov-Smirnov test	X	
Shapiro-Wilk test	X	

Table E.10: Hypothesis testing for normal distribution. H_0 : Normal distributed sample at $\alpha = 0.05$

Time averaging window of 60 seconds, Sabro

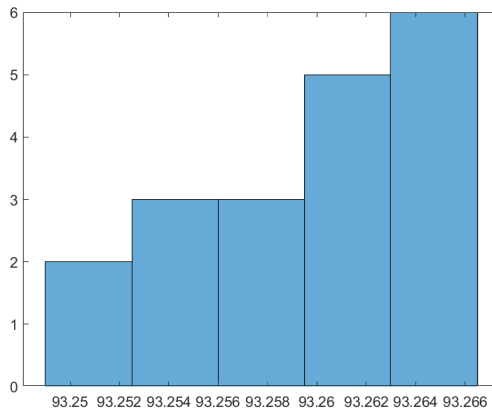


Figure E.31: Histogram - 60 seconds

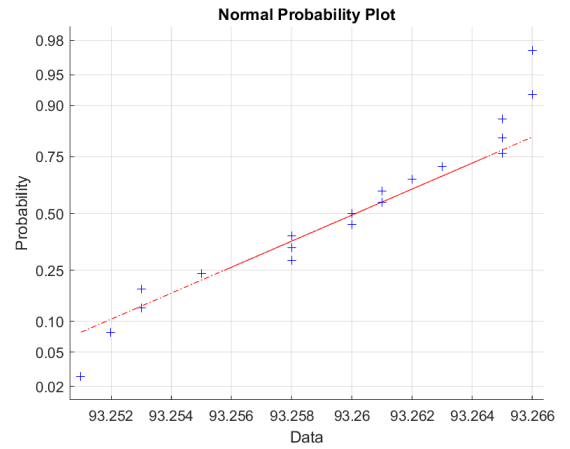


Figure E.32: Norm plot - 60 seconds

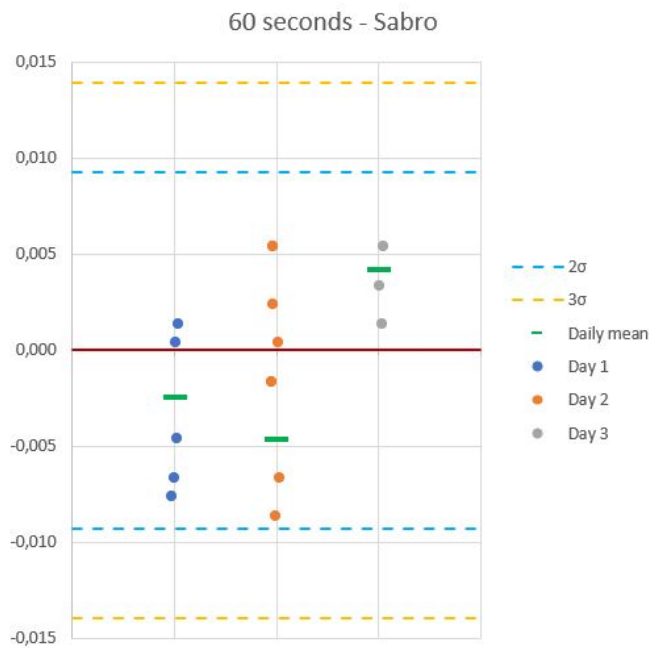


Figure E.33: Plots of observations from different days of collection. 60 second averaging time window

	Accepted	Rejected
Kolmogorov-Smirnov test	X	
Shapiro-Wilk test	X	

Table E.11: Hypothesis testing for normal distribution. H_0 : Normal distributed sample at $\alpha = 0.05$

Time averaging window of 120 seconds, Sabro

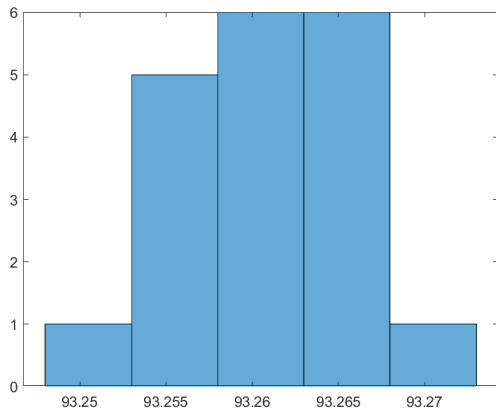


Figure E.34: Histogram - 120 seconds

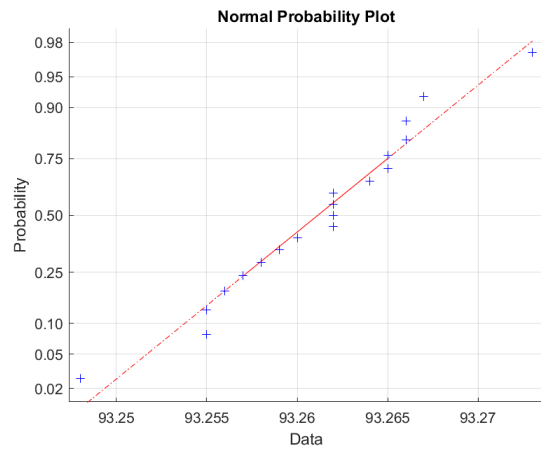


Figure E.35: Norm plot - 120 seconds

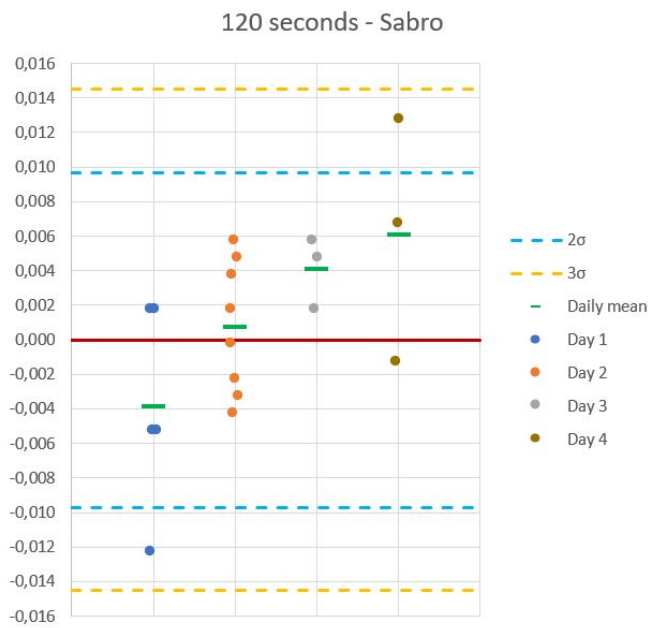


Figure E.36: Plots of observations from different days of collection. 120 second averaging time window

	Accepted	Rejected
Kolmogorov-Smirnov test	X	
Shapiro-Wilk test	X	

Table E.12: Hypothesis testing for normal distribution. H_0 : Normal distributed sample at $\alpha = 0.05$

Time averaging window of 240 seconds, Sabro

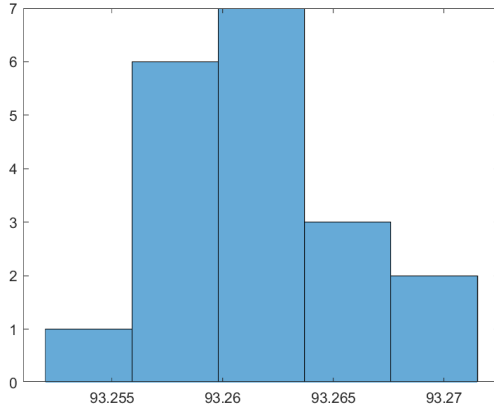


Figure E.37: Histogram - 240 seconds

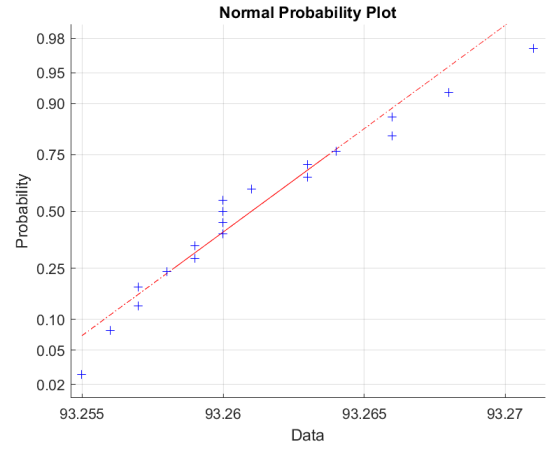


Figure E.38: Norm plot - 240 seconds



Figure E.39: Plots of observations from different days of collection. 240 second averaging time window

	Accepted	Rejected
Kolmogorov-Smirnov test	X	
Shapiro-Wilk test	X	

Table E.13: Hypothesis testing for normal distribution. H_0 : Normal distributed sample at $\alpha = 0.05$

Time averaging window of 600 seconds, Sabro

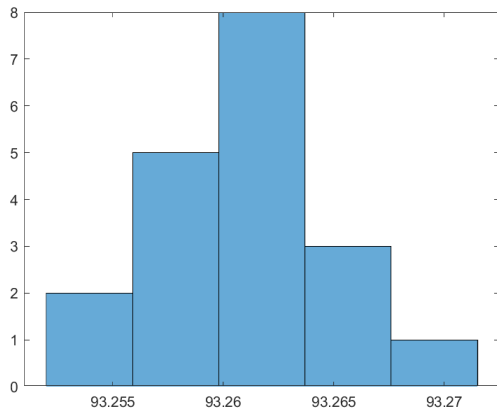


Figure E.40: Histogram - 600 seconds

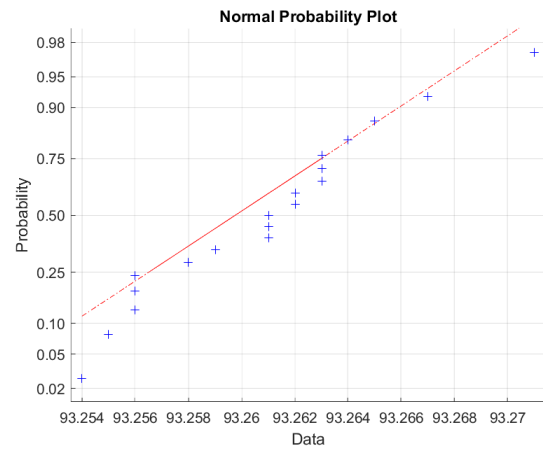


Figure E.41: Norm plot - 600 seconds

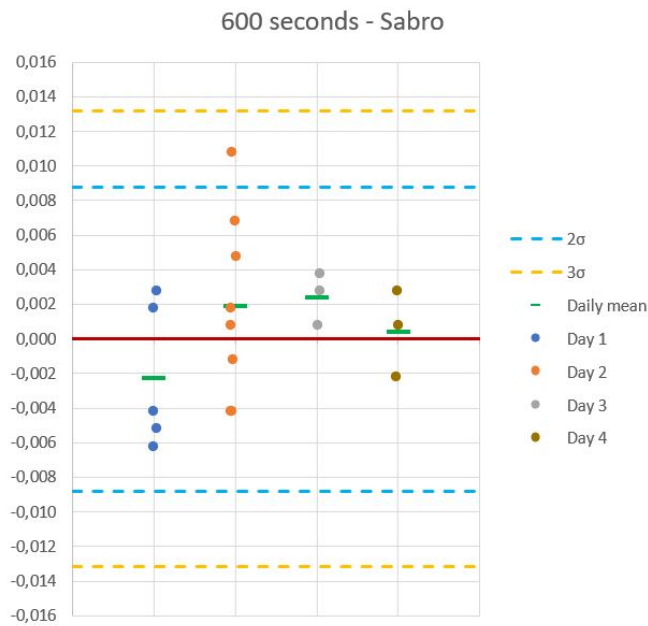


Figure E.42: Plots of observations from different days of collection. 600 second averaging time window

	Accepted	Rejected
Kolmogorov-Smirnov test	X	
Shapiro-Wilk test	X	

Table E.14: Hypothesis testing for normal distribution. H_0 : Normal distributed sample at $\alpha = 0.05$

**Individual data
examination of baseline
distance test**

F

Baseline 1 (22 m)

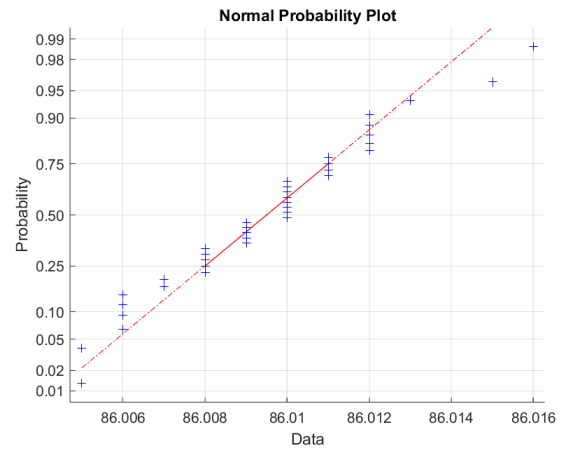
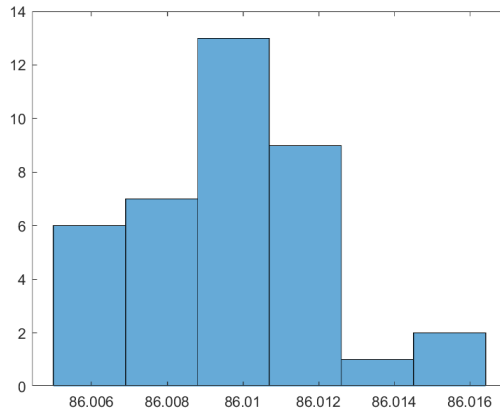


Figure F.1: Histogram - Baseline 1 (22 m)

Figure F.2: Norm plot - Baseline 1 (22 m)

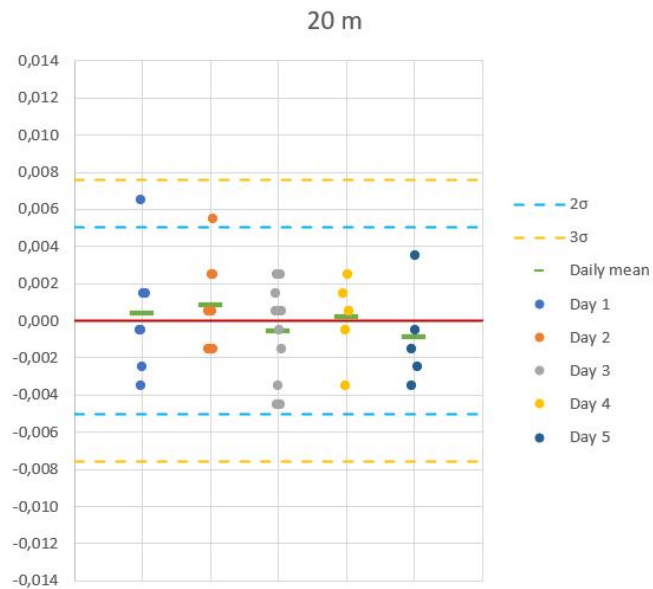


Figure F.3: Plots of observations from different days of collection. Baseline 1 (22 m)

	Accepted	Rejected
Kolmogorov-Smirnov test	X	
Shapiro-Wilk test	X	

Table F.1: Hypothesis testing for normal distribution. H_0 : Normal distributed sample at $\alpha = 0.05$

Baseline 2 (286 m)

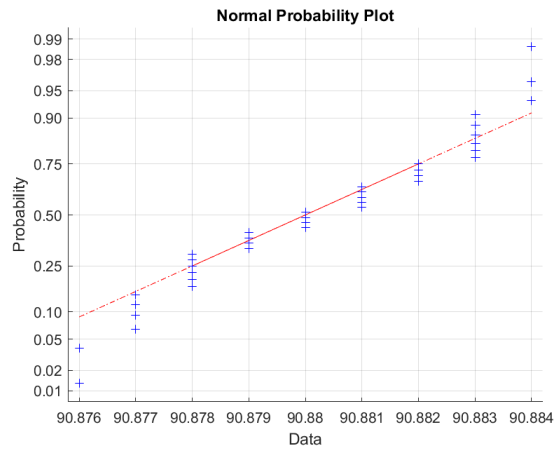
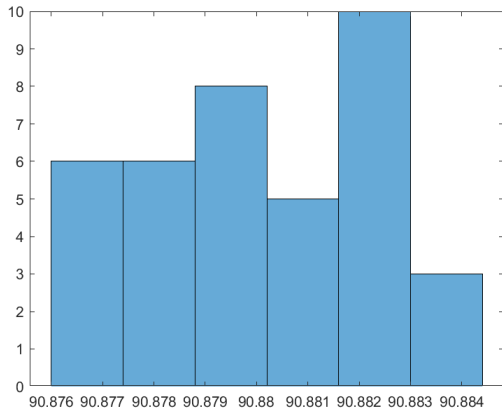


Figure F.4: Histogram - Baseline 2 (286 m)

Figure F.5: Norm plot - Baseline 2 (286 m)

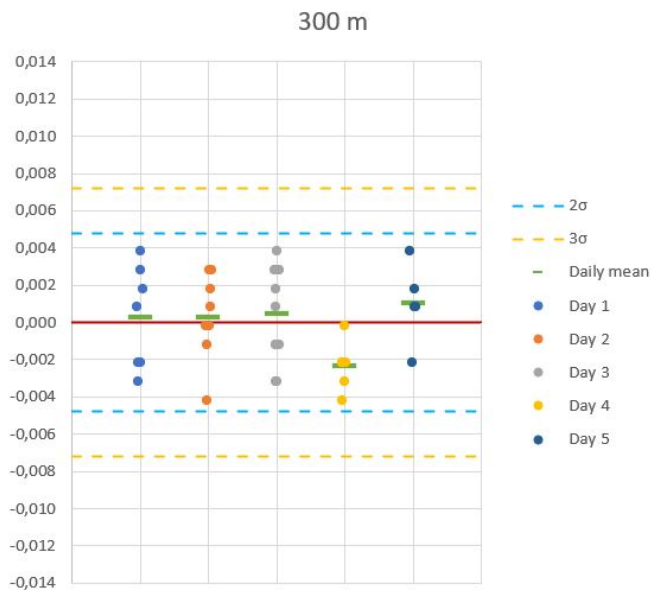


Figure F.6: Plots of observations from different days of collection. Baseline 2 (286 m)

	Accepted	Rejected
Kolmogorov-Smirnov test	X	
Shapiro-Wilk test		X

Table F.2: Hypothesis testing for normal distribution. H_0 : Normal distributed sample at $\alpha = 0.05$

Baseline 3 (686 m)

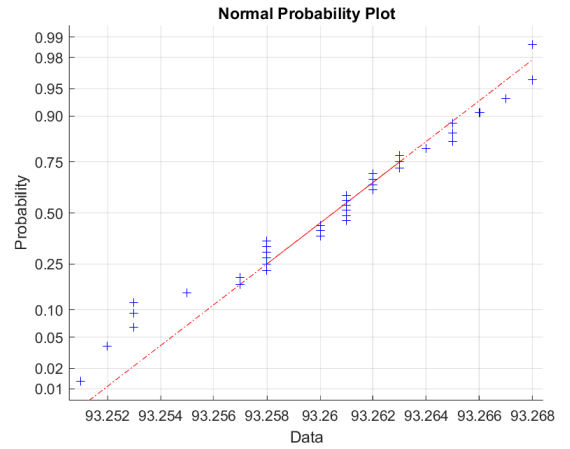
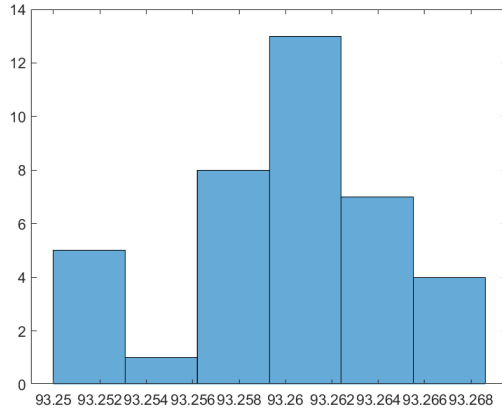


Figure F.7: Histogram - Baseline 3 (686 m)

Figure F.8: Norm plot - Baseline 3 (686 m)

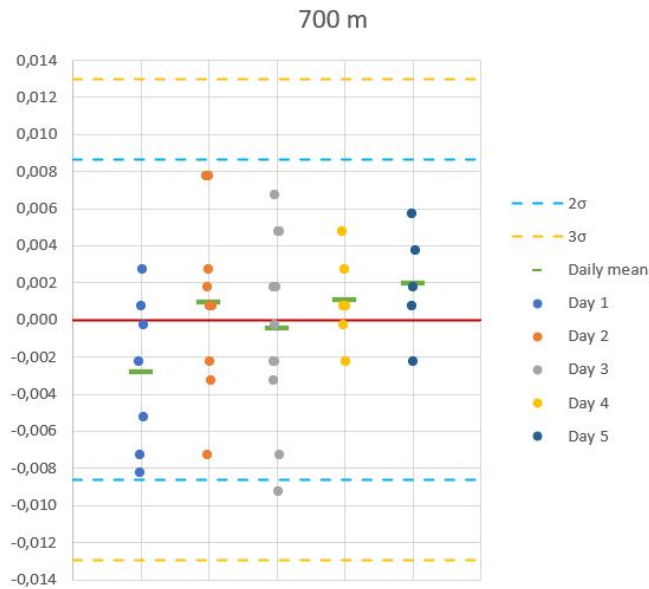


Figure F.9: Plots of observations from different days of collection. Baseline 3 (686 m)

	Accepted	Rejected
Kolmogorov-Smirnov test	X	
Shapiro-Wilk test	X	

Table F.3: Hypothesis testing for normal distribution. H_0 : Normal distributed sample at $\alpha = 0.05$

Baseline 4 (1.409 m)

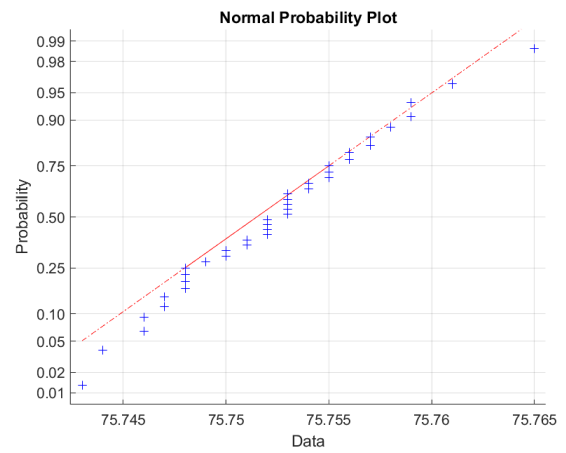
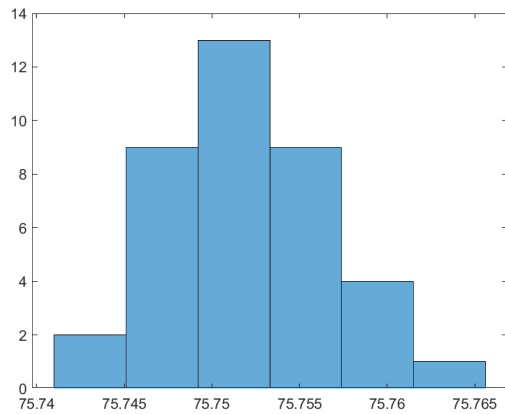


Figure F.10: Histogram - Baseline 4 (1.409 m) Figure F.11: Norm plot - Baseline 4 (1.409 m)

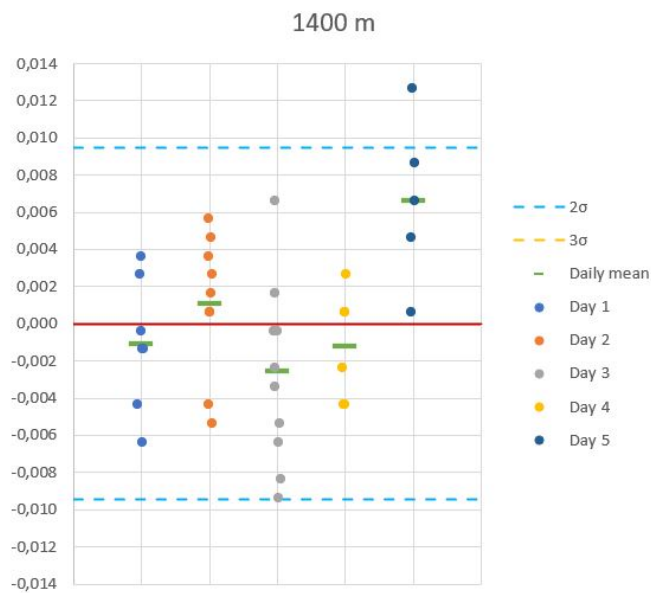


Figure F.12: Plots of observations from different days of collection. Baseline 3 (1.409 m)

	Accepted	Rejected
Kolmogorov-Smirnov test	X	
Shapiro-Wilk test	X	

Table F.4: Hypothesis testing for normal distribution. H_0 : Normal distributed sample at $\alpha = 0.05$

Baseline 5 (2.944 m)

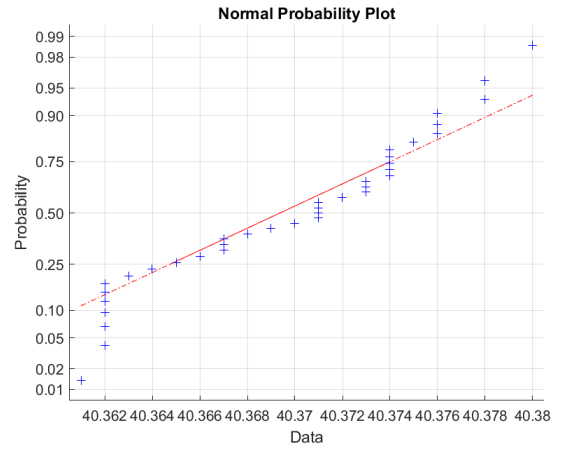
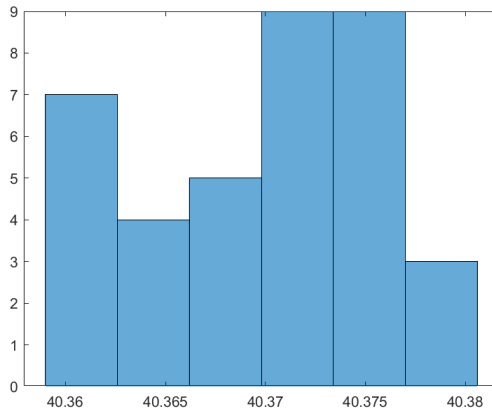


Figure F.13: Histogram - Baseline 5 (2.944 m) Figure F.14: Norm plot - Baseline 5 (2.944 m)

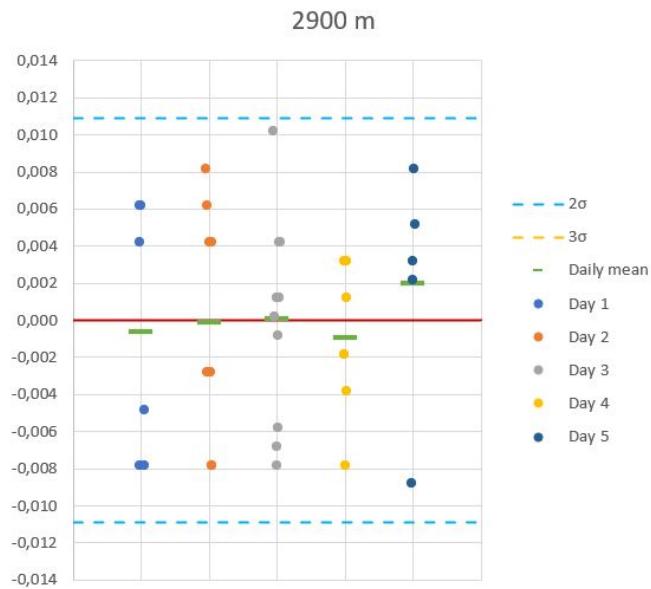


Figure F.15: Plots of observations from different days of collection. Baseline 4 (2.944 m)

	Accepted	Rejected
Kolmogorov-Smirnov test	X	
Shapiro-Wilk test		X

Table F.5: Hypothesis testing for normal distribution. H_0 : Normal distributed sample at $\alpha = 0.05$

Baseline 6 (4.469 m)

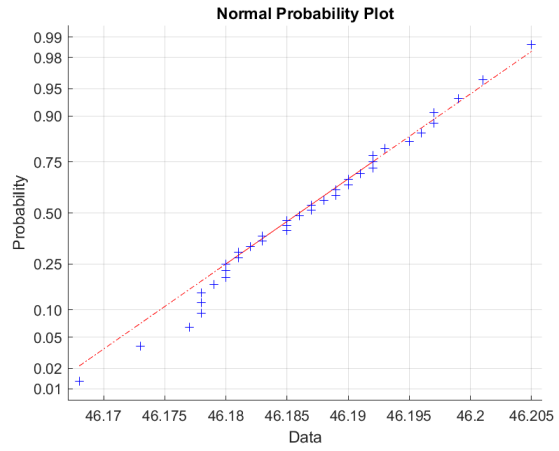
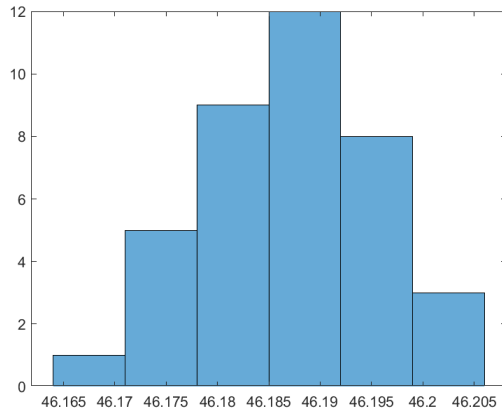


Figure F.16: Histogram - Baseline 6 (4.469 m) Figure F.17: Norm plot - Baseline 6 (4.469 m)

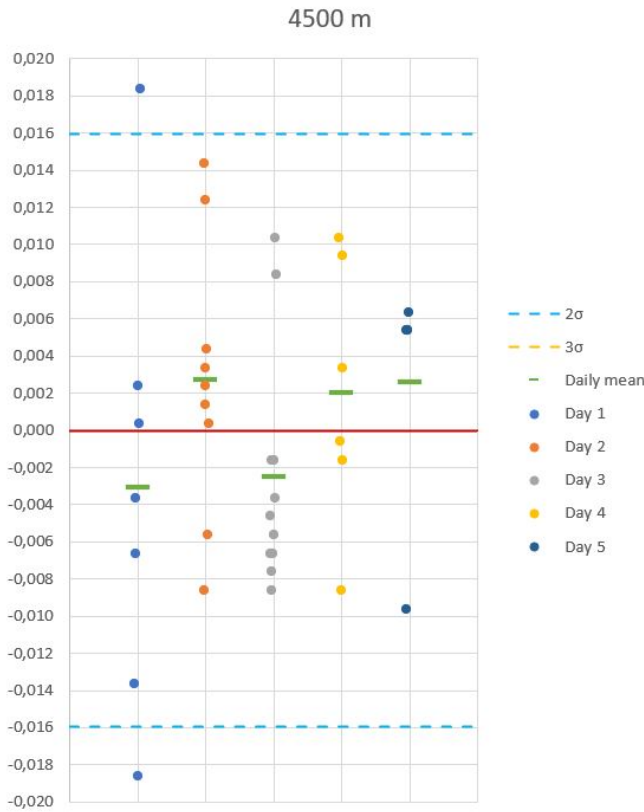


Figure F.18: Plots of observations from different days of collection. Baseline 6 (4.469 m)

	Accepted	Rejected
Kolmogorov-Smirnov test	X	
Shapiro-Wilk test	X	

Table F.6: Hypothesis testing for normal distribution. H_0 : Normal distributed sample at $\alpha = 0.05$

Baseline 7 (7.401 m)

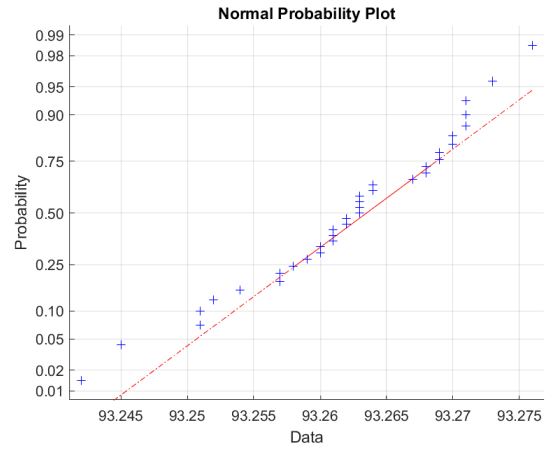
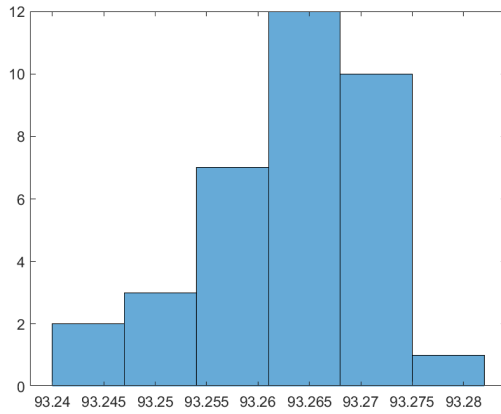


Figure F.19: Histogram - Baseline 7 (7.401 m) Figure F.20: Norm plot - Baseline 7 (7.401 m)

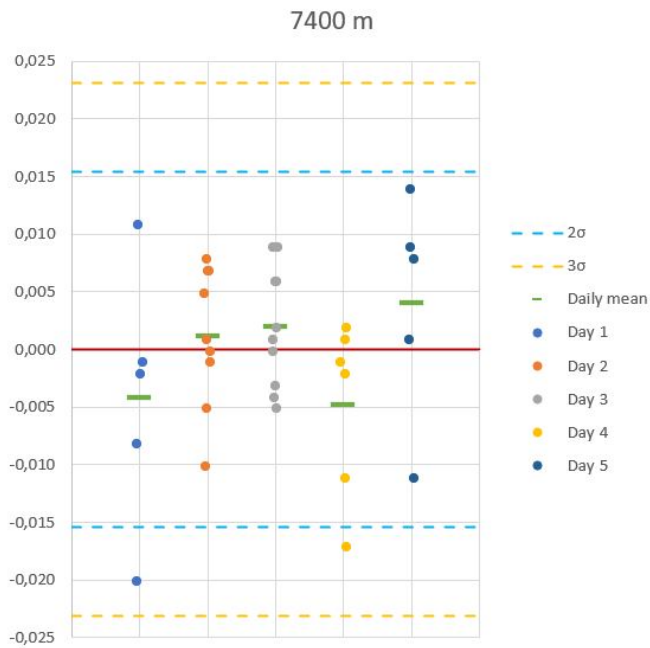


Figure F.21: Plots of observations from different days of collection. Baseline 7 (7.401 m)

	Accepted	Rejected
Kolmogorov-Smirnov test	X	
Shapiro-Wilk test	X	

Table F.7: Hypothesis testing for normal distribution. H_0 : Normal distributed sample at $\alpha = 0.05$

Baseline 8 (12.401 m)

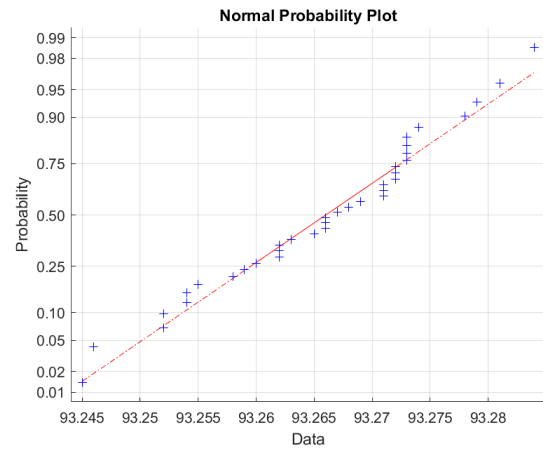
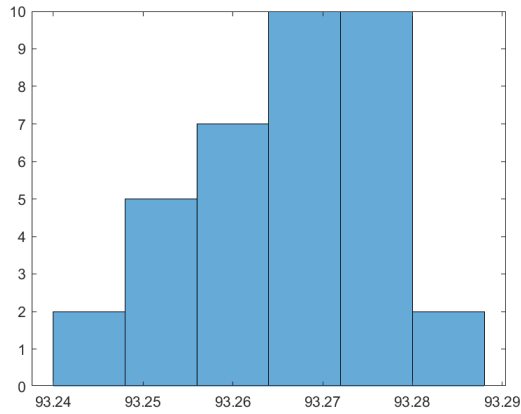


Figure F.22: Histogram - Baseline 8 (12.401 m) Figure F.23: Norm plot - Baseline 8 (12.401 m)

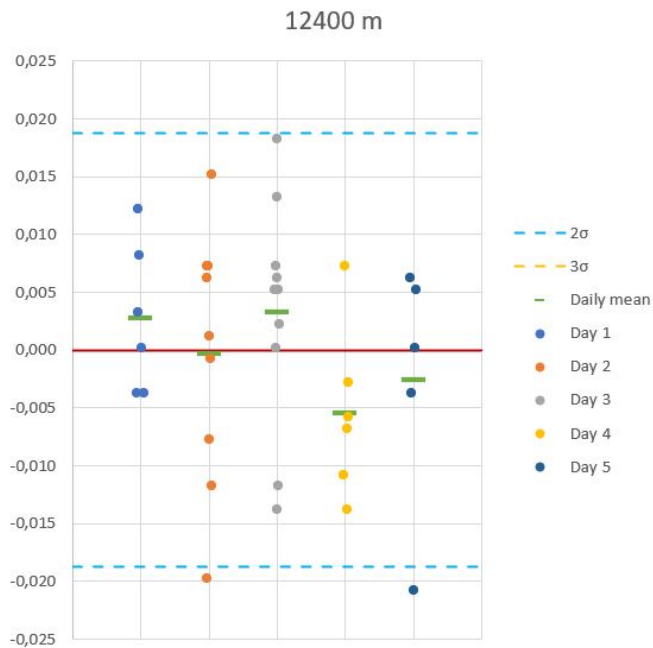


Figure F.24: Plots of observations from different days of collection. Baseline 8 (12.401 m)

	Accepted	Rejected
Kolmogorov-Smirnov test	X	
Shapiro-Wilk test	X	

Table F.8: Hypothesis testing for normal distribution. H_0 : Normal distributed sample at $\alpha = 0.05$

Baseline 9 (21.991 m)

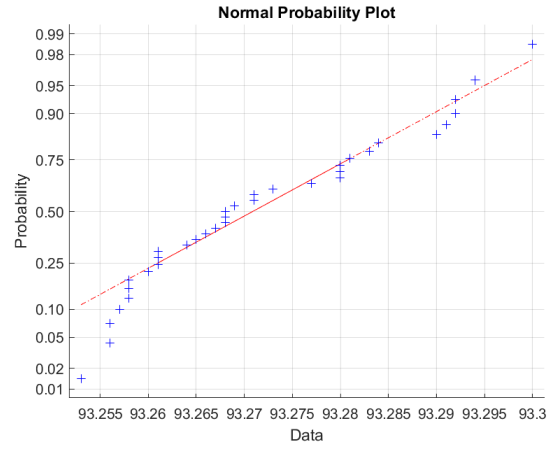
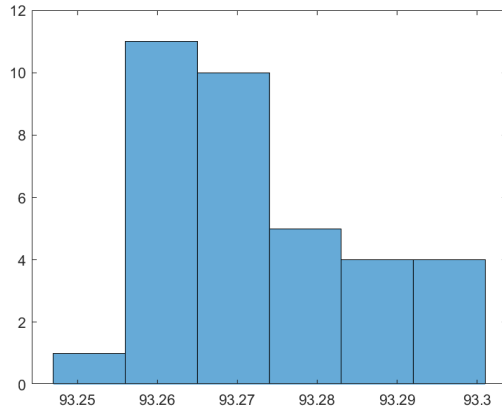


Figure F.25: Histogram - Baseline 9 (21.991 m) Figure F.26: Norm plot - Baseline 9 (21.991 m)

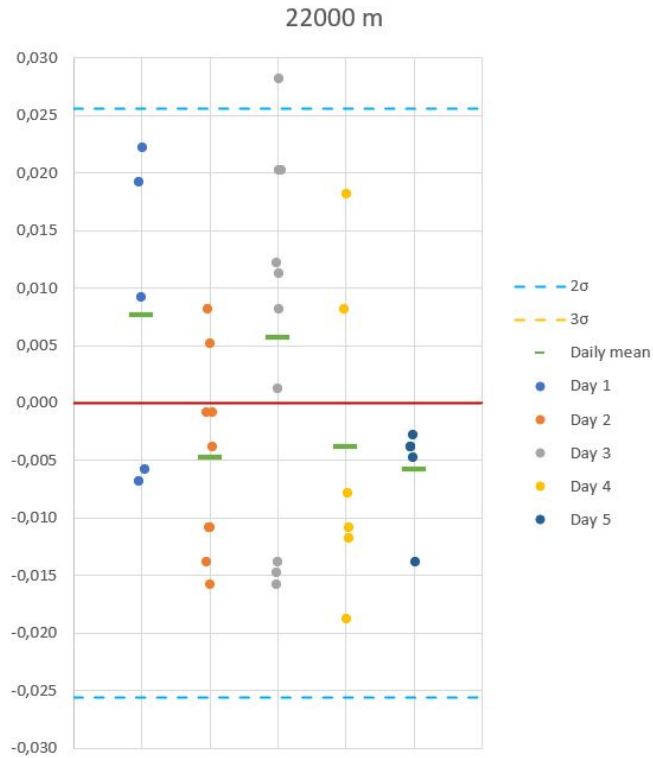


Figure F.27: Plots of observations from different days of collection. Baseline 9 (21.991 m)

	Accepted	Rejected
Kolmogorov-Smirnov test		X
Shapiro-Wilk test		X

Table F.9: Hypothesis testing for normal distribution. H_0 : Normal distributed sample at $\alpha = 0.05$

Baseline 10 (32.561 m)

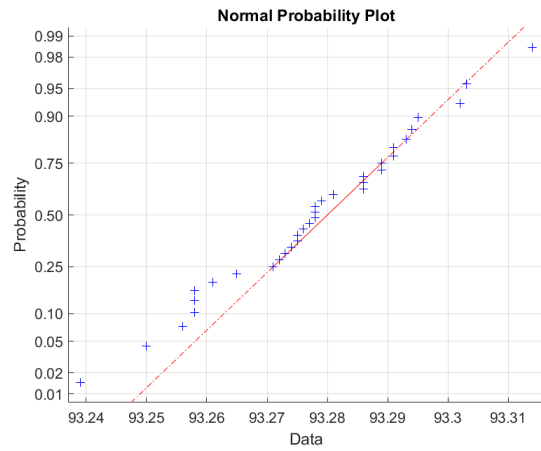
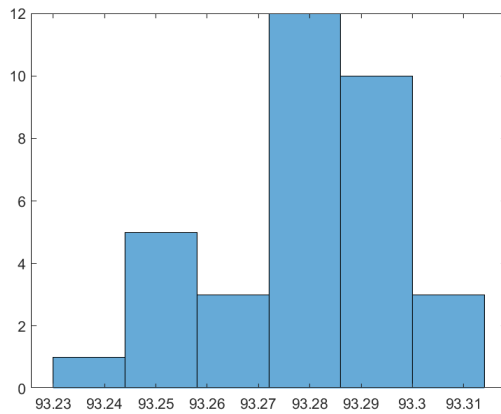


Figure F.28: Histogram - Baseline 10 (32.561 m) Figure F.29: Norm plot - Baseline 10 (32.561 m)

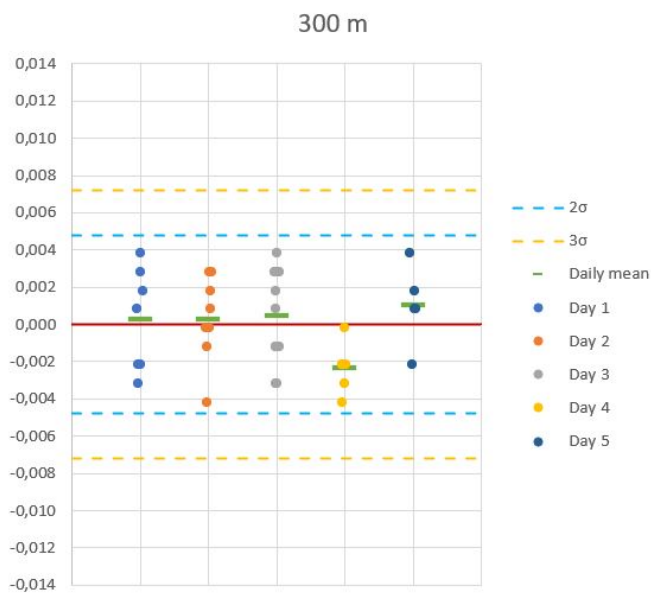


Figure F.30: Plots of observations from different days of collection. Baseline 10 (32.561 m)

	Accepted	Rejected
Kolmogorov-Smirnov test	X	
Shapiro-Wilk test	X	

Table F.10: Hypothesis testing for normal distribution. H_0 : Normal distributed sample at $\alpha = 0.05$

Baseline 11 (Smartnet IMAX)

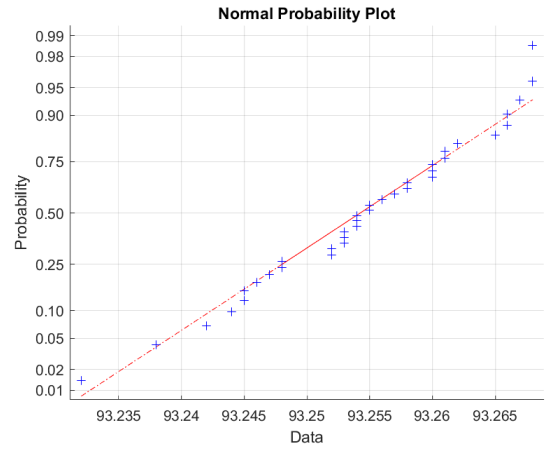
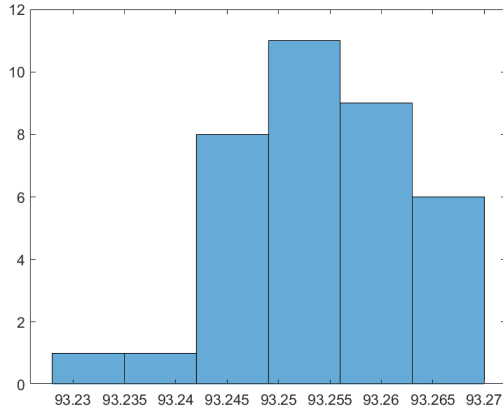


Figure F.31: Histogram - (Smartnet IMAX)

Figure F.32: Norm plot - (Smartnet IMAX)

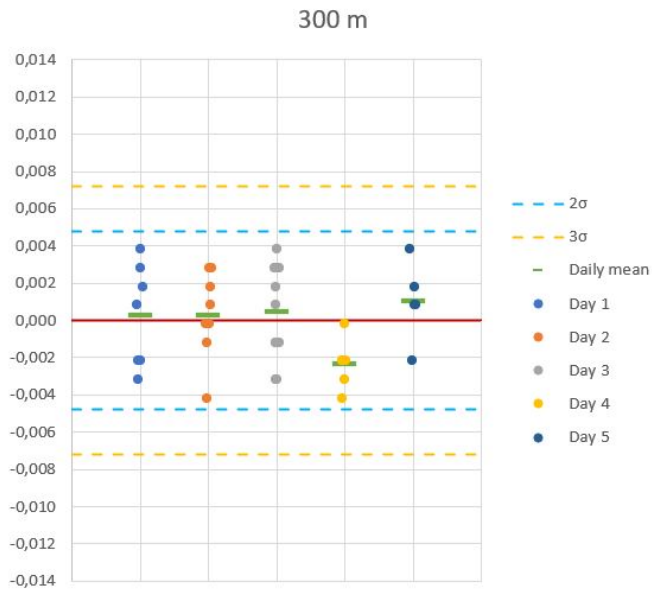


Figure F.33: Plots of observations from different days of collection. Baseline 11 (Smartnet IMAX)

	Accepted	Rejected
Kolmogorov-Smirnov test		X
Shapiro-Wilk test	X	

Table F.11: Hypothesis testing for normal distribution. H_0 : Normal distributed sample at $\alpha = 0.05$

Precision of a height difference



Precision (1σ) of a height difference between two points, when both points are measured with SRTK GNSS, with a basic error of 2.4 mm and a distance-dependent error of 1.3 mm/km. Dark green cells visualize distance where both the GNSS error and the geoid error are verified. Light green cells visualize distances where the geoid error are verified, but only when the points are in the same direction from the base station, and the GNSS error is verified. Yellow cells visualize where only the GNSS error is verified, and the geoid model may begin to contribute with a lack of precision (not modelled).

Point 1 [m]																					
	0	250	500	750	1000	1250	1500	1750	2000	2250	2500	2750	3000	3250	3500	3750	4000	4250	4500	4750	5000
0	3,5	3,7	3,9	4,2	4,4	4,7	4,9	5,2	5,5	5,7	6,0	6,3	6,6	6,9	7,1	7,4	7,7	8,0	8,3	8,6	8,9
250	3,7	3,9	4,1	4,3	4,6	4,8	5,1	5,3	5,6	5,9	6,1	6,4	6,7	7,0	7,3	7,5	7,8	8,1	8,4	8,7	9,0
500	3,9	4,1	4,3	4,5	4,8	5,0	5,3	5,5	5,8	6,0	6,3	6,6	6,8	7,1	7,4	7,7	7,9	8,2	8,5	8,8	9,1
750	4,2	4,3	4,5	4,8	5,0	5,2	5,4	5,7	5,9	6,2	6,4	6,7	7,0	7,2	7,5	7,8	8,1	8,3	8,6	8,9	9,2
1000	4,4	4,6	4,8	5,0	5,2	5,4	5,6	5,9	6,1	6,4	6,6	6,9	7,1	7,4	7,7	7,9	8,2	8,5	8,7	9,0	9,3
1250	4,7	4,8	5,0	5,2	5,4	5,6	5,8	6,1	6,3	6,5	6,8	7,0	7,3	7,5	7,8	8,1	8,3	8,6	8,9	9,1	9,4
1500	4,9	5,1	5,3	5,4	5,6	5,8	6,0	6,3	6,5	6,7	7,0	7,2	7,5	7,7	8,0	8,2	8,5	8,7	9,0	9,3	9,6
1750	5,2	5,3	5,5	5,7	5,9	6,1	6,3	6,5	6,7	6,9	7,2	7,4	7,6	7,9	8,1	8,4	8,6	8,9	9,2	9,4	9,7
2000	5,5	5,6	5,8	5,9	6,1	6,3	6,5	6,7	6,9	7,1	7,4	7,6	7,8	8,1	8,3	8,6	8,8	9,1	9,3	9,6	9,8
2250	5,7	5,9	6,0	6,2	6,4	6,5	6,7	6,9	7,1	7,3	7,6	7,8	8,0	8,2	8,5	8,7	9,0	9,2	9,5	9,7	10,0
2500	6,0	6,1	6,3	6,4	6,6	6,8	7,0	7,2	7,4	7,6	7,8	8,0	8,2	8,4	8,7	8,9	9,2	9,4	9,7	9,9	10,2
2750	6,3	6,4	6,6	6,7	6,9	7,0	7,2	7,4	7,6	7,8	8,0	8,2	8,4	8,6	8,9	9,1	9,3	9,6	9,8	10,1	10,3
3000	6,6	6,7	6,8	7,0	7,1	7,3	7,5	7,6	7,8	8,0	8,2	8,4	8,6	8,9	9,1	9,3	9,5	9,8	10,0	10,3	10,5
3250	6,9	7,0	7,1	7,2	7,4	7,5	7,7	7,9	8,1	8,2	8,4	8,6	8,9	9,1	9,3	9,5	9,7	10,0	10,2	10,4	10,7
3500	7,1	7,3	7,4	7,5	7,7	7,8	8,0	8,1	8,3	8,5	8,7	8,9	9,1	9,3	9,5	9,7	9,9	10,2	10,4	10,6	10,9
3750	7,4	7,5	7,7	7,8	7,9	8,1	8,2	8,4	8,6	8,7	8,9	9,1	9,3	9,5	9,7	9,9	10,1	10,4	10,6	10,8	11,1
4000	7,7	7,8	7,9	8,1	8,2	8,3	8,5	8,6	8,8	9,0	9,2	9,3	9,5	9,7	9,9	10,1	10,4	10,6	10,8	11,0	11,3
4250	8,0	8,1	8,2	8,3	8,5	8,6	8,7	8,9	9,1	9,2	9,4	9,6	9,8	10,0	10,2	10,4	10,6	10,8	11,0	11,2	11,5
4500	8,3	8,4	8,5	8,6	8,7	8,9	9,0	9,2	9,3	9,5	9,7	9,8	10,0	10,2	10,4	10,6	10,8	11,0	11,2	11,4	11,7
4750	8,6	8,7	8,8	8,9	9,0	9,1	9,3	9,4	9,6	9,7	9,9	10,1	10,3	10,4	10,6	10,8	11,0	11,2	11,4	11,7	11,9
5000	8,9	9,0	9,1	9,2	9,3	9,4	9,6	9,7	9,8	10,0	10,2	10,3	10,5	10,7	10,9	11,1	11,3	11,5	11,7	11,9	12,1

Point 2 [m]